

ACTIVE AND REACTIVE POWER CONTROL OF A DFIG BASED WIND ENERGY CONVERSION SYSTEM BY VECTOR CONTROL

Ibrahim Ahmad A.¹, D. Anitha², Sadokpam Romita Devi³

^{1, 2, 3} Department of Electrical and Electronics Engineering, S.R.M University, Chennai (India)

ABSTRACT

The paper deals with a design and implementation of a doubly fed induction generator (DFIG) wind energy conversion system (WECS) connected to the power grid. A back-to-back AC/DC/AC converter is incorporated between the stator and the rotor windings of a DFIG, in order to obtain variable speed operation. The DFIG can be controlled from sub-synchronous speed to super synchronous speed operation. The main objective of the paper is to control the flow of the Active and Reactive powers produced by the DFIG based wind energy conversion system. A vector control strategy with stator flux orientation is applied to both the grid side converter and the rotor side converter for the independent control of Active and reactive powers produced by the DFIG based wind energy conversion system. The system along with its control circuit was simulated in a Matlab/simulink and the results are presented and discussed.

Keywords: Active and Reactive powers, back-to-back converters, DFIG, Vector control, WECS

I. INTRODUCTION

Renewable energy sources are abundant all over the world and can easily be accessed. In the past, most of the electricity generated in the world was generated from the conventional sources of energy such as: Gas, oil, hydrothermal and coal. These are non renewable energy sources that emits large amount of carbon dioxide into the atmosphere, which results in the global warming there by polluting the environment [1, 2].

Nowadays due to the rapid development of modern electricity production technologies, the old methods are being replaced. Among these technologies renewable energy sources are the most widely used due to their smaller size, low cost per unit and their environmental friendly nature [1].

Among all the renewable energy sources wind energy conversion system is the promising and fastest growing source of energy in the world, this renewable and clean source of energy have always been available and its being employed for electricity generation over the years. The rising share of wind energy conversion system, in the existing power system has created many opportunities and challenges [2].

The main objective and aim of this paper is the control of the active and reactive power produced by the stator of the DFIG. The paper is divided into five sections; the first section gives the introduction, the second section discusses the operating principles of the system, the third section gives the dynamic model of a DFIG. The vector control of DFIG based wind energy conversion system for efficient and good performance is discussed in section four. The last section gives the simulation results and conclusion.

II. OPERATING PRINCIPLES OF A DFIG

The stator is directly connected to the AC mains, where as the wound rotor is fed from the Power Electronic Converters via slip rings to allow DIFG to operate at a variety of speeds in response to changing wind speed. The idea is to introduce a frequency converter between the variable frequency induction generator and fixed frequency grid. The DC capacitor linking stator-side and rotor-side converters allows the storage of power from induction generator for further generation [8]. To achieve full control of grid current, the DC-link voltage must be boosted to a level higher than the amplitude of grid line-to-line voltage. The slip power can flow in both directions, i.e. to the rotor from the supply and from supply to the rotor and hence the speed of the machine can be controlled from either rotor-side or stator-side converter in both super and sub-synchronous speed ranges. As a result, the machine can work as a generator or a motor in both super and sub-synchronous operating modes realizing four operating modes [8][10]. Below the synchronous speed in the motoring mode and above the synchronous speed in the generating mode, rotor-side converter operates as a rectifier and stator-side converter as an inverter, where slip power is returned to the stator. Below the synchronous speed in the generating mode and above the synchronous speed in the motoring mode, rotor-side converter operates as an inverter and stator-side converter as a rectifier, where slip power is supplied to the rotor. At the synchronous speed, slip power is taken from supply to excite the rotor windings and in this case machine behaves as a synchronous machine [8].

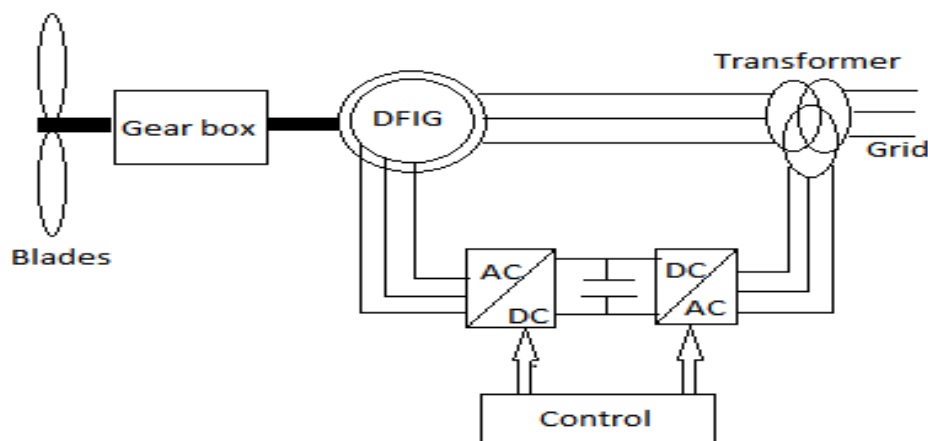


Fig. 1 Power Flow Diagram of DFIG

This arrangement has a number of advantages which include: rotor speed variation from sub-synchronous speed to super synchronous speed based on the wind speed, independent control of the active and reactive powers, and reduced flicker [4]. Generally two control schemes namely mechanical and electrical control system represent the overall control schemes of DFIG, which are both characterized by different objectives. However, the main aim is to control the power injected into the grid. The active power supply to the grid is generally controlled by the rotor side converter (RSC) whereas the reactive power injection is controlled by both the rotor side and grid side converters (GSC) as in [2]. The grid side converter also can realize the control of the DC link voltage and network power factor by using the grid voltage oriented vector control strategy [4].

III. DYNAMIC MODELLING OF A DFIG

In order to investigate the actual behavior of the DFIG, dynamic equation needs to be considered for more realistic observation. From the view point of the machine's control, the d-q representation of an induction machine leads to control flexibility [4]. The dynamic behavior of the DFIG in synchronous reference frame can

be represented by the Park equations, provided all the rotor quantities are referred to the stator side. The stator and rotor voltages are expressed as follows [3-4]:

$$\begin{aligned} V_{ds} &= R_s I_{ds} + p\varphi_{ds} - \omega_s \varphi_{qs} \\ V_{qs} &= R_s I_{qs} + p\varphi_{qs} + \omega_s \varphi_{ds} \\ V_{dr} &= R_r I_{dr} + p\varphi_{dr} - (\omega_s - \omega_r) \varphi_{qr} \\ V_{qr} &= R_r I_{qr} + p\varphi_{qr} + (\omega_s - \omega_r) \varphi_{dr} \end{aligned} \quad \text{Where } p = \frac{d}{dt} \quad (1)$$

The flux linkage equations of the stator and rotor can be related to the current and expressed as:

$$\begin{aligned} \varphi_{ds} &= L_{ss} I_{ds} + L_m I_{dr} \\ \varphi_{qs} &= L_{ss} I_{qs} + L_m I_{qr} \\ \varphi_{dr} &= L_{rr} I_{dr} + L_m I_{ds} \\ \varphi_{qr} &= L_{rr} I_{qr} + L_m I_{qs} \end{aligned} \quad (2)$$

The electromagnetic torque developed by the DFIG is related to the torque supplied by the turbine and can be expressed as:

$$T_e = 1.5p(\varphi_{ds} I_{qs} - \varphi_{qs} I_{ds}) \quad (3)$$

For stable operation and independent control of the active and reactive powers of the system, a model based on PI controllers is developed as shown in figure 2 using the dynamic model equations below.

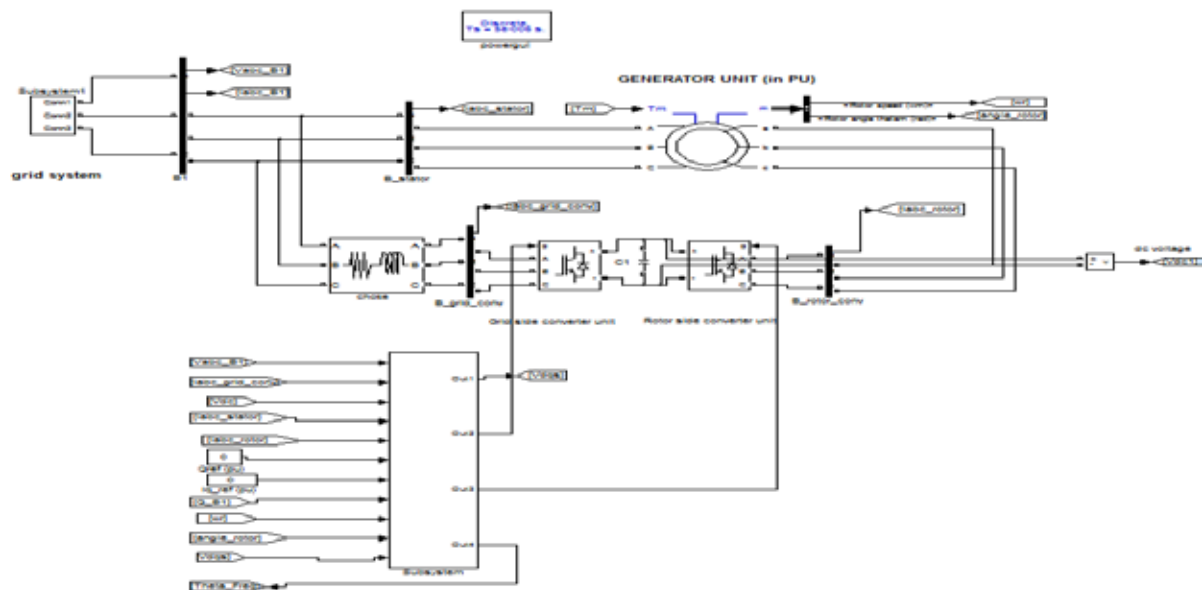


Fig. 2 Closed loop diagram of a DFIG WECS

IV. THE VECTOR CONTROL STRATEGY

The vector control concept is used for controlling a DFIG system, which is based on the transformation of a three phase variables to the synchronous frame variables, in d-q reference frames. The reference frame is aligned to the stator of the machine rotating at synchronous speed, in which the q-axis component of the rotor current is controlled to achieve the control of active power production by the DFIG while the d-axis component of the rotor current is controlled to achieve the control of reactive power production. The grid side converter is controlled to maintain the DC-link voltage constant.

The following assumptions are considered in the simulation of vector control strategy [4].

- Stator voltage drop across resistance is neglected.
- The q-axis leads the d-axis by 90^0 in the direction of rotation
- The stator flux vector is aligned with the d-axis of the stator
- The amplitude and frequency of the stator or grid voltage is assumed to be constant.
- The magnetizing current of the stator is assumed to be determined by the grid.

The above assumptions lead to the following

$$\begin{aligned} V_{ds} &= 0 & \varphi_{ds} &= \varphi_s \\ V_{qs} &= V_s & \varphi_{qs} &= 0 \end{aligned} \quad (4)$$

Neglecting stator resistance

$$\begin{aligned} V_{ds} &= 0 = p\varphi_{ds} - \omega_s\varphi_{qs} \\ V_{qs} &= V_s = p\varphi_{qs} + \omega_s\varphi_{ds} \\ V_{dr} &= R_r I_{dr} + p\varphi_{dr} - (\omega_s - \omega_r)\varphi_{qr} \\ V_{qr} &= R_r I_{qr} + p\varphi_{qr} + (\omega_s - \omega_r)\varphi_{dr} \end{aligned} \quad (5)$$

And the fluxes becomes

$$\begin{aligned} \varphi_{ds} &= L_{ss}I_{ds} + L_m I_{dr} \\ 0 &= L_{ss}I_{qs} + L_m I_{qr} \\ \varphi_{dr} &= L_{rr}I_{dr} + L_m I_{ds} \\ \varphi_{qr} &= L_{rr}I_{qr} + L_m I_{qs} \end{aligned} \quad (6)$$

Then,

$$\begin{aligned} V_{dr} &= R_r I_{dr} \left(L_{rr} - \frac{L_m^2}{L_{ss}} \right) pI_{dr} - \left[(\omega_s - \omega_r) \left(L_{rr} - \frac{L_m^2}{L_{ss}} \right) \right] I_{qr} \\ V_{qr} &= R_r I_{qr} + \left(L_{rr} - \frac{L_m^2}{L_{ss}} \right) pI_{qr} + (\omega_s - \omega_r) \left[\left(L_{rr} - \frac{L_m^2}{L_{ss}} \right) I_{dr} + \frac{L_m V_s}{\omega_s L_{ss}} \right] \end{aligned} \quad (7)$$

The active and reactive powers produced in the stator, the rotor fluxes and voltages can be written in terms of rotor currents as:

$$\begin{aligned} P_s &= -\frac{L_m V_s}{L_{ss}} * I_{qr} \\ Q_s &= -\frac{V_s^2}{\omega_s L_{ss}} - \frac{L_m V_s}{L_{ss}} * I_{dr} \end{aligned} \quad (8)$$

Then, the reference currents interms of the active and reactive powers can be written as:

$$\begin{aligned} I_{qr} &= -\frac{L_{ss} P_s}{L_m V_s} \\ I_{dr} &= \left(Q_s - \frac{V_s^2}{\omega_s L_{ss}} \right) * -\frac{L_{ss}}{V_s L_m} \end{aligned} \quad (9)$$

V. SIMULATION RESULTS

The DFIG based wind energy conversion system was simulated, for the active and reactive power control on the matlab/simulink platform. In this section the simulation results for the system operation are shown.

The stator dq-axis currents are shown in Figure (5) & (6). These figures represent a good pursuit, except that the present of oscillations during the transient time. A very good decoupling between the two components of the currents is obtained, which ensures the decoupling between the components of the rotor currents shown in

Figure (3) and (4), and eventually result in decoupling the active and reactive powers shown in Figure (7) and (8) respectively, which leads to a good control of the power flow between the grid and the machine at all time. The grid side voltage and currents waveforms are shown in figure (9) and (10), figure (11) shows the dc link voltage.

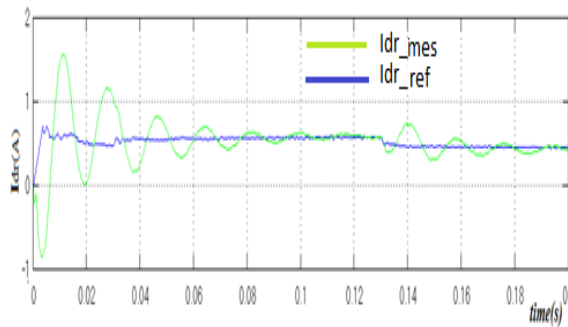


Fig. 3 Rotor d-axis currents

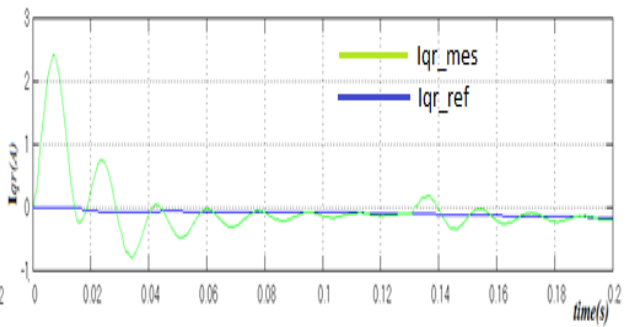


Fig. 4 Rotor q-axis currents

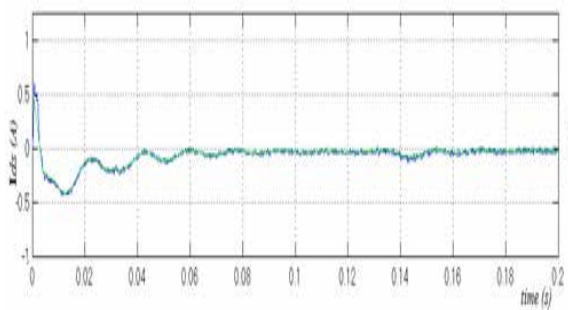


Fig. 5 Stator d-axis currents

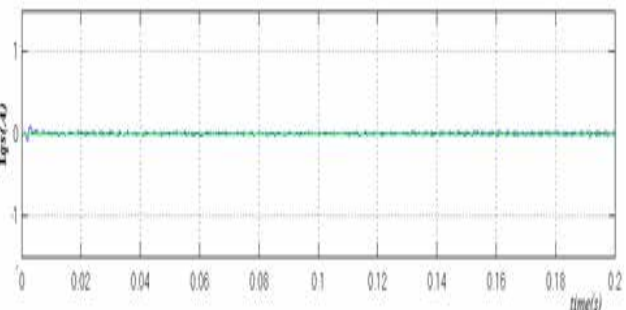


Fig. 6 Stator q-axis currents

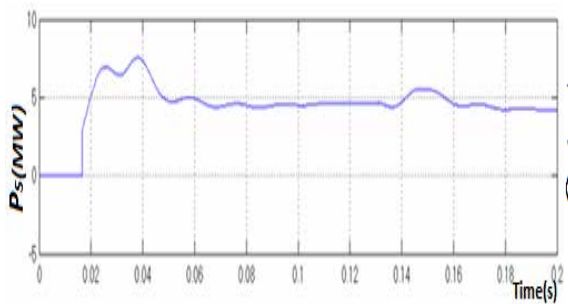


Fig. 7 Stator Active power

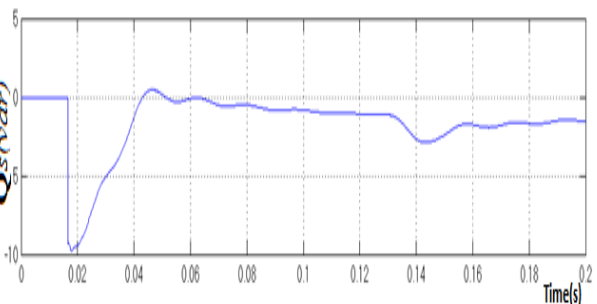


Fig. 8 Stator Reactive power

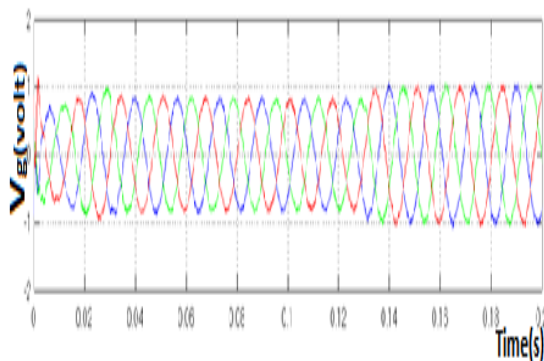


Fig. 9 Grid voltage waveforms

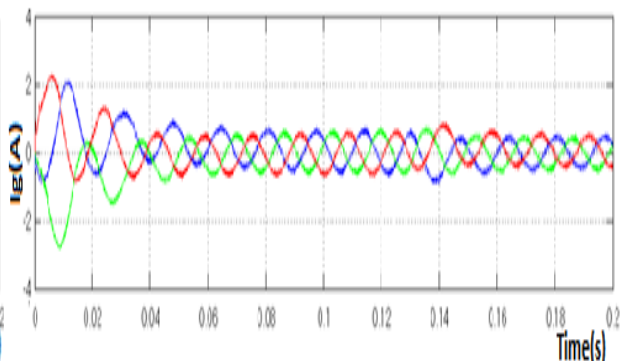


Fig. 10 Grid current waveforms

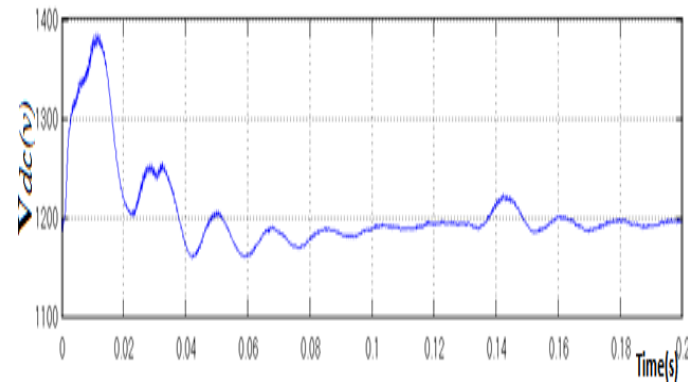


Fig. 11 DC-Link voltage

VI. CONCLUSION

The simulation of the system was carried out on a matlab/simulink, using the parameters listed below. And its overall control system model has been presented in this paper. The simulation test confirms the dynamic performance and the independent control of active and reactive powers by the vector control scheme.

Machine Parameters

Parameters	values
Power	7.5MW
Voltage	575V
Frequency	60HZ
Pole pairs	3
Stator resistance	0.0071
Rotor resistance	0.0050
Stator inductance	0.171
Rotor inductance	0.1560
Magnetizing inductance	2.9
Inertial constant	5.04
DC link capacitor	0.060
DC voltage	1200V

VII. ACKNOWLEDGMENT

The authors would like to thank and acknowledge the help and the support of our able professor Dr. S.S. Dash and Dr. N. Challammal of EEE Dept. SRM University, Chennai.

REFERENCES

- [1] Abdulla Asuhaimi, B mohd Zin, Mahmoud pesaran H.A, Azhar B. Khairuddin, Leila Jahanshaloo, Omid Shariati. An overview on DFIG controls and contributions to wind based electricity generation, science direct 27 (2013) 692-708.
- [2] H.T. Jadhav, Ranjit Roy 'A comprehensive review on the grid integration of doubly fed induction generator'science direct in electrical power and energy systems 49 (2013) 8 – 18.

- [3] K. Kerrouche, A mezouar, Kh. Belgacem, 'Decoupled control of DFIG by vector control for wind energy conversion system' energy procedia 42 (2013) 239 – 248.
- [4] Md Arifujjaman, M.T. Iqbal, J.E. Quaicoe, 'Vector control of a DFIG wind turbine, Journal of electrical and electronic engineering 9 (2009) 1057 – 1066.
- [5] B Hamane, M Bhenganem, A.M Bouzid, A.Belabbes, M. Bouhamida, A.Draou, 'control for variable speed wind turbine driving a DFIG using Fuzzy – PI control, energy procedia 18 (2012) 476 – 485.
- [6] S. Benelgali, M.E.H. Benbouzid, and J.F Charpentier, 'Comparison of DFIG and PMSG for marine current turbine applications' in international conference on electrical machines ICEM 2010 rome.
- [7] Jose liuz Dominguez-Garcia' Oriol gomis-Bellmunt, Lluís Trilla-Romero, Adria Junyent-Ferre, 'Indirect vector control of a squirrel cage induction generator wind turbine' computers and mathematics with applications 64 (2012) 102 - 114.
- [8] Srinath vanikuru, Satish Sukhsavasi 'Active and Reactive power control of a DFIG driven by a wind turbine' international journal of power system operation and energy management, ISSN 2231-4407 volume-1, issue-2, 2011.
- [9] Andreas Peterson 'Analysis, modeling and control of a DFIG for wind turbines' Doktorsavhandlingar vid Chalmers tekniska högskola Ny serie nr. 2282 ISSN 0346-718x ISBN 91-7291-600-1, 2005.
- [10] Ashish kumar aggarwal et'al 'study of wind turbine driven dfig using ac/dc/ac converter' thesis submitted on DFIG wind turbine.

EVALUATION OF DELAY FOR MULTI-RATE SIGNAL BY USING FARROW FILTER

Mousumi De¹, Biswajit Basak²

¹ M.Tech Scholar, Microwave & Communication Engineering,
MCKV Institute of Engineering, Howrah, (India)

² Assistant Professor, Dept of ECE, Hooghly Engineering & Technology College,
Hooghly, (India)

ABSTRACT

The discrete time systems process the data at more than one sampling rate is called multi-rate system. In this case the sampling rates of signals are unequal at various parts of the system. In all available communication channels achieving maximum signal transfer without any noise, the only frequency processor synchronized with the sampling rate. In this paper evaluate the differential delay of Farrow filters in different sampling frequencies.

I. INTRODUCTION

Multi-rate systems are used extensively in all areas of digital signal processing (DSP). Their function is to alter the rate of the discrete-time signals, by adding or deleting a portion of the signal samples. They are essential in various standard signal processing techniques such as signal analysis, de-noising, compression and so forth. During the last decade, however, they have increasingly found applications in new and emerging areas of signal processing, as well as in several neighboring disciplines such as digital communications.

One example is sampling rate conversion by arbitrary conversion factors where the traditional interpolators and decimators used for integer and rational-factor conversion fail or imply very high interpolation and decimation factors. An efficient structure

for adjustable FD filtering is the so called Farrow structure which makes use of a number of fixed FIR sub-filters and only one variable parameter.

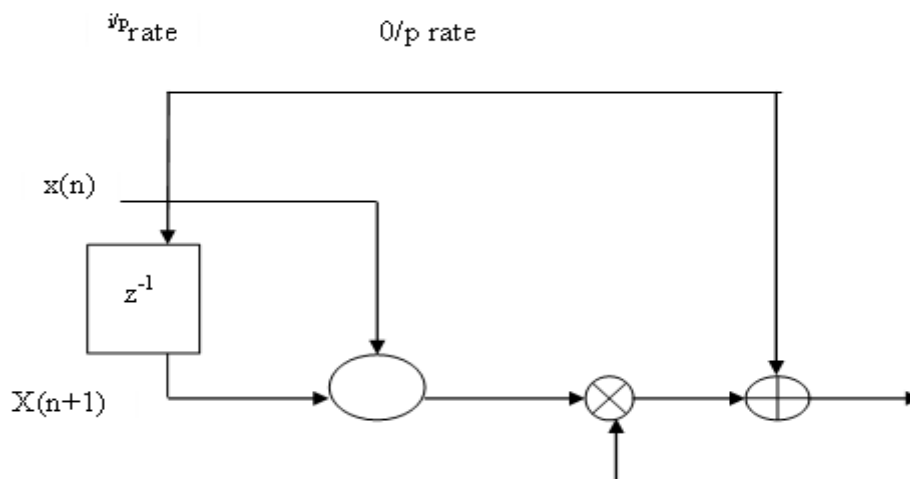


Diagram: Farrow Structure

The farrow filters is another class of digital filters which are used extensively in arbitrary sample rate conversions and fractionally delaying the samples. They have polyphase structure and are very efficient for digital filtering. Field-programmable gate array (FPGA) has become an extremely cost-effective means of off-loading computationally intensive digital signal processing algorithms to improve overall system performance.

In this paper the farrow filters are implemented for fractional delay and arbitrary change in sample rate conversion. This filters gives a better performance than the common filter structures in terms of speed of operation, cost, and power consumption in real-time. The proposed filter structures have wide applications in the designing of sample rate converters, analog to digital converter, decimators and interpolators.

II. FARROW FILTER AND DELAY

When the decimation factor $1/R$ or the interpolation factor R is an integral value, then the conversion of sampling rate can be performed conveniently with the aid of fixed digital filters (Farrow, 1998). In case of a scenario where the factors are irrational, it will be impossible to use fixed digital filters directly. Moreover, if R is considered as the ratio of two relatively large prime integers, then, in the case of the conventional poly-phase implementation, it is quiet essential that the orders of the required filter become very large (Oh et al., 1999). In nutshell, it means that a large number of coefficients need to be stored in coefficient memory. In sampling rate conversion by non-integer factor, it is required to determine the values between existing samples. In this case, it is very convenient to use interpolation filters. Among them, polynomial based filters are generally assumed to provide an efficient implementation form directly in digital domain. Such filters witness an effective implementation through Farrow structure or its higher version (Farrow, 1998; Hentschel and Fettweis, 2000). The main advantage of the Farrow structure is based on the presence of fixed finite-impulse response (FIR) filters as one of its ingredients. Thus, there is only one changeable parameter being the so-called fractional interval μ . Besides this, the control of μ is easier during the operation than in the corresponding coefficient memory implementations, and the concept of arithmetic preciseness; not the memory size limits the resolution of μ . These characteristics of the Farrow structure make it a very attractive structure to be implemented using a VLSI circuit or a signal processor (Vesma, 1999; Fettweis and Hentschel, 2000).

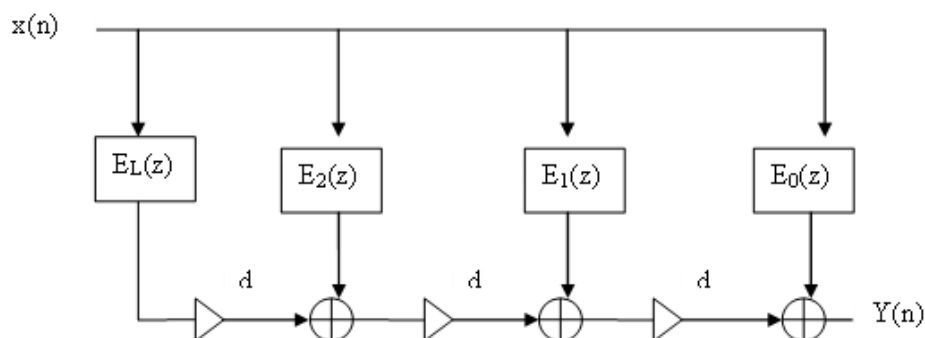


Diagram: Farrow Filter

The dashed line separates the filter into a section running at the input signal's sampling-rate and a section running at the output sampling-rate. Note that the output is re-labeled to be $y[m]$ rather than $y[n]$. This is due to different input and output rates. Notably, the fractional delay denoted as β_m will now change at every instant an output sample occurs. The first time an input is used, β_m will take on the value 0.3 and the output will be computed as

$$Y[m] = 0.5 (x [n-1] - x [n]) + x[n] = 0.5 x [n-1] + 0.5 x [n] \quad \dots(1)$$

Before the input sample changes, one more output sample will be computed. β_m will take the value 0 and the output will simply be

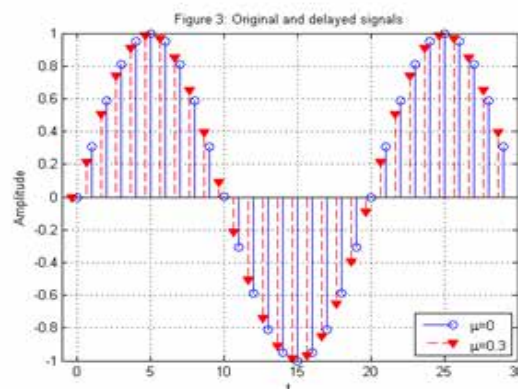
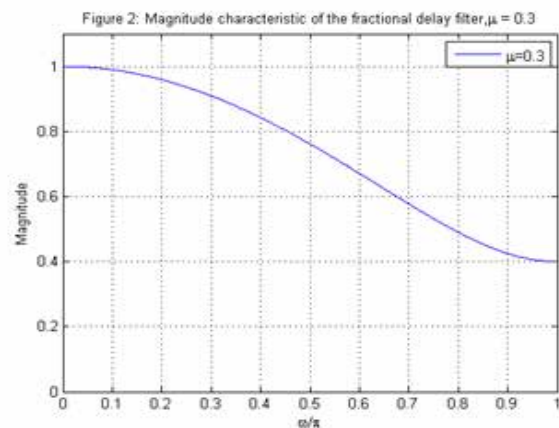
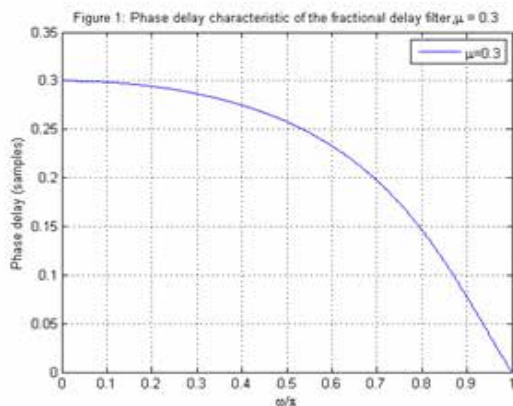
$$Y(m + 1) = x [n] \quad \dots(2)$$

Subsequently, the input sample will change; β_m will be once again set to 0.5 and so forth. In summary, when increasing the sampling rate by a factor of two, β_m will cycle between the values {0.5, 0} twice as fast as the input, producing an output each time it changes. In the general case, it is simply a matter of determining which values β must take. The formula is simply

$$\beta_m = (m f_s / f'_s) \bmod 1 \quad \dots(3)$$

Where f_s is the input sampling rate and f'_s is the output sampling rate. In order to perform a non integer SRC (sample rate conversion), Farrow structure or its modifications directly can be used. However, in many cases, it becomes more efficient to use cascaded structures engineered by the modification of the Farrow structure and fixed FIR, or multistage FIR filter (Babic et al., 2001, 2002, 2005; Meyer and Bease, 2007). The main advantage of using the cascaded structures instead of the direct modification of the Farrow structure lies in the fact that in case of joint optimization of the two building blocks the computational complexity to generate practically the same filtering performance is dramatically reduced. This is because of the following reasons. First, the implementation of a fixed linear phase FIR interpolator is not very costly, compared to the Farrow structure. Second, most importantly, the requirements for implementing the modification of the Farrow structure become significantly milder. This is mainly because the FIR filter takes care of pass-band and stop-band shaping, where the Farrow-based structure should only take care of attenuating images of FIR filter.

III. SIMULATION RESULTS



IV. DISCUSSION

A farrow filter is a filter of digital type having as main function to delay the processed input signal a fractional of the sampling period time. There are several applications where such signal delay value is required, examples of such systems are: timing adjustment in all-digital receivers (symbol synchronization), conversion between arbitrary sampling frequencies, echo cancellation, speech coding and synthesis, musical instruments modeling etc. In order to achieve the fractional delay filter function, two main frequency-domain specifications must be met by the filter. The filter magnitude frequency response must have an all-pass behavior in a wide frequency range, as well as its phase frequency response must be linear with a fixed fractional slope through the bandwidth.

In this paper consider the input and the output rates in the case of a fractional filter are identical. Just generate the first 30 samples of the signal $x[n] = \sin(0.1\pi n)$ and perform the fractional delay filtering for the delay factor $\mu = 0.3$. Plot the input sequence $\{x[n]\}$ and the delayed sequence $\{y[n]\}$. At first generate the delay signal from 0 to 0.3 and apply it over the sinc function with first 30 samples. Get the fig 1, fig2 and fig 3 respectively.

V. CONCLUSION

This paper has considered a multirate approach for fractional-delay filtering. According to the results one of the most challenging approaches for designing fractional delay filters is the use of frequency domain optimization methods. The use of MATLAB as a design and simulation platform is a very useful tool to achieve a fractional delay filter that meets best the required frequency specifications dictated by a particular application.

REFERENCES

- [1] Diaz-Carmona, J.; Jovanovic-Dolecek, G. & Ramirez-Agundis, A. (2010). Frequency-based optimization design for fractional delay FIR filters. *International Journal of Digital Multimedia Broadcasting*, Vol.2010, (January 2010), pp. 1-6, ISSN 1687-7578.
- [2] Erup, L.; Gardner, F. & Harris, F. (1993). Interpolation in digital modems-part II: implementation and performance. *IEEE Trans. on Communications*, Vol.41, (June 1993), pp. 998-1008.
- [3] Farrow, C. (1988). A continuously variable digital delay element, *Proceedings of IEEE Int.*
- [4] H. Johansson and P. Löwenborg, "Reconstruction of nonuniformly sampled bandlimited signals by means of digital fractional delay filters," *IEEE Trans. Signal Processing*, vol. 50, no. 11, pp. 2757–2767, Nov. 2002.
- [5] C. W. Farrow, "A continuously variable digital delay element," in *Proc. IEEE Int. Symp. Circuits Syst.*, Espoo, Finland, June 7–9, 1988, vol. 3, pp. 2641–2645.
- [6] J. Vesma and T. Saramäki, "Optimization and efficient implementation of FIR filters with adjustable fractional delay," in *Proc. IEEE Int. Symp. Circuits Syst.*, Hong Kong, June 9–12, 1997, vol. IV, pp. 2256–2259.
- [7] Delay calculation of farrow filter in multirate filter Evaluation of delay for multirate signal by using farrow filter.

DESIGN AND IMPLEMENTATION OF MICROCONTROLLER BASED TECHNOLOGY FOR AUTOMATIC CONTROL OF BRAKING SYSTEM IN VEHICLES

H Prakash¹, Rashmi H K²

¹Assistant Professor, Department of Mechanical Engineering,
JSSATE, Bangalore, VTU, Belgaum, (India)

²Assistant Professor, Department of Electronics and Communication Engineering,
PNSIT, Bangalore, VTU, Belgaum, (India)

ABSTRACT

Most of the accidents in four wheeled vehicles occur because of failure of breaking systems. Manual method of applying breaks is always dangerous as it leads to accidents. Unconsciousness of driver, failure in the linkages of breaking systems, road conditions, uncontrollable speed of the vehicle and manual operation of breaking systems are the reasons of accidents. It is necessary to control breaks automatically through electronics devices to minimize the accident problems. In this research paper we propose an effective methodology for automatic control of breaking system to avoid accidents. In this technology we used micro controller, relays, IR transmitter, IR receiver and embedded C for effective function of breaking control system. This complete system can be fitted on to dashboard of a vehicle and effectively used for automatic control of braking system. In this research we implemented this technology for prototype model and experimentation is carried out. Based on the experimentation we can make a conclusion of using this technology for real time implementation.

Keywords: *Embedded C, Hydraulic brake system, IR receiver, IR transmitter, Microcontroller,*

I. INTRODUCTION

With the current fast development in information technology, there has been a tremendous increase in the number of cars. Cars have become a major tool of transportation in the current society. Car safety system becomes important as traffic density is increasing every day. Because it is always difficult to apply brake in such traffic density it is required to design and implement an effective technology which automatically controls the braking system of car to provide safety to the vehicle. There are three kinds of systems for automatic control of braking system namely ultrasonic system, radar system and infra red system. Ultrasonic systems are widely used in many applications, whose strength lies in its wide range of detection and anti-interference. Moreover, the original material is cheap and production cost is low, making its price more widely acceptable. Its weakness lies in the valid radius of detection that is rather limited and in its accuracy in obstacle detection that is the lowest among the three. Ultrasonic systems are generally used in middle and low-end cars. The radar system is difficult to use in cars as it is not cost effective. Here we used infrared based technology to implement our research as the infrared system can have long-distance detection and accuracy outshining that of ultrasonic and cost effective

II. LITERATURE REVIEW

Honda company developed idea of using ABS (Anti lock braking system) to control the car speed. But ABS has its own braking distance and it avoids the collisions only when driver applies brake at right time. Volvo introduced XC60SUV technology for intelligent braking control. This technology has capability to sense and avoids collision only when the vehicle speed is below 50 KMPH. Volvo's laser assisted braking system could not work in rainfall and snowfall. William K. Lennon and Kevin M. Passino, discussed about fuzzy model reference learning controller, genetic model reference adaptive controller and general genetic adaptive controller in their research. Cirovic, Velimir, Aleksendric, and Dragan discussed about their model predictive control (MPC) based braking system. Here we presented an idea of designing and implementation of microcontroller based technology for automatic control of braking system to avoid accidents.

III. WORKING OF BRAKE SYSTEM

Fig 3.1 shows principle of working of a typical hydraulic braking system. In a hydraulic brake system, when the brake pedal is pressed, a pushrod exerts force on the piston(s) in the master cylinder, causing fluid from the brake fluid reservoir to flow into a pressure chamber through a compensating port. This results in an increase in the pressure of the entire hydraulic system, forcing fluid through the hydraulic lines toward one or more calipers where it acts upon one or two caliper pistons sealed by one or more seated O-rings (which prevent leakage of the fluid). The brake caliper pistons then apply force to the brake pads, pushing them against the spinning rotor, and the friction between the pads and the rotor causes a braking torque to be generated, slowing the vehicle. Heat generated by this friction is either dissipated through vents and channels in the rotor or is conducted through the pads, which are made of specialized heat-tolerant materials such as Kevlar or sintered glass. Subsequent release of the brake pedal/lever allows the spring(s) in the master cylinder assembly to return the master piston(s) back into position. This action first relieves the hydraulic pressure on the caliper and then applies suction to the brake piston in the caliper assembly, moving it back into its housing and allowing the brake pads to release the rotor. Fig. 3.2 describes the different components of a car braking system.

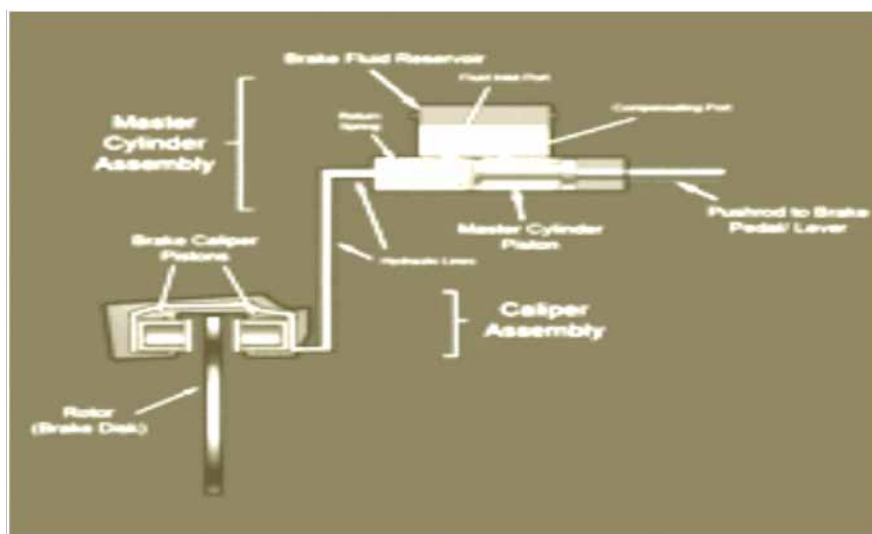


Fig. 3.1: Working Principle of Hydraulic Braking System

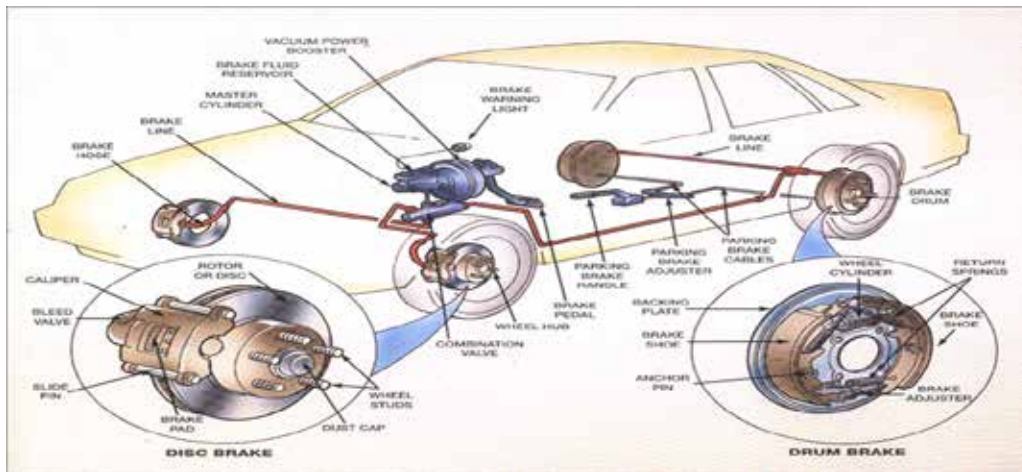


Fig. 3.2: Components of Braking System in a Car

IV.WORKING OF MICROCONTROLLER BASED AUTOMATIC BRAKING SYSTEM (MBABS)

Fig 4.1 shows the block diagram of working principle of proposed research. Microcontroller is the heart of the system. Here we used 8051 based P89V51RD2 microcontroller. The IR transmitter circuit transmits the Infra-Red rays continuously and if any obstacle like other vehicle, human being are detected then IR transmitter circuit produce the reflected rays. These reflected rays are received by IR receiver and these are compared with the comparator circuit and suitable signal will be given to microcontroller. Based on the input signal microcontroller will generate suitable control signal. This signal will be received by relay to control the motor. Motor is connected to brake pedal the car and actuates it to control the speed of the car. If there is no obstacle then motor will bring the vehicle speed to normal. In this research we implemented this technology for prototype model and experimentation is carried out. Based on the experimentation we can make a conclusion of using this technology for real time implementation.

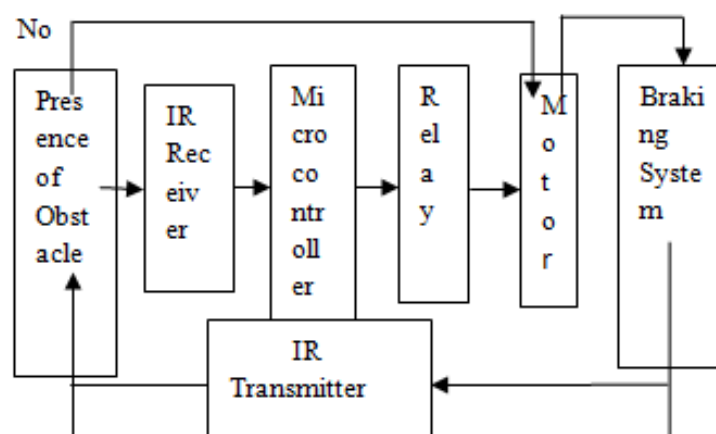


Fig 4.1: Working principle of Microcontroller based Automatic braking system

V. DESIGN AND DEVELOPMENT

5.1 Microcontroller

The main centre part of the project is the microcontroller. Here we used the 8051 based Philips P89V51RD2 microcontroller. The P89V51RD2 are 80C51 microcontrollers with 64kB flash and 1024 B of data RAM. A key feature of the P89V51RD2 is its X2 mode option. The design engineer can choose to run the application with the conventional 80C51 clock rate (12 clocks per machine cycle) or select the X2 mode (six clocks per machine cycle) to achieve twice the throughput at the same clock frequency.

5.1.1 Features of Microcontroller

80C51 CPU with 5V operating voltage from 0 to 40 MHz, 64 KB of on-chip flash user code memory with ISP and IA, SPI and enhanced UART, Four 8-bit I/O ports with three high-current port 1 pin, Three 16-bit timers/counters, Programmable watchdog timer, Eight interrupt sources with four priority levels, Second DPTR register, Low EMI mode (ALE inhibit), TTL- and CMOS-compatible logic levels, Brownout detection, Low power modes, Power-down mode with external interrupt wake-up, Idle mode

5.1.2 Block Diagram of Microcontroller

Block diagram of microcontroller used in our research is shown in fig 3.1.1

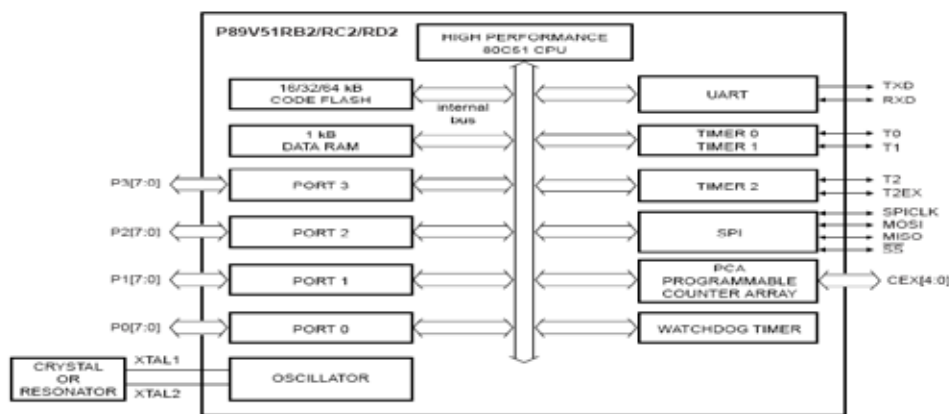


Fig 5.1.1: Block Diagram of Microcontroller

5.1.3 PIN diagram of P89V51RD2 microcontroller

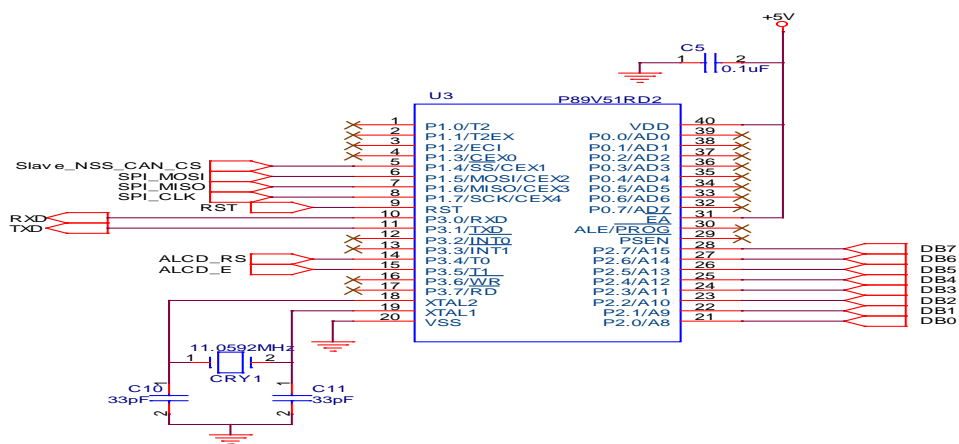


Fig 5.1.2: PIN diagram of P89V51RD2

PIN diagram of P89V51RD2 Microcontroller is shown in the fig 3.1.2

5.2 Piezoelectric Sensor

A piezoelectric sensor is a device that uses the piezoelectric cause to measures the load, hastening, strain or force. And it converts them to an electrical signal.

5.3 Relay

A relay is an electrical switch that uses an electromagnet to move the switch from the off to on position instead of a person moving the switch. It takes a relatively small amount of power to turn on a relay but the relay can control something that draws much more power. Ex: A relay is used to control the air conditioner in your home. The AC unit probably runs off of 220VAC at around 30A. That's 6600 Watts! The coil that controls the relay may only need a few watts to pull the contacts together.

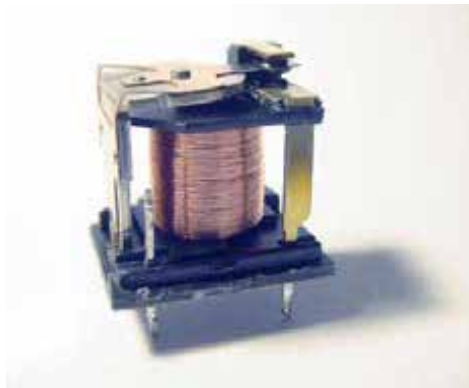


Fig 5.3: Relay

Fig 5.3 shows the schematic representation of a relay. The contacts at the top are normally open (i.e. not connected). When current is passed through the coil it creates a magnetic field that pulls the switch closed (i.e. connects the top contacts). Usually a spring will pull the switch open again once the power is removed from the coil

5.4 IR Transmitter and Receiver

To monitor the density of the traffic, we used a few sets of IR transmitter and receiver sensors on the sides of the roads. One side IR transmitter will be placed and right opposite to the IR transmitter, an IR receiver will be kept. This set of IR transmitter and receiver will be kept on roads at different intervals. The IR transmitters are connected to supply, so that they will transmit high signal all the time. The IR receivers are connected to the comparator circuit, to get digital signals. A low power operational amplifier LM324 IC has been used to develop a comparator circuit. Two set of LM324 IC has been used in this project. The circuit diagram of the comparator is shown in fig 3.4.

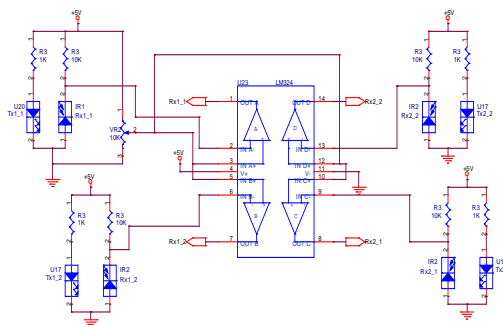


Fig 5.4 Comparator Circuit

of the C programming language and standard libraries are altered or enhanced to address the peculiarities of an embedded target processor.

VI. IMPLEMENTATION OF RESEARCH

6.1. Circuit Diagram

We prepared prototype model of vehicle braking system along with controller to implement our technology. Fig 6.1 shows the overall circuit diagram of the microcontroller based automatic braking system. Based on the circuit diagram we assembled the components to experiment our technology. Fig 6.2 shows complete hardware set up of the research.

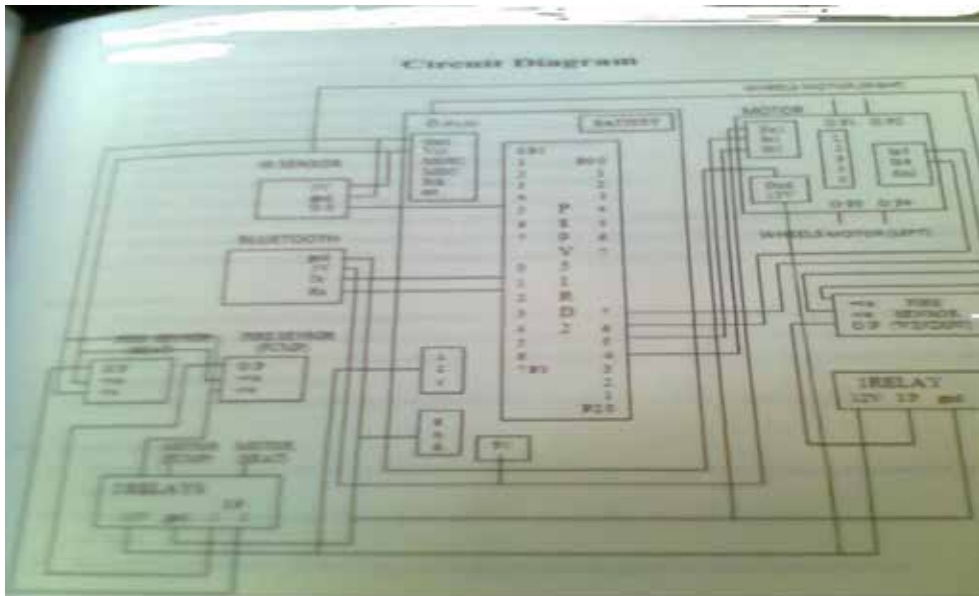


Fig: 6.1 Overall Circuit Diagram Of The Microcontroller Based Automatic Braking System.

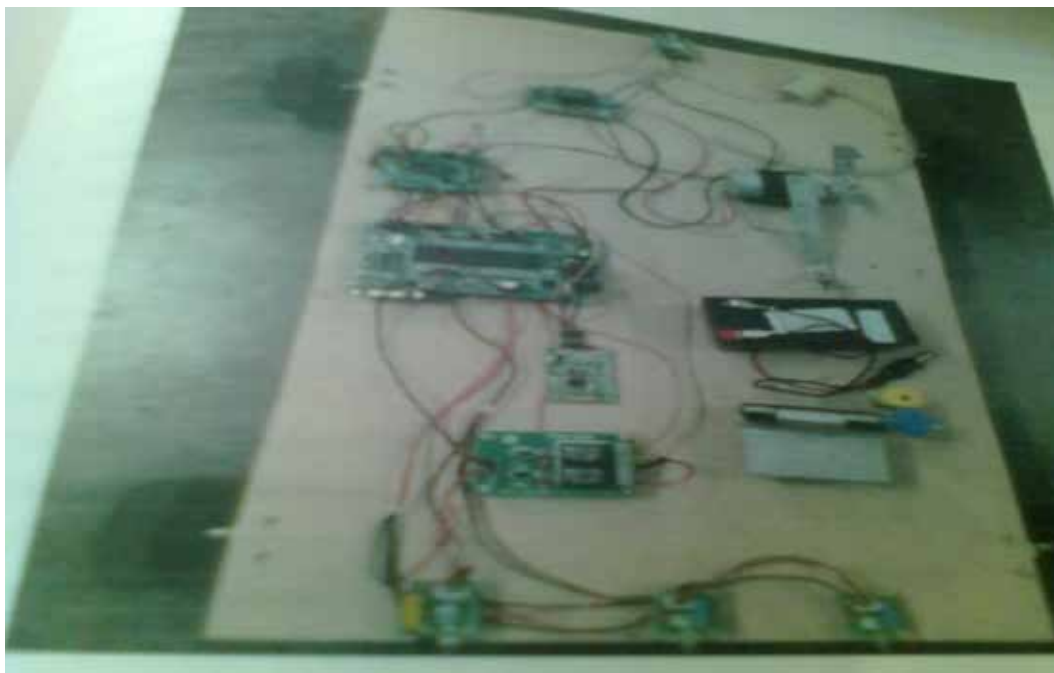


Fig 6.2 Hardware Set Up Of the Research

VII. EXPERIMENTATION AND RESULT

We conducted many experiments to test our technology. We used android based mobile phone to control the vehicle movements. By swiping the screen of mobile phone we tried to control all the movements of the car model and whenever vehicle senses an obstacle automatic application of brake is achieved. The result obtained is satisfactory. Same technology can be incorporated for real time system.

VIII. CONCLUSION AND FUTURE SCOPE

Based on the series of experimentation and the results obtained which are satisfactory we can conclude that the microcontroller based technology can be used for automatic application of brakes in car. It avoids accidents by intelligently identifying the obstacles. Proximity of this technology for sensing obstacle and application of brake is 15 inches. This may be difficult in case of real implementation. This can be set up with advanced sensors to sense the obstacles in for distance so that smooth application of brake can be achieved.

BIBLIOGRAPHY

- [1] Automobile Engineering Vol 1and Vol 2, Kripal Singh, Standard publishers, 2011
- [2] Adaptive control, second edition, Karl J Astrom and Bjorn Wittnmark, Dover publishers, NY, 2008

RELIABILITY CENTERED MAINTENANCE MODELLING ON POWER SYSTEMS

Ahmed Tijjani Dahiru

*Department of Electrical/Electronics Technology, School of Technical Education
Federal College of Education, Bichi, Kano, Nigeria*

ABSTRACT

Sound maintenance management in power systems could be influenced by application of appropriate reliability modelling. The aggressive approach needed to retract the power sector in Nigeria should include expansion, upgrading and automation in the national grid system. This is necessary in view of current generation and transmission capacities as well as operational parameters in distribution systems obtained within the national grid. The changes needed in the context of Nigeria's power system, should as well be supported by proper maintenance management. This paper therefore explore the deplorable conditions upon which Nigeria's power system operates. It also review various risk and reliability assessment tools and their effects on various fields of technological development. The paper henceforth proposes the modelling of Reliability Centred Maintenance (RCM), as an appropriate tool for reliability enhancement. The RCM approach is chosen for its advantages in reduced frequency of maintenance which could eventually reduce running cost and quick wear. The modelling is also seen to be a step towards realizing an automated control and protection as well as self healing.

Keywords: Cost Benefits, Energy, Maintenance, Modelling, Power Grid, Reliability Enhancement.

I. INTRODUCTION

Like many countries south of the Sahara, management of power sector in Nigeria has not been efficient enough to maintain sufficient supply of electricity to consumers. The insufficient supply to some extent is attributed to issues such as, government's direct and 100% involvement in power investments, which could have had influences on employments, contracts and other services etc.

Government's direct involvement however could not have been the only problem in this regard, as new techniques in procurements, maintenance etc., were not employed in maintenance management. Right now Nigeria is battling to bring revolutions in electrical power sector through privatization of all its companies holding stakes. When that is achieved, a well trained personnel and methods must be in place to turn things around. Thus there should be an upgraded style in running the affairs of maintenance programmes.

To be in tune with the global style in the management of maintenance especially in power systems, studies need to be carried out by analyzing system failures using tools such as Failure Modes Effect Analysis (FMEA), Failure Mode Effect and Criticality Analysis (FMECA), Fault Tree Analysis (FTA), Ishikawa Diagrams etc., thereby arriving at solutions using Reliability Centered Maintenance (RCM).

II. AN OVERVIEW OF RELIABILITY AND RISK ASSESSMENT TOOLS

Failures recorded on military hardware such as aircrafts, weaponry, during events of Korean, Vietnam wars etc. Automobiles used before, during and after the Second World War. Then cars were increasingly used widely for private purposes. And of recent calamities on space crafts such as Columbia were few among events that motivated aggressive revolution in reliability engineering.

Much of the failures recorded on larger systems such an aircraft were simply traced to remote failures on parts such as joints, components of a particular sub-system etc. For the whole system to be brought to full working condition, the maintenance action of sub-systems, parts or components, which may cost much in terms of time and resources, a trend not friendly for safety of personnel and consumers and for economy of investments and patronage.

Measures taken to develop and implement changes in the system of maintenance for reliability enhancements and risk reduction include [5][6][7];

- (i) *Fish Bone (Ishikawa) Diagram*: This is a technique developed by Kaoru Ishikawa in 1990 to improve process of tracing of faults in a system, such as machines or part(s), production processes, and also applied to industrial personnel managements etc.
- (ii) *Fault Tree Analysis*: This is a bottom-up approach of a systems' failure analysis.
- (iii) *Failure Mode Effect Analysis (FMEA)*: An analysis of failure likely to occur within a system that takes top-bottom approach.
- (iv) *Failure Mode Effect and Criticality Analysis (FMECA)*: A further analysis to FMEA, which prioritize failures as regard their severities for effective maintenance action (for systems on active use) or design modifications (for systems on drawing boards) for the purpose of risk reduction and mitigations.

The techniques of risk assessment or risk assessment tools mentioned above are few examples developed to improve system reliability. The unique difference or features of Reliability Centered Maintenance, RCM (not mentioned above) is that it is focused on reduction of not failures or faults alone, but the frequency of maintenance itself, whereas most of the tools among which the above stated belong emphasize on somehow application of regular maintenance. This is particularly important in reducing the maintenance cost, which is part of running cost of all investments.

Per capita energy consumption of every nation portrays its economic strength to large extent. Nigeria's per capita energy consumption barely 140 kw-h was far below the global average [1]. The major problem with energy crises in Nigeria is rooted the system of power generation. While the installed capacities of the individual generating stations were grossly inadequate when converged together on grid system for a population roughly half that of the United States, the 4500MW (installed capacity) is incredibly one out of nearly two hundred and sixtieth of the U.S installed capacity [15][19]. Moreover, performances of the power stations are much below the installed capacities as stressed by Iwayemi [3] that less than 40% on average was realized within the period of 35 years (1970 – 2005).



Fig. 1. Typical Unhealthy Distributed Generation Common to Nigeria's Consumer Points

The somehow poor performances of the power generating plants in Nigeria based on their installed capacities may be attributed to all or one of the following two factors;

- (i) The capacities of the transmission stations with a total capacity of 4000MW [2] which could not support the full capacity utilization and further expansion of the generating capacities.
- (ii) The outdated system of maintenance management, procurements and poor quality assurance being applied at all the stages of power systems, namely generation, transmission and distribution.

The generation system in Nigeria has suffered neglect in terms of upgrading for many years. This is among the primary factors contributing to the deterioration of the system. Other problems are basically operational, which include shortages of water in the reservoirs in hydro systems and shortage of gas supplies to the turbines of the thermal stations due to vandalism and other socio-economic factors in the Niger-Delta region and the problem of oil and gas sectors. Thus there may be multi-faceted approaches, which issues of safety and maintainability is the subject within this context.

Table 1 Summary of Thermal Station's Installed Capacities in Nigeria. [2]

Country's Thermal Plant	Total Thermal Units	Total Thermal Installed Capacity (MW)	Total Thermal Available Units
11	93	5976	44

Table 2 Summary of Hydro Station's Installed Capacities in Nigeria [2]

Country's Hydro Plant	Total Hydro Units	Total Hydro Installed Capacity (MW)	Total Hydro Available Units
3	111	7876	58

Conventionally transmission stages are central to in power systems. The bulk of electricity generated are transported to the load centers using transmission facilities such as power transformers, high voltage switch gears and circuit breakers, insulators, cable and harnesses supported by high rising towers. It is very common scene, buildings being erected under very high voltage Nigerian transmission lines. Other factors may include the use of obsolete equipments and continued implementation of outdated maintenance practices. While the existing equipments cannot support modern maintenance techniques, the evolving maintenance management system must be supported using modern equipments.

The distribution system is the most troubled portion of power system in Nigeria. It is common to have consumer units with insufficient protection such as cut-out fuses, proper earthing, ELCBs etc. Many consumers are found looping through other consumers in cascades to avoid tariffs, as the existing tariff is sub-standard and outdated. The system is also plagued by the use of wrong size equipments and other materials such as cables, insulators etc.

Individual performance of the three sectors of power system mentioned earlier resulted in frequent load shedding and total power outages which could be linked directly to the implication of the low per capita energy consumption recorded and mentioned earlier.



Fig. 2 Typical Maintenance Handling At Nigeria's Distribution Networks

III. THE RCM APPROACH TO IMPROVED MAINTENANCE

Now that the power sector is undergoing series of aggressive reforms through privatization and commercialization, and National Independent Power Project (NIPP) schemes, it is expected that reliability, safety and efficiency in Nigeria's power industry could be enhanced through a well developed and implemented Reliability Centered Maintenance (RCM) for the improvement of per capita energy consumption and the gross domestic product, GDP. Thus, the aim can be achieved according to the following detailed objectives;

- Analyzing types of failures occurring in the generation, transmission and distribution systems of electricity in Nigeria as a case study.
- Explore various methods of failure analysis and risks assessment techniques and the suitability of the reliability centered maintenance on the case study.

- Develop a model for maintenance management structure according to Reliability Centered Maintenance (RCM) techniques on the case study.

The Nigerian power grid as described previously, by convention operates in stages namely generation, transmission and distribution. Failures recorded were as a result of lapses from all the stages mentioned. Thus development and implementation of RCM should be on all the stages. This could effectively be achieved by sampling units making up the grid system, generating station, transmission sub-station, distribution sub-station, Control Centre, etc. The modelling and implementations could be in phases or stages by which an illustrative diagram of the initial phase is shown in fig. 1.

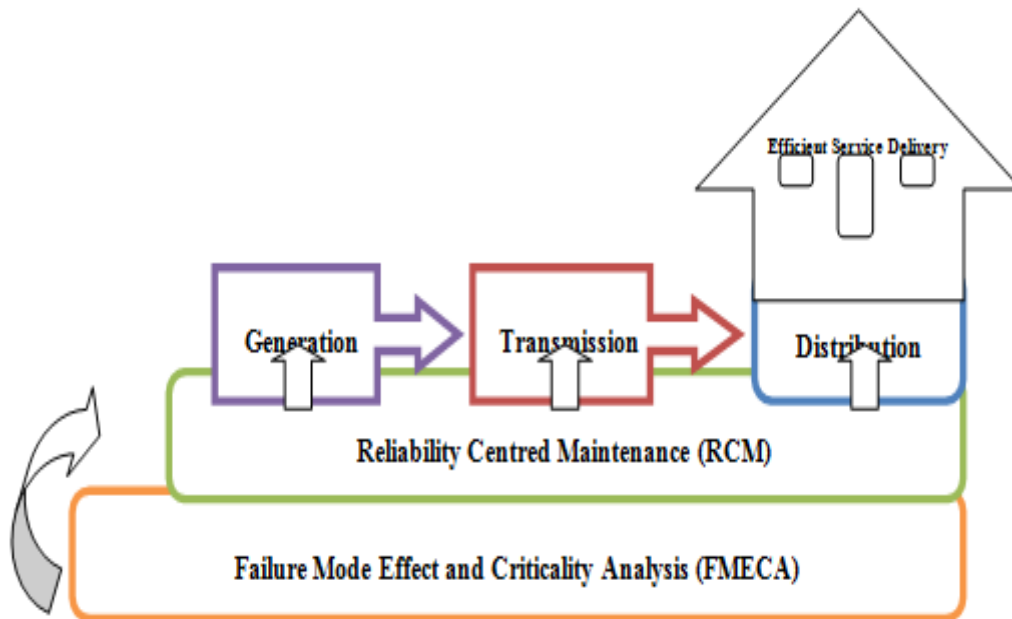


Fig.3 Initial Stage of RCM Modelling On Grid System

The performance of FMECA is known to precede RCM, which is a good reason for inclusion of FMECA in the process even though it can importantly be standalone. In the process therefore it is expected that FMECA would effectively support RCM. The RCM modelling over a grid system ensures efficiency and quality of service to the consumers.

IV. CONCLUSIONS

As obtained in industries of developed societies such as aviation, space missions, defense, maritime, manufacturing etc., where safety and investment securities are priorities, risks due to failures are well mitigated over the years of evolutions of reliability engineering. It is opined that frequency of maintenance practices somehow reduce the useful life span of an item, thus comparing to human anatomy, the more human body experiences surgeries, the weaker the part or the entire body becomes. This implies RCM modelling proposed in this paper could be centered around reduction in number of failures occurring in power systems and their frequencies which contribute to the acceleration of wear and tear of equipments and parts of the system. It is also expected that the developed technique will tremendously reduce the costs involved in traditional maintenance practices. Other benefits to be derived include improvement of productivity through reduction in downtime and a drive towards system automation. These achievements are made possible despite major challenges such as the size of the power grid and laborious nature of FMECA.

REFERENCES

- [1] United nations Statistics Division, (2010). *Gross Domestic Product Per Capita*. [Online]. Available: <http://www.un.org/Dept/unsd>. [Accessed: 9 Mar 2012].
- [2] Sambo, A.S. et al. “*Electricity Generation and the present challenges in the Nigeria Power Sector*”. Presented at the world energy conference, 2010. [Online]. Available: <http://www.worldenergy.org/congresspapers/70.pdf>. [Accessed: 08 Mar 2012].
- [3] Iwayemi, A. “*Nigerian Dual Energy Problems*” Presented at the 31st IAEE International Conference. IAEE.Istanbul, 2008. [Online]. Available: <http://www.ieaa.org/en/publications/proceedings.aspx>. [Accessed: 19 Feb 2012].
- [4] Dhillon, B.S. *A Modern Engineering Maintenance Approach*, 1st ed. Boca Raton: CRC Press LLC, 2002.
- [5] Andrews, J.D. and Moss, T.R., *Reliability and Risk Assessment*, 2nd ed. London: Professional Engineering Publishing Limited, 2002.
- [6] Smith, D.J., *Reliability Maintainability and Risk: Practical Methods for Engineers*, 5th ed. Oxford: Butterworth-Heinemann, 1997.
- [7] Kumamoto, H. and Henley, E.J., *Probabilistic Risk Assessment and Management for Engineers and Scientists*, 5th ed. New York: IEEE Press, 1996.
- [8] Henley, E.J. and Kumamoto, H., *Probabilistic Risk Assessment: Reliability Engineering, Design and Analysis*, 1st ed. New York: IEEE Press, 1992.
- [9] The United States Department of Defense Handbook. *Designing and Developing Maintainable Products and Systems*. Vol I (1997, Aug 4). [Online]. Available: http://www.barringer1.com/mil_files/MIL-HDBK-470A.pdf. [Accessed: 06 Jun 2012]
- [10] Department of Army Headquarters, Washington DC. Technical Manual (2006, 22 Jul). *Survey for Reliability and Availability Information for Power Distribution, Power Generation, And Heating and Ventilating and Air Conditioning (HVAC) Components for Commercial, Industrial And Utility Installation*. [Online] Available: http://www.barringer1.com/mil_files/TM-5-698-5.pdf [Accessed: 06 Jun 2012]
- [11] The United States Department of Defense, *Military Standard: Procedure for Performing a Failure Mode Effect and Criticality Analysis*. (1980, Nov 2). [Online]. Available: <http://www.sre.org/Pubs/Mil-Std-1629A.pdf> [Accessed: 31 Aug 2012]
- [12] Fahimi, A. B., Kawasinski, A., Davoudi, A., Balog, R. S. and Kilani, M., (2012, Mar). *Charge It: Power the More Electrified Planet*. *IEEE Power and Energy Magazine*. [Online]. Available: <http://www.ieee-pes.org/images/pdf/2012-pe-smart-grid-compendium.pdf>. [Accessed: 3 Feb. 2013].
- [13] Schulz R.W., “Maintenance Contribution to Customer Satisfaction in Electrical Power Generation,” MSc thesis, School of Engineering Design and Technology, University of Bradford, Bradford, 2005.
- [14] The US Department of Labor Occupational Safety & Health Administration, eTool: Electrical Power, (2012, March). *Underground Distribution Substation*. [Online]. Available: http://www.osha.gov/SLTC/etools/electric_power. [Accessed: 23 May 2012].
- [15] U.S. and World Population Clock (2010). [Online]. Available: <http://www.census.gov/popclock/>. [Accessed: 02 Jan 2014].
- [16] Garza, L.” A Case Study Of The Application Of Reliability Centered Maintenance (RCM) In The Acquisition Of The Advanced Amphibious Assault Vehicle (AAAV)”. M.S Thesis, Naval Postgraduate School Monterey, California, 2002. [Online]. Available: <http://www.dtic.mil/dtic/tr/fulltext/u2/a411338.pdf>. [Accessed: 09 Jan 2014].

- [17] Afefy, I. H. (Oct, 2010). Reliability-Centered Maintenance Methodology and Application: A Case Study. Scientific Research. [Online]. Available: http://file.scirp.org/Html/3_8101205_3165.htm. [Accessed: 09 Jan 2014].
- [18] Martinez, J. "Application Of Reliability-Centered Maintenance in Facility Management" M.S Thesis, Worcester Polytechnic Institute, 2007. [Online]. Available: http://www.wpi.edu/Pubs/ETD/Available/etd-120606-132430/unrestricted/job_3074-Microsoft_Word_-_RCM_in_Facility_Management.pdf. [Accessed: 09 Jan 2014].
- [19] US Energy Information Administration: Independent Statistics and Analysis, (2013 Dec). *Electric Power Generating Capacities*. [Online]. Available: <http://www.eia.gov/electricity/data.cfm#gencapacity>. [Accessed: 11 Jan 2014].

REMOVAL OF SALT AND PEPPER NOISE THROUGH UNSYMMETRIC TRIMMED MEDIAN FILTER

R. R. Kadam¹, Prof. M. S. Biradar²

^{1,2}*Department of Electronics & Telecommunication,*

CAYMET Siddhant College of Engineering, Pune University, Pune, (India)

ABSTRACT

Here a modified decision based unsymmetrical trimmed median filter algorithm for the restoration of gray scale, and colour images that are highly corrupted by salt and pepper noise is proposed. This algorithm replaces the noisy pixel by trimmed median value when other pixel values, 0's and 255's are present in the selected window and when all the pixel values are 0's and 255's then the noise pixel is replaced by mean value of all the elements present in the selected window. This proposed algorithm shows better results than the Standard Median Filter (MF), Decision Based Algorithm (DBA), Modified Decision Based Algorithm (MDBA), and Progressive Switched Median Filter (PSMF). The proposed algorithm is tested against different gray scale and colour images and it gives better Peak Signal-to-Noise Ratio (PSNR) and Image Enhancement Factor (IEF).

Index Terms: Median Filter, Salt and Pepper Noise, Unsymmetrical Trimmed Median Filter

I. INTRODUCTION

Bit errors in transmission or introduced during the signal acquisition causes impulse noise in images. There are two types of impulse noise, they are salt and pepper noise and random valued noise. Salt and pepper noise can corrupt the images where the corrupted pixel takes either maximum or minimum gray level. Several nonlinear filters have been proposed for restoration of images contaminated by salt and pepper noise. Among these standard median filter has been established as reliable method to remove the salt and pepper noise without damaging the edge details. However, the major drawback of standard Median Filter (MF) is that the filter is effective only at low noise densities [1]. When the noise level is over 50% the edge details of the original image will not be preserved by standard median filter. Adaptive Median Filter (AMF) [2] performs well at low noise densities. But at high noise densities the window size has to be increased which may lead to blurring the image. In switching median filter [3], [4] the decision is based on a pre-defined threshold value. The major drawback of this method is that defining a robust decision is difficult. Also these filters will not take into account the local features as a result of which details and edges may not be recovered satisfactorily, especially when the noise level is high. To overcome the above drawback, Decision Based Algorithm (DBA) is proposed [5]. In this, image is de noised by using a 3×3 window. If the processing pixel value is 0 or 255 it is pro-cessed or else it is left unchanged. At high noise density the median value will be 0 or 255 which is noisy. In such case, neighboring pixel is used for replacement. This repeated replacement of neighbouring pixel produces streaking effect

[6]. In order to avoid this drawback, Decision Based Unsymmetric Trimmed Median Filter (DBUTMF) is proposed [7]. At high noise densities, if the selected window contains all 0's or 255's or both then, trimmed median value cannot be obtained. So this algorithm does not give better results at very high noise density that is at 80% to 90%. The proposed Modified Decision Based Un-symmetric Trimmed Median Filter (MDBUTMF) algorithm re-moves this drawback at high noise density and gives better Peak Signal-to-Noise Ratio (PSNR) and Image Enhancement Factor (IEF) values than the existing algorithm. The rest of the paper is structured as follows. A brief introduction of unsymmetrical trimmed median filter is given in Section II. Section III describes about the proposed algorithm and different cases of proposed algorithm. The detailed description of the proposed algorithm with an example is presented in Section IV. Simulation results with different images are presented in Section V. Finally conclusions are drawn in Section VI.

II. PROPOSED ALGORITHM

The proposed Modified Decision Based Unsymmetric Trimmed Median Filter (MDBUTMF) algorithm processes the corrupted images by first detecting the impulse noise. The processing pixel is checked whether it is noisy or noisy free. That is, if the processing pixel lies between maximum and minimum gray level values then it is noise free pixel, it is left unchanged. If the processing pixel takes the maximum or minimum gray level then it is noisy pixel which is processed by MDBUTMF. The steps of the MDBUTMF are elucidated as follows.

Step 1: Select 2-D window of size 3×3 . Assume that the pixel being processed is.

Step 2: If then is an uncorrupted pixel and its value is left unchanged.

Step 3: If or then is a corrupted pixel then two cases are possible as given in Case i) and ii).

Case i): If the selected window contains all the elements as 0's and 255's. Then replace with the mean of the element of window.

Case ii): If the selected window contains not all elements as 0's and 255's. Then eliminate 255's and 0's and find the median value of the remaining elements. Replace with the median value.

Step 4: Repeat steps 1 to 3 until all the pixels in the entire image are processed. The pictorial representation of each case of the proposed algorithm is shown in Fig. 1.

The detailed description of each case of the flow chart shown in Fig.1.

III. ILLUSTRATION OF MDBUTMF ALGORITHM

Each and every pixel of the image is checked for the presence of salt and pepper noise. Different cases are illustrated in this Section. If the processing pixel is noisy and all other pixel values are either 0's or 255's is illustrated in Case i). If the processing pixel is noisy pixel that is 0 or 255 is illustrated in Case ii). If the processing pixel is not noisy pixel and its value lies between 0 and 255 is illustrated in Case iii). Case i): If the selected window contains salt/pepper noise as processing pixel (i.e., 255/0 pixel value) and neighbouring pixel values contains all pixels that adds salt and pepper noise to the image:

$$\begin{bmatrix} 0 & 255 & 0 \\ 0 & \langle 255 \rangle & 255 \\ 255 & 0 & 255 \end{bmatrix}$$

where "255" is processing pixel, i.e., (P_{ij}) .

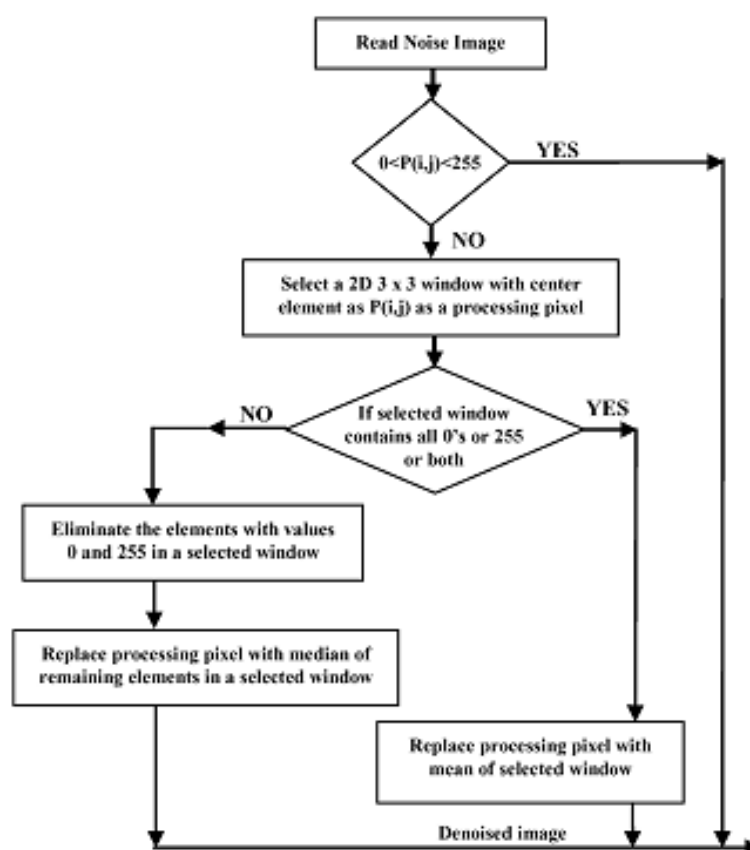


Fig. 1. Flow chart of MDBUTMF.

Since all the elements surrounding are 0's and 255's. If one takes the median value it will be either 0 or 255 which is again noisy. To solve this problem, the mean of the selected window is found and the processing pixel is replaced by the mean value. Here the mean value is 170. Replace the processing pixel by 170. Case ii): If the selected window contains salt or pepper noise as processing pixel (i.e., 255/0 pixel value) and neighbouring pixel values contains some pixels that adds salt i.e., 255 pixel value) and pepper noise to the image:

$$\begin{bmatrix} 78 & 90 & 0 \\ 120 & \langle 0 \rangle & 255 \\ 97 & 255 & 73 \end{bmatrix}$$

where "0" is processing pixel, i.e., $P(i, j)$.

Now eliminate the salt and pepper noise from the selected window. That is, elimination of 0's and 255's. The 1-D array of the above matrix is [78 90 0 120 0 255 97 255 73]. After elimination of 0's and 255's the pixel values in the selected window will be [78 90 120 97 73]. Here the median value is 90. Hence replace the processing pixel by 90.

Case iii): If the selected window contains a noise free pixel as a processing pixel, it does not require further processing. For example, if the processing pixel is 90 then it is noise free pixel:

$$\begin{bmatrix} 43 & 67 & 70 \\ 55 & \langle 90 \rangle & 79 \\ 85 & 81 & 66 \end{bmatrix}$$

where "90" is processing pixel, i.e., $P(i, j)$.

Since “90” is a noise free pixel it does not require further processing.

IV. RESULT

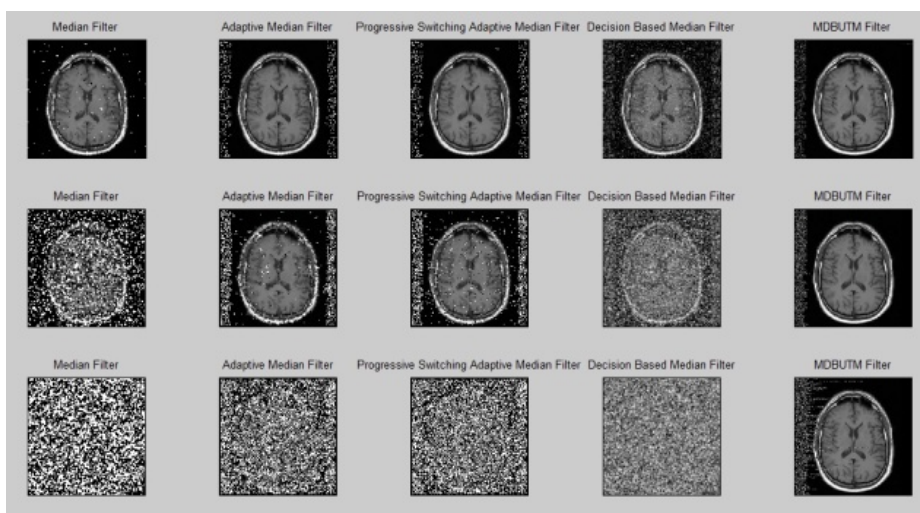


Fig: Results of different algorithms for image corrupted by 30%, 60% and 90% noise densities, respectively.

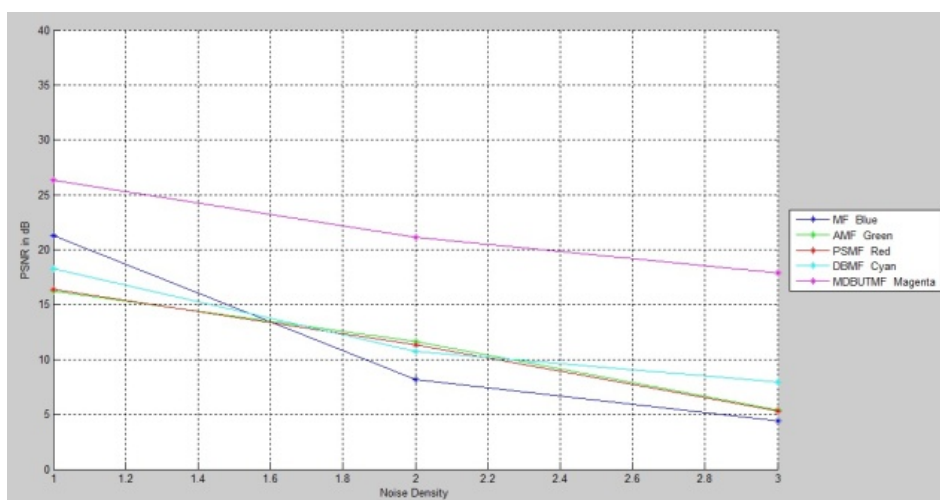


Fig: Comparison graph of PSNR at different noise densities.

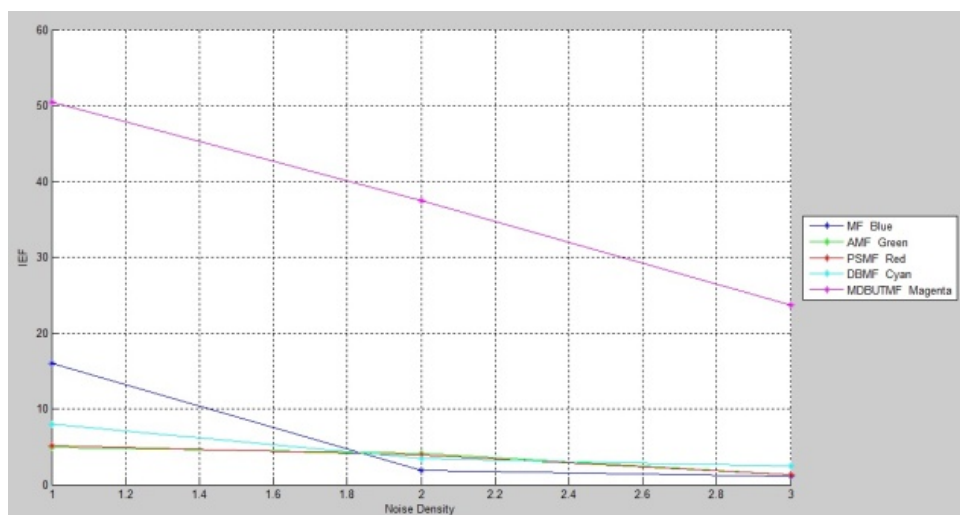


Fig: Comparison graph of IEF at different noise densities.

IV. CONCLUSION

In this letter, a new algorithm (MDBUTMF) is proposed which gives better performance in comparison with MF, AMF and other existing noise removal algorithms in terms of PSNR and IEF. The performance of the algorithm has been tested at low, medium and high noise densities on both gray-scale and colour images. Even at high noise density levels the MDBUTMF gives better results in comparison with other existing algorithms. Both visual and quantitative results are demonstrated. The proposed algorithm is effective for salt and pepper noise removal in images at high noise densities.

REFERENCES

- [1] J. Astola and P. Kuosmanen, 1997, *Fundamentals of Nonlinear Digital Filtering*, Boca Raton, FL: CRC.
- [2] H. Hwang and R. A. Haddad, "Adaptive median filter: New algorithms and results," *IEEE Trans. Image Process.* vol. 4, no. 4, pp. 499–502, Apr..
- [3] S. Zhang and M. A. Karim, Nov. 2002 "A new impulse detector for switching median filters," *IEEE Signal Process. Lett.*, vol. 9, no. 11, pp. 360–363.
- [4] P. E. Ng and K. K. Ma, Jun. 2006 "A switching median filter with boundary discriminative noise detection for extremely corrupted images," *IEEE Trans. Image Process.*, vol. 15, no. 6, pp. 1506–1516.
- [5] K. S. Srinivasan and D. Ebenezer, Mar. 2007 "A new fast and efficient decision based algorithm for removal of high density impulse noise," *IEEE Signal Process. Lett.*, vol. 14, no. 3, pp. 189–192.
- [6] V. Jayaraj and D. Ebenezer, 2010. "A new switching-based median filtering scheme and algorithm for removal of high-density salt and pepper noise in image," *EURASIP J. Adv. Signal Process.*
- [G] S. Esakkirajan, T. Veerakumar, Adabala N. Subramanyam, and C.H PremChand, 2011, "removal of high density salt and pepper noise in images" *IEEE Signal processing letters*, VOL. 18.
- [7] K. Aiswarya, V. Jayaraj, and D. Ebenezer, 2010 "A new and efficient algorithm for the removal of high density salt and pepper noise in images and videos," in *Second Int. Conf. Computer Modelling and Simulation*, pp. 409–413.

NUCLEAR REACTOR CORE PRESSURE LOSS ADJUSTMENT WITH NEURAL APPROACH

Hema.K¹ , Dr.S.Muralidharan²

¹Assistant Professor, Department of Electronics & Instrumentation Engg.,
Greater Noida Institute of Technology, Greater Noida, U.P, (India)

²Department of Electrical & Electronics Engineering, Mepco Schlenk Engineering College, Sivakasi,
Virudhunagar District, Tamil Nadu, (India)

ABSTRACT

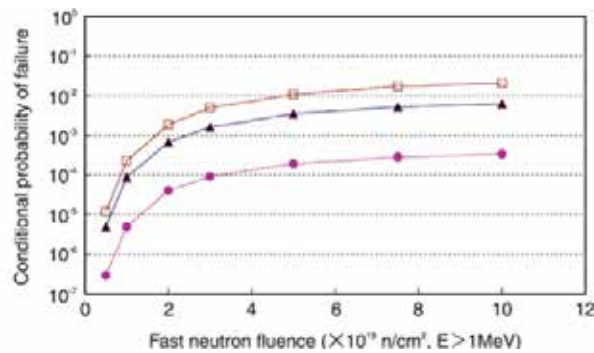
To investigate loss of pressure control on nuclear reactor design models artificial neural networks supports plant operators by training with process parameter database pertaining to accident conditions. The pressure-loss adjusting member can suppress problems due to a flow of a primary coolant, while easily distributing the flow rate of the primary coolant to fuel assemblies. Accordingly, the flow rate of light water flowing toward the fuel assembly can be reduced by arranging the pressure-loss adjusting member between a lower nozzle of a fuel assembly having a small pressure-loss and the lower core support plate, and rattling or the like of the pressure-loss adjusting member can be suppressed by engaging the core support plate engaging unit with the lower core support plate. The pressure distribution and flow patterns in a unit cell, corresponding to 1/4 of fuel assembly, of the top fuel region are obtained with Computational Fluid Dynamics (CFD) model. ANN provides a better diagnostic and prognostic system essential for the identification of pressure loss scenarios in reactor core.

Keywords: Artificial neural network, CFD Models, Pressure loss adjusting member, Simulation.

I. INTRODUCTION

Most commercial reactors use pressure vessel to prevent to prevent boiling in the core which would lead to nuclear meltdown [1]. Thermal stratification, rupture of the pressurizer, spray nozzle failure, mechanically clogged piping may lead to loss of pressure control which have been the reports on Analysis of Severe Accidents in Pressurized Heavy Water Reactors [2]. During an inspection on March 2002 Davis-Besse Nuclear Power Station identified a football-sized cavity in the units' reactor vessel head. The cavity was next to a leaking nozzle with a through-wall crack and was in an area of the vessel head that had been covered with boric acid deposits for several years [3]. When a loss-of-coolant accident occurs in a reactor, the emergency core cooling system injects water in the Reactor Pressure Vessel (RPV), resulting in cooling of the inside of the vessel with high pressure maintained. This induces a high tensile stress at the inner surface of the RPV, so called Pressurized Thermal Shock (PTS). The structural integrity of the RPV during PTS should be evaluated assuming the existence of a flaw at the inner surface [4].

An important aspect of nuclear reactor core analysis involves the determination of the optimal coolant flow distribution and pressure drop across the core. On the one hand, higher coolant flow rates will lead to better heat transfer coefficients. On the other hand, higher flow rates will also result in larger pressure drops across the core, hence larger required pumping powers and larger dynamic loads on the core components



. Thus, the role of the hydrodynamic and thermal-hydraulic core analysis is to find proper working conditions that assure both safe and economical operation of the nuclear power plant. Artificial Neural Network attempt to simulate, within specialized hardware or sophisticated software, with multiple layers of neurons. A general characteristic of a neural network is the ability that quickly recognizes the various conditions or states of a complex system once it has been suitably trained. Transient data was generated and first order resilient back propagation with batch mode training was used. Training of ANN was carried out on a typical Pentium IV processor with 1.5GHz and 512MB of RAM [5]. In this paper the Resilient Back propagation algorithm is used as a local adaptive learning scheme. The motivation behind this algorithm is to eliminate the influence of the magnitude of the partial derivative. Only the sign of the derivative can determine the direction of the weight update. The size of the weight changes is determined by a separate update value. In the training phase, the P prototypes of the learning dataset are presented to the network in sequential and iterative manner. Regressors are used to describe the nonlinear and linear functions. MATLAB has a number of verification techniques available to validate the model structures that are identified. Validation is required to verify that the model structure replicates the behavior of the identified system within acceptable levels.

II. PRESSURE LOSS ADJUSTING CHAMBER

In the pressurized water reactor, fuel assemblies are mounted on a lower core support plate provided in a lower part of a reactor vessel. Light water circulating in the reactor internal flows upward from below the core support plate, passes through the holes in the lower core support plate and then the holes in the lower nozzle, and flows toward the fuel assembly on the lower nozzle. Accordingly, the light water circulates in the primary cooling system, while being exposed to the heat at the time of a fuel reaction. At the time of circulation of light water, light water passes through the holes in the lower core support plate and in the lower nozzle and flows to the circumference of the fuel assembly. However, a flow rate of light water flowing to the circumference of the fuel assembly may be different according to an arrangement position of the fuel assembly. Further, when the performance of the reactor at the time of operation is considered, it may be desired to adjust the flow rate thereof to the fuel assembly. Therefore, the conventional reactor may have a structure for adjusting the flow rate of light water flowing to the fuel assemblies.

One can identify several mechanisms that will cause pressure drop along the fuel assembly:

1. Friction losses from the fuel rod bundle
2. Local losses from the spacer grids
3. Local losses at the core inlet and exit (contraction and expansion)
4. Elevation pressure drop (Fig 1)

The total pressure drop can be calculated from the following equation:

$$\Delta p_{\text{tot}} = -\Delta p_{\text{fric}} - \Delta p_{\text{loc}} - \Delta p_{\text{elev}} = \frac{4C_f L}{D_h} \left(+ \sum_i \xi_i \frac{G^2}{2\rho} \right) + L\rho g \sin\phi \quad (1)$$

Here C_f is the Fanning friction coefficient, L is the length of the channel, G is the mass flux, D_h is the channel hydraulic diameter and ρ is the coolant density.

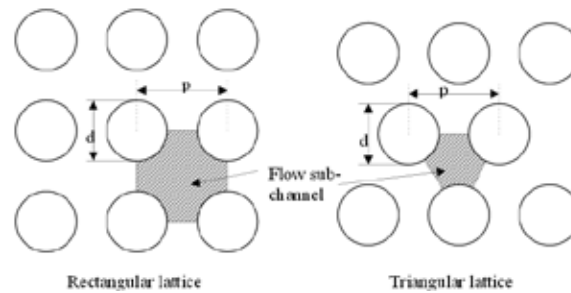


Fig 1 Fuel Assembly

2.1 Primary and Secondary Cooling system

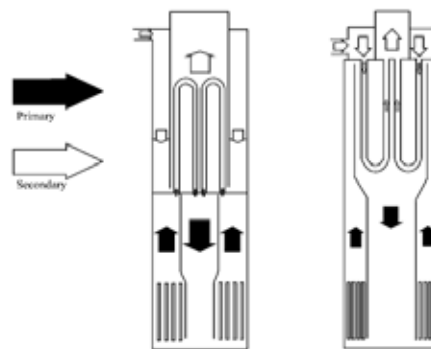


Fig 2 Cooling System

The time of extracting energy is separated into a primary cooling system and a secondary cooling system in PWR. In the primary cooling system, light water exposed to heat at the time of a fuel reaction is made high-temperature and high-pressure water [11]. Pressurizing light water circulating in the reactor does not allow light water to boil. In the secondary cooling system, light water circulating in the secondary cooling system is exposed to heat of the high-temperature and high-pressure water in the primary cooling system so that light water is brought to a boil, and energy is extracted as high-temperature and high-pressure steam. The pressure drop inside the tubes is so high, that natural convection at full power in the primary side is not established for reasonable module heights. Since the module must be extracted from the top, after removing the fuel element from the bottom, the total length should not exceed 12 m. When the water of the secondary system flows inside the tubes, the pressure drop is higher, because of the two-phase flow (Fig 2). But in the secondary system pumps establish the flow. The decay heat can still be removed by natural circulation in secondary circuit at low flow. Steam drums are used to collect and separate the vapor. In order to fulfill the natural convection requirement at decay heat, the position of the steam drum must be determined to provide the buoyancy force necessary to balance the pressure drop.

As the fluid travels up the length of the fuel assembly, there are pressure losses associated with frictional, gravity, form, and acceleration factors. The largest factor is the frictional pressure drop. This consists of a relation of a frictional factor, geometry, and velocity of the fluid. For turbulent flow, the frictional term can be solved for

using the McAdams relation for smooth pipes of $f = 0.184 \cdot Re^{-0.2}$. It is important to remember to use a hydraulic diameter and area associated with fuel rods. For example, for a square array, the area equals the pitch squared minus the cross sectional area of the rod and the hydraulic diameter is four times the area divided by the perimeter of a rod. When grid spacers are introduced, the pressure loss is greatly increased [12] Grid spacers are used for support of the fuel rods from vibration but also external loads of the coolant. Another advantage of spacers is that they increase the heat transfer coefficient by creating additional mixing and direction of the coolant. Modern day spacers provide proper mixing to allow for a swirling affect along the length of a section of the rod. As the mixing increases, the pressure loss increases.

2.2 CFD Model

Pressure distribution and flow fields in reactor core have significant impacts on fuel performance as well as the integrity of reactor vessel internals. Steeper pressure drops are observed at locations where the flow area is reduced at the entrances to the top grid, top nozzle, hold down device, and upper core plate hole. Moderate effects on the pressure decrease and recovery are obtained by refining the meshes in the fluid region adjacent to hold-down device and region in front of the upper core plate hole.

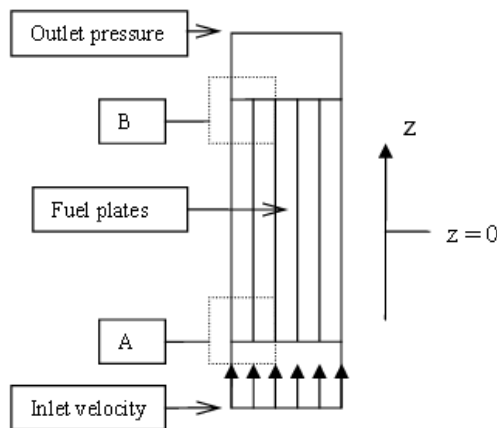


Fig 3 Boundary conditions on Fuel Assembly

Under normal operating conditions, the core is cooled with forced circulation. The average velocity in coolant channels is 8.2 m/s which corresponds to 5.08 m/s of inlet velocity at the inlet of the “lower plenum” (Fig 3). The pressure drop under normal operating condition is reported to be 240 kPa . Corresponding CFD simulations show a pressure drop of only 180 kPa. Errors can be further reduced using neural network. The pressure drop is calculated by, Loss Coefficient = $\frac{\Delta P}{\frac{1}{2} \rho V^2}$ where the P is the difference of the area-averaged total pressures at the entrance of the top grid and at the outlet of the upper core plate hole, ρ is the density, and V is the inlet velocity.

TABLE 1 CFD Model

Inlet velocity (m/s)	Pressure Drop of Assembly CFD with Structure Details (Pa)
0.01	131.7
0.025	349.1
0.05	773.3

0.1	1650.3
0.5	6188.5
1.0	14819
2.0	45279

III. ARTIFICIAL NEURAL NETWORK

A neural network model of the thermodynamics of a power plant can be used to determine the influence of changes in different variable upon the heat rate through the use of sensitivity coefficients, where the signs indicate the directions of change in the variable that will improve heat rate, and the magnitude indicates the relative importance of the different variables. This information can be used to provide guidance to the plant operators and engineers as to where they should expand their efforts to improve the heat rate. ANN based modeling for pressure drop coefficient for cyclone separators is done by [11].

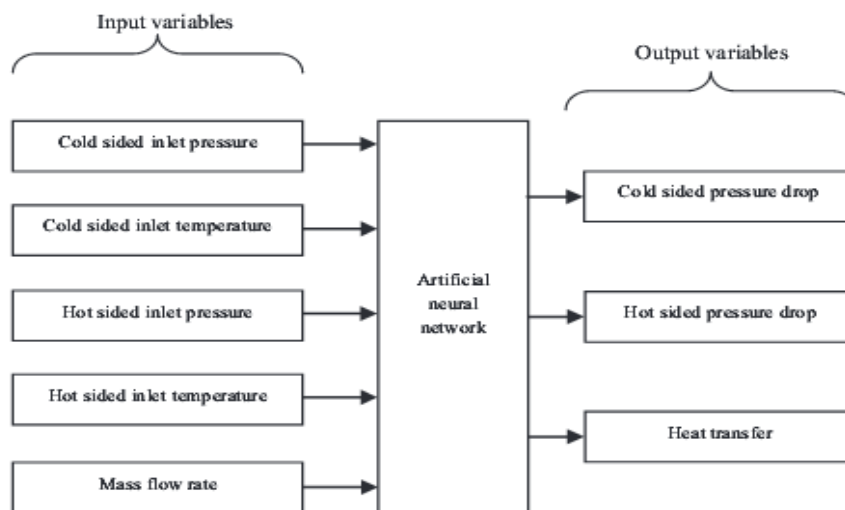


Fig 4 ANN Modeling of Reactor Core Pressure Drop

Resilient back Propagation algorithm is a local adaptive learning scheme performing supervised batch learning in feed forward neural networks. The basic principle of this algorithm is to eliminate the harmful influence of the size of the partial derivative on the weight step. RPROP modifies the size of the weight step taken adaptively, and the mechanism for adaptation in RPROP does not take into account the magnitude of the gradient as seen by a particular weight, but only the sign of the gradient (positive or negative). This allows the step size to be adapted without having the size of the gradient interfere with the adaptation process [13].

Resilient Back propagation Algorithm is generally much faster than the standard steepest descent algorithm. It also has a very good feature that it requires only a modest increase in memory requirements. It is a systematic method to train the neural network. The purpose of it is to eliminate the harmful effects of the magnitudes of the partial derivatives. Only the sign of the derivative is used to determine the direction of the weight update and the magnitude of the derivative has no effect on the weight update. Different trials have been carried out in the training phase to get the optimal values for different number of hidden nodes and learning rates for back propagation algorithm. Fig 5 shows mean square error parameter with respect to the number of iterations for

various learning rates and number of hidden nodes. At first the value of learning rate was varied keeping number of hidden nodes constant. Then the number of hidden nodes was varied keeping learning rate constant.

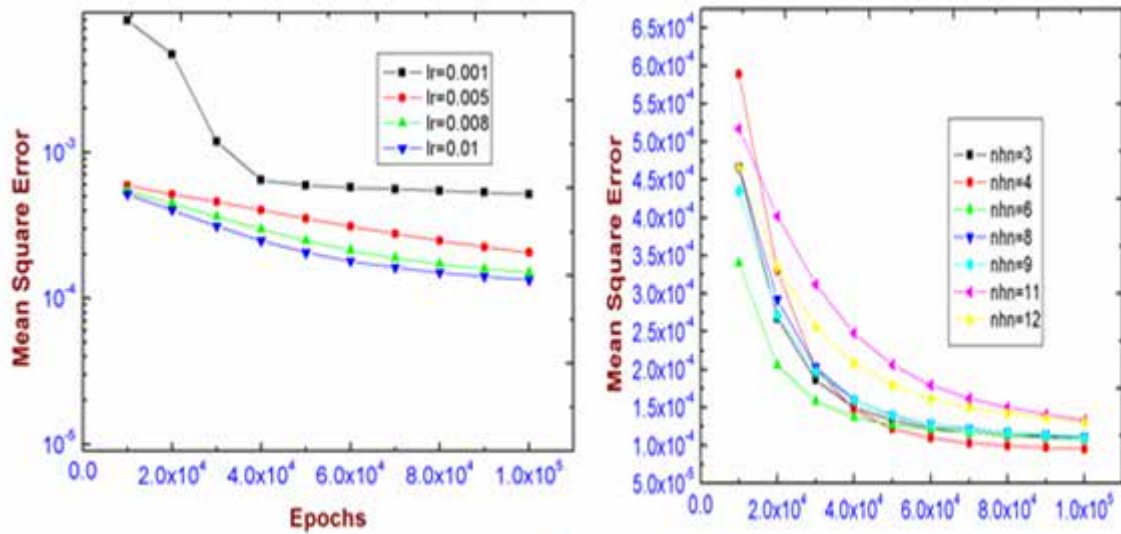


Fig 5 Epochs Vs Mean Square Error

After repeating the above process Q times the mean MSE (mMSE) and standard deviation of MSE sdMSE) were calculated respectively:

$$mMSE = \frac{\sum_{i=1}^Q MSE_i}{Q} \tag{2}$$

$$sdMSE = \sqrt{\frac{1}{Q} \sum_{i=1}^Q (MSE_i - mMSE)^2} \tag{3}$$

The difference between mean MSE values for training and validating were compared.

IV. SIMULATED RESULTS

ARMAX structure estimates different set of zeros but same set of poles for the system and the noise model. This structure is especially suitable when the stochastic dynamics are dominating in nature and the noise enters early into the process e.g. load disturbances [17].

$$A(z)y(t) = B(z)u(t) + C(z)e(t) \tag{4}$$

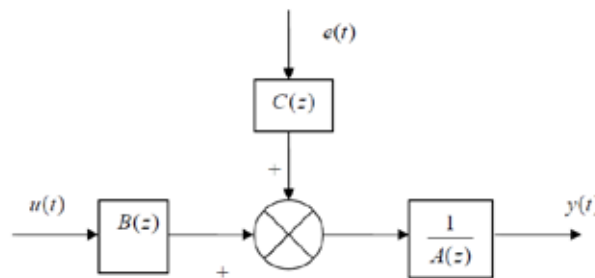


Fig 6 ARMAX Structure

For identification, the reactor is visualized as a system with fraction of total drop as input and the global power (in percentage of maximum power produced) as output. From the simulator it is known that the set point is 15.51MPa. The main pressuriser heaters are switched on at about 15.51MPa and increase linearly to about

15.41MPa where the main heaters maximum power of 315kW is reached. The pressuriser spray valves are opened at a minimum value and increase linearly to a maximum value. In none of the simulated data sets could a maximum value for the spray mass flow be reached [21].

TABLE 2 Simulated Pressurizer data sets

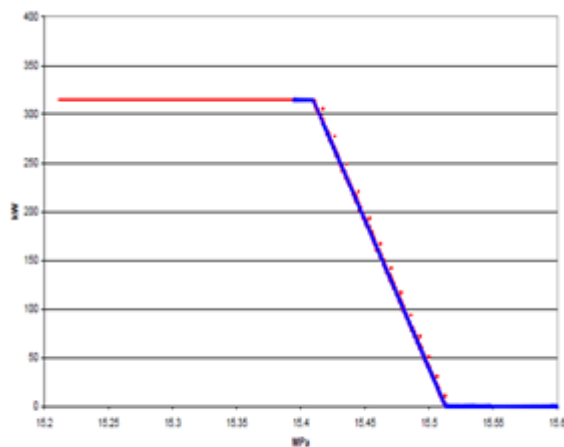
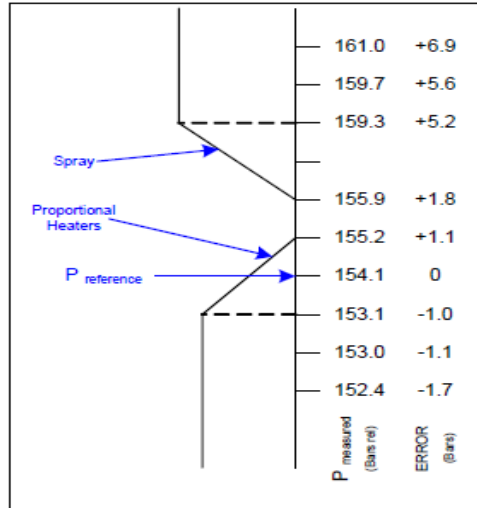


Fig 7 Heater Power Vs Pressure

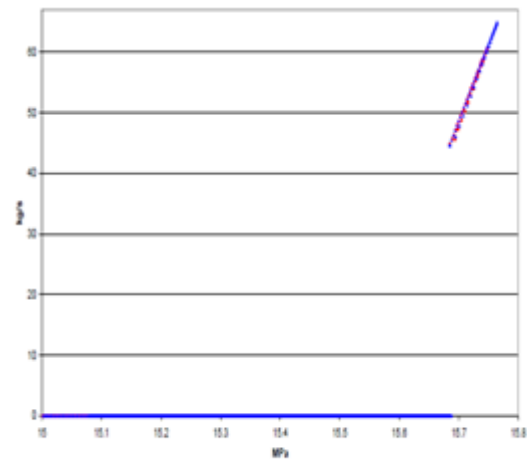


Fig 8 Mass Flow rate Vs Pressure

The identification is carried out using the $arx()$, $armax()$, $bj()$, $oe()$ functions of System Identification Toolbox of MATLAB and higher order discrete transfer function models have been estimated from the measured input output data [24]. Now, the most appropriate model structure can be judged from the prediction error of the models. The statistical measure of the quality of the identified model can be judged using Akaike’s Information Criterion (AIC)

$$AIC = \log \left\{ \det \left[\frac{1}{N} \sum_{t=1}^N \varepsilon(t, \theta_N) \varepsilon^T(t, \theta_N) \right] \right\} + \frac{2d}{N} \tag{5}$$

where, N is the number of measurement points

θ is the identified system parameters and

d is the number of parameters to be identified.

V. CONCLUSION

Fuel criticality due to loss of pressure control and cooling malfunction makes the reactor unstable. CFD Model analyses the pressure distributions and flow patterns in the assembly. Nodes representing fluid volumes or thermal masses are connected with one-dimensional heat and fluid flow elements to represent a thermal system. The type of element determines the pressure drop; mass and heat flow characteristics. Thus the flow distribution at the core inlet is influenced by the flow field in the reactor pressure vessel and the flow distribution between the loops. The calculated pressure loss coefficients can be used to increase accuracy of severe accident analysis with core meltdown. CFD validates and evaluates the pressure loss coefficient Neural networks can capture complex dynamics of the system like hindered lower plenum geometry yielding satisfactory predictions. Selected model structures available in the MATLAB System Identification Toolbox with validation techniques are used for the verifying the system model. Partition coefficients at higher pressure, improved numerical stability can be worked on for more improved performance.

REFERENCES

- [1] Edwards R.M , Lee K.Y, Schultz M.A. State-feedback assisted classical control , An incremental approach to control modernization of existing and future nuclear reactors and power plants, *Nucl. Technol.* 1990, 92, 167–185.
- [2] Ben-Abdenour A, Edwards R.M., Lee K.Y. LQR/LTR robust control of nuclear reactors with improved temperature performance. *IEEE Trans. Nucl. Sci.* 1992, 39, 2286–2294.
- [3] Arab-Alibeik H, Setayeshi, S. Improved temperature control of a PWR nuclear reactor using LQG/LTR based controller. *IEEE Trans. Nucl. Sci.* 2003, 50, 211–218.
- [4] Osakabe K , Onizawa K. et al., Development of Probabilistic Fracture Mechanics Analysis Code PASCAL ver.2 for Reactor Pressure Vessel, , *IEEE Trans. Nucl. Sci.* vol.6, no.2, p.161-171,2007.
- [5] Santosh, Gopika Vinod, R.K. Saraf, A.K. Ghosh and H.S. Kushwaha, “Application of artificial neural networks to nuclear power plant transient diagnosis”, *Reliability Engineering and System Safety*, Vol. 92, pp.1486-1472,2007.
- [6] YangQuan Chen, Kevin L. Moore, “Relay feedback tuning of robust PID controllers with iso-damping property”, *IEEE Transactions on Systems, Man and Cybernetics-Part B: Cybernetics*, Volume 35, Issue 1, pp. 23-31, February 2005.
- [7] G. Datatreya Reddy, Y. Park, B. Bandyopadhyay, A.P. Tiwari, “Discrete-time output feedback sliding mode control of a large PHWR”, *Automatica*, Volume 45, Issue 9, pp. 2159-2163, September 2009.
- [8] G.L. Sharma, B. Bandopadhyay and A. P. Tiwari, “Spatial control of a large pressurized heavy water reactor by fast output sampling technique”, *IEEE Transactions on Nuclear Science*, Volume 50, Issue 5, pp. 1740-1751, October 2003.
- [9] G.L. Sharma, B. Bandopadhyay and A. P. Tiwari, “Fault-tolerant spatial control of a large pressurized heavy water reactor by fast output sampling technique”, *IEEE Proceedings-Control Theory and Applications*, Volume 151, Issue 1, pp. 117-124, January 2004.
- [10] A.P. Tiwari, B. Bandyopadhyay and H. Werner, “Spatial control of a large PHWR by piecewise constant periodic output feedback”, *IEEE Transactions on Nuclear Science*, Volume 47, Issue 2, pp. 289-402, April 2000.
- [11] B. Su Y, Artificial neural network-based modeling of pressure drop coefficient for cyclone separators, *Chemical engineering research and design*, 88, 606-613,2009.

- [12] Nidal F. Shilbayeh and Mahmoud Z. Iskandarani “Effect of Hidden Layer Neurons on the Classification of Optical Character Recognition Typed Arabic Numerals”. *Journal of Computer Science* 4 (7):578 – 584, 2008.
- [13] Man Gyun Na and Belle R. Upadhyay, “Application of model predictive control strategy based on fuzzy identification to an SP-100 space reactor”, *Annals of Nuclear Energy, Volume 33, Issue 17-18, pp. 1467-1478, November-December 2006.*
- [14] Man Gyun Na and Belle R. Upadhyaya, “Model predictive control of an SP-100 space reactor using support vector regression and genetic optimization”, *IEEE Transactions on Nuclear Science, Volume 53, Issue 4, pp. 2318-2327, August 2006.*
- [15] George T. Bereznaï and Naresh K. Sinha, “Adaptive control of nuclear reactors using] Neural Network Toolbox, Signal Processing Toolbox, Statistics Toolbox of MATLAB digital computer”, *IEEE Transactions on Nuclear Science, Volume 18, Issue 4, pp. 387-397, August 1971.*
- [16] Zhengyu Huang, Robert M. Edwards and Kwang Y. Lee, “Fuzzy-adapted recursive sliding-mode controller design for a nuclear power plant control”, *IEEE Transactions on Nuclear Science, Volume 51, Issue 1, pp 256-266, February 2004.*
- [17] Monotosh Das, Ratna Ghosh, Bhaswati Goswami, Amitava Gupta, A. P. Tiwari, R. Balasubramanian and A. K. Chandra, “Networked control system applied to a large pressurized heavy water reactor”, *IEEE Transactions on Nuclear Science, Volume 53, Issue 5, Part 2, pp. 2948-2956, October 2006.*
- [18] Moon Ghu Park and Nam Zin Cho, “Time-optimal control of nuclear reactor power with adaptive proportional-integral-feed forward gains”, *IEEE Transactions on Nuclear Science, Volume 40, Issue 3, pp. 266-270, June 1993.*
- [19] R.K. Sinha and A. Kakodkar, “Design and development of the AHWR-the Indian thorium fuelled innovative nuclear reactor”, *Nuclear Engineering and Design, Volume 236, Issue 7-8, pp. 683-700, April 2006.*
- [20] A.P. Tiwari, B. Bandyopadhyay and G. Govindarajan, “Spatial control of a large pressurized heavy water reactor”, *IEEE Transactions on Nuclear Science, Volume 43, Issue 4, pp. 2440-2453, August 1996.*
- [21] D.B. Talange, B. Bandyopadhyay and A.P. Tiwari, “Spatial control of a large PHWR by decentralized periodic output feedback and model reduction techniques”, *IEEE Transactions on Nuclear Science, Volume 53, Issue 4, pp. 2308-2317, August 2006.*
- [22] S.R. Shimjith, A.P. Tiwari, M. Naskar, B. Bandyopadhyay, “Space-time kinetics modeling of advanced heavy water reactor for control studies”, *Annals of Nuclear Energy, Volume 37, Issue 3, pp. 310-324, March 2010.*
- [23] Yoon Joon Lee and Man Gyun Na, “Robust controller design for the nuclear reactor power by extended frequency response method”, *Nuclear Engineering and Technology, Volume 38, Issue 6, August 2006.*
- [24] Neural Network Toolbox, Signal Processing Toolbox, Statistics Toolbox of MATLAB.

DESIGN OF QUATERNARY ADDER FOR HIGH SPEED APPLICATIONS

Ms. Priti S. Kapse¹, Dr. S. L. Haridas²

¹Student, M. Tech. Department of Electronics, VLSI, GHRACET, Nagpur, (India)

²H.O.D. of Electronics and communication VLSI, GHRACET, Nagpur, (India)

ABSTRACT

Routing has become the main contributor in many areas of design such as area, delay and power. Multiple Valued Logic (MVL) offers a means to reduce the routing since each wire in MVL can carry the twice as much information as single binary wire. Reducing this routing directly leads to the reduction of overall circuit area and power consumption. Rapid advancement in VLSI technology makes it possible to couple several binary inputs to form a multivalued input for faster processing. In this paper, we present the Quaternary Signed Digit number(QSD) system which comes under the Multiple Valued Logic(MVL); to achieve fast processing by achieving the carry free arithmetic operations. This approach can greatly enhance the performance of digital signal processing(DSP) system.

Keywords: *Multiple Valued Logic, Quaternary Signed Digit, Carry Free Operations, VLSI.*

INTRODUCTION

For many years digital devices have been designed using binary logic. Even today also, the latest computing systems are designed and developed using binary logic only. Then why there is a need of inventing multi valued logic over binary logic??? With the advancing technology, interconnections are the main contributor for delay, area and power consumption. One of the solution for the problem of interconnection is that: what if we will develop the idea of transmitting the number of logic levels through a single wire. Since, multi valued logic scheme allows more data to be grouped in single digit, researchers seems the use of multivalued logic as a solution for the above problem.so, researchers have been working on the idea of using multivalued logic for many years. Existing VLSI technology has put some limitations on the selection of number of logic states, therefore researchers seems the use of Quaternary logic systems to be best in this regards. The paper is organized as follows: In this paper we review some work related to QSD number system. Section2 explains basic concept of performing any operation in QSD number system. Section3 explains quaternary signed digit number system. Section4 explains converter of decimal to Quaternary Signed Digit number.Section5 explains converter of QSD number to decimal number. Section6 explains QSD adder. Conclusion of paper is given in Section7.

VLSI designers has the main challenge of less chip area and high operation speed for faster calculations since in **today's** microprocessors millions of operations are performed per second[2]. In binary system, speed is limited by formation and propagation of carry. When the number or length of bits are large, carry formation and propagation problem becomes worst. We can achieve a carry free arithmetic operation by using higher radix number system such as QSD (Quaternary Signed Digit). Signed digit number system has redundancy associated with it. The redundancy provided in signed digit number system offers the possibility of carry free arithmetic operations which in terms allows for faster processing. In signed digit representation of the system; the add time for two redundant signed digit

numbers is a constant independent of the word length of the operands which is the key to high speed computation. Binary signed digit numbers allows limited carry propagation with a more complex addition process which requires very large circuit for implementation[1][4]. A higher radix based representation of binary signed digit numbers such as quaternary allows carry free arithmetic operations as well as it offers the important advantage of logic simplicity and storage density[5]. Quaternary logic is a promising alternative for the complex binary circuit as it will reduce the circuit area and circuit cost and power efficiency at the same time.

II. QUATERNARY SIGNED DIGIT NUMBERS

Quaternary is the base four numeral system which uses the digits 0, 1, 2 and 3 to represent any real number. QSD numbers are represented with the digit set from -3 to +3 i.e. with $\{\bar{3}, \bar{2}, \bar{1}, 0, 1, 2, 3\}$. $\bar{3}, \bar{2}, \bar{1}$, represents the signed numbers -3, -2, -1 respectively. Signed digit numbers have redundancy associated with it therefore quaternary is also called as base-4 redundant number system. Degree of redundancy increases with increase of radix[6]; therefore higher radix number systems usually have higher redundancy.

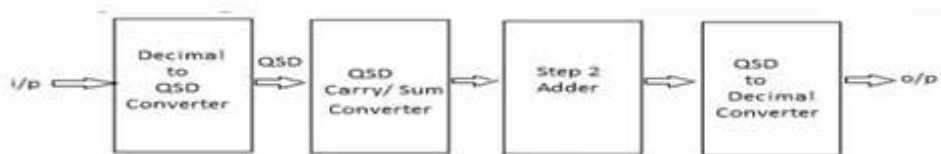
Redundancy allows multiple representation of any integer quantity i.e. $6_{10} = 12_{QSD} = 2\bar{2}_{QSD}$. In QSD, numbers are represented using 3 bit 2's complement notation. In general decimal signed digit number (D) can be represented in terms of quaternary signed digit number (Q) as follows;

$$D = \sum_i X_i \cdot 4^i$$

Where; X_i can be any value or digit from the digit set $\{\bar{3}, \bar{2}, \bar{1}, 0, 1, 2, 3\}$ for achieving the appropriate decimal representation. In this number system; a QSD negative number is nothing but the QSD complement of the QSD positive number[7], i.e. $\bar{3} = 3$; $3' = \bar{3}$; $\bar{2} = 2$; $2' = \bar{2}$; $\bar{1} = 1$; $1' = \bar{1}$. For eg. $233_{10} = 3\bar{3}\bar{2}\bar{1}_{QSD}$ and $-233_{10} = \bar{3}\bar{3}\bar{2}\bar{1}_{QSD}$. In QSD single decimal number can be represented in multiple ways. Operation on large number of digits such as 64, 128, or more can be implemented with constant delay and complexity. A high speed and area effective adders and multipliers can be implemented using QSD number system.

III. BASIC CONCEPT

For performing any operation in QSD; first convert the binary or any other input into quaternary signed digit (QSD).



IV. DECIMAL NUMBER TO QSD NUMBER CONVERTER:

As mentioned before; for any operation to get performed in QSD, we have to first convert the binary or any other input into quaternary signed digit (QSD) number. Now, we will go through some ideas related to the conversion of decimal number to QSD number[1]. For this purpose we exploit some fundamentals as they play an important role in corresponding algorithm. As the numbers can be positive and can also be negative. In digital system, positive numbers are called as unsigned numbers whereas the negative numbers are called as signed numbers. The input decimal number is given as, in the form of n-bit binary number, as Modelsim and Xilinx software takes the input in the form of binary only. Binary numbers are of two types; Unsigned binary numbers and Signed binary numbers.

Unsigned binary numbers have only magnitude and this number is always positive. Signed binary number consist of magnitude as well as sign. In the decimal number system, sign of a number is indicated by “+” or “-” symbol before the leftmost number. However; in the binary number system, the sign of a number i.e. whether the number is positive or negative is indicated by the leftmost bit which is called as MSB (Most Significant Bit). For a positive binary number, the leftmost bit is always “0” and for a negative binary number, the leftmost bit is always “1”. Thus in signed binary numbers since the MSB i.e. n th bit represents sign, magnitude is represented by the remaining “ $n-1$ ” bits as shown. Whereas in unsigned binary numbers all n -bits are used to represent the magnitude. It is very important to understand the location of MSB while studying the signed and unsigned number system. The leftmost bit i.e. b_{n-1} is called MSB in unsigned integer whereas the leftmost bit b_{n-1} in signed integer represents sign bit and it's MSB is b_{n-2} bit as shown in fig. (a) and (b). As the Modelsim and Xilinx software takes the input in form of binary, this algorithm depicts that, it takes any n digit decimal number as input and convert it into it's equivalent quaternary signed digit number whether the decimal input is positive or negative number. If the given input decimal number is positive then we will get a QSD number at the output in which each digit will be positive. This QSD output is represented with 3 bit 2's complement notation in simulation result. If the given input decimal number is negative, then after conversion we will get the corresponding QSD number at the output in which each digit will be negative. This QSD output can also be represented in 3 bit 2's complement notation in simulation result.

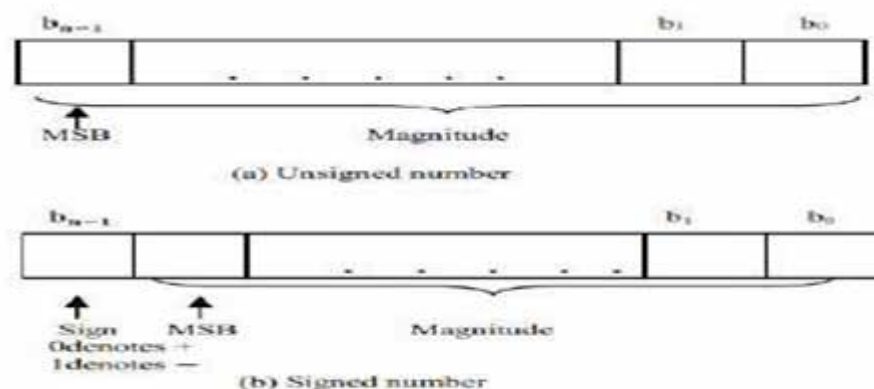


Fig. 1: Formats for representation of integers

The conversion of a decimal number into corresponding QSD number can be performed by modulo-4 arithmetic, in which the given decimal number is successively divided by 4 and by keeping the track of the remainders. This process continues until the quotient becomes zero. When we divide the given decimal number by 4, the quotient which we get is nothing but the just another QSD number and remainder is nothing but the digit qsd_0 i.e. (LSB) least significant bit of our output QSD number. Further dividing the quotient by 4 gives the new quotient and the remainder which is the next digit i.e. qsd_1 . Continuing the process of dividing the new quotient by 4; determining the remainder (one digit) in each step will produce all digits of the QSD integer, and this process continues until quotient becomes zero. It is important to note that; the least significant bit (LSB) is generated first and most significant bit (MSB) is generated last. We can say that; collection of remainders forms the collection of QSD digits which in terms forms the resultant QSD number.

This algorithm first find out the value of leftmost input bit i.e. if the leftmost bit is “1”, algorithm determines that given input decimal number is negative and binary number indicates 2's complement represented number and if the leftmost bit is “0”, algorithm determines that given input decimal number is positive and binary number indicates unsigned number. It is important to note that; “0” is neither positive nor negative hence if decimal input is 0 in the

form of binary then output will always be 0. Decimal number that can be represented with 4-bits , 8-bits , 16-bits etc. in 2's complement binary form are -8 to +7 , -128 to +127 , -32768 to +32767 etc. respectively. Operation on these large numbers are performed with constant delay and less complexity in QSD number system.

V. QUATERNARY TO DECIMAL NUMBER CONVERTER

Any n-digit QSD number can be converted into it's equivalent decimal number by using the following equation;

$$D = \sum_{i=0}^{n-1} X_i \cdot 4^i$$

Where; X_i can be any value or digit from the digit set $\{\bar{3}, \bar{2}, \bar{1}, 0, 1, 2, 3\}$ for achieving the appropriate decimal representation. For required decimal representation, each digit in the QSD number is multiplied by its quaternary weight. In general QSD integer is expressed by; QSD = $qsd_{n-1} qsd_{n-2} qsd_{n-3} \dots \dots qsd_1 qsd_0$ which represents the equivalent decimal value as; $D(QSD) = qsd_{n-1} \times 4^{n-1} + qsd_{n-2} \times 4^{n-2} + \dots \dots + qsd_1 \times 4^1 + qsd_0 \times 4^0$. In this way QSD number is converted into its equivalent decimal number by using above equation. Some examples are;

$$10\bar{2}1_{QSD} = 1 \times 4^3 + 0 \times 4^2 + \bar{2} \times 4^1 + 1 \times 4^0$$

$$= 64 + 0 - 8 + 1$$

$$= (57)_{10}$$

$$\bar{1}0\bar{2}\bar{1}_{QSD} = (-57)_{10}$$

VI. QSD ADDER

Adders are most commonly used in numerous electronic applications and serves as the basic building block of various arithmetic operations. As we know that the speed of the digital processor mainly depends on the speed of the adders used in the system. System speed can be increased by increasing the speed of addition. Speed of the system is limited by the carry formation and propagation especially when the number of bits are large. In QSD number system , carry propagation chain are eliminated which reduce the computation time substantially, thus enhancing the speed of the machine[8]. As mentioned before, range of the QSD number varies from -3 to +3. Carry free addition can be achieved by exploiting the redundancy of QSD numbers and QSD addition.

There are two steps involved in carry free addition;

STEP 1 :Generates an intermediate carry and sum from the QSD input i.e. from addend and augend.

STEP 2 :Combines the intermediate sum of current digit with the carry of the lower significant digit.

To prevent carry from further rippling two rules are define;

RULE 1:States that the magnitude of intermediate sum must be less than or equal to 2 or it must not be greater than 2.

RULE 2:States that the magnitude of intermediate carry must be less than or equal to 1 or it must not be greater than 1.

Consequently the magnitude of second step output cannot be greater than 3, which can be represented by a single digit QSD number hence no further carry is required. Outputs of all possible combinations of QSD inputs i.e addend and augend are shown in table 1.

Table 1

THE OUTPUTS OF ALL POSSIBLE COMBINATIONS OF A PAIR OF ADDEND (A) AND AUGENDS (B)

B A	-3	-2	-1	0	1	2	3
-3	-6	-5	-4	-3	-2	-1	0
-2	-5	-4	-3	-2	-1	0	1
-1	-4	-3	-2	-1	0	1	2
0	-3	-2	-1	0	1	2	3
1	-2	-1	0	1	2	3	4
2	-1	0	1	2	3	4	5
3	0	1	2	3	4	5	6

We can see that output ranges from -6 to +6 and these output values can be represented in QSD format as shown in table 2.

Output values in the range from +3 to -3 can be represented by single digit QSD number but when these output values exceeds from the above range more than one QSD digit is required to represent that value. In this two digit QSD number, LSB represents sum bit and MSB represents intermediate carry bit. This intermediate carry propagates from lower significant digit to higher significant digit position and to prevent this propagation QSD number representation is used[9]. QSD number has redundancy associated with it in which same decimal number can be represented in more than two QSD representations. But we chose only those QSD coded number which meet our defined rules(as shown in table2) to prevent the further rippelton of carry.

Table 2 THE INTERMEDIATE CARRY AND SUM BETWEEN -6 TO 6

Sum	QSD represented number	QSD coded number
-6	$\bar{2}2, \bar{1}2$	$\bar{1}2$
-5	$\bar{2}3, \bar{1}1$	$\bar{1}1$
-4	$\bar{1}0$	$\bar{1}0$
-3	$\bar{1}1, 0\bar{3}$	$\bar{1}1$
-2	$\bar{1}2, 0\bar{2}$	$0\bar{2}$
-1	$\bar{1}3, 0\bar{1}$	$0\bar{1}$
0	00	00
1	01, $\bar{1}\bar{3}$	01
2	02, $\bar{1}\bar{2}$	02
3	03, $\bar{1}\bar{1}$	$\bar{1}\bar{1}$
4	10	10
5	11, $\bar{2}\bar{3}$	11
6	12, $\bar{2}\bar{2}$	12

To prevent carry propagation, these two digits i.e. n^{th} intermediate sum and $n - 1^{th}$ intermediate carry bits should never form the pair (3,3) (3,2) (3,1) ($\bar{3}, \bar{3}$) ($\bar{3}, \bar{2}$) ($\bar{3}, \bar{1}$) . In this way, when intermediate sum and intermediate carry go upto maximum value of 2 and 1 respectively, final result of operation will become carry free. Mapping between the 3-bit 2's complement inputs (addend and augend) and outputs (intermediate carry and sum) are shown in binary format in table 3. Intermediate carry ranges between -1 to +1 and can be represented with 2 bit binary number but

we have taken the 3-bit representation of carry bit for bit compatibility. Outputs of all possible combinations of intermediate sum and intermediate carry is shown table 4.

Table 3

INPUT				OUTPUT				
QSD		Binary		Dec	QSD		Binary	
Ai	Bi	Ai	Bi	Su	Ci	Si	Ci	Si
3	3	011	011	6	1	2	01	010
3	2	011	010	5	1	1	01	001
2	3	010	011	5	1	1	01	001
3	1	011	001	4	1	0	01	000
1	3	001	011	4	1	0	01	000
2	2	010	010	4	1	0	01	000
1	2	001	010	3	1	-1	01	111
2	1	010	001	3	1	-1	01	111
3	0	011	000	3	1	-1	01	111
0	3	000	011	3	1	-1	01	111
1	1	001	001	2	0	2	00	010
0	2	000	010	2	0	2	00	010
2	0	010	000	2	0	2	00	010
3	-1	011	111	2	0	2	00	010
-1	3	111	011	2	0	2	00	010
0	1	000	001	1	0	1	00	001
1	0	001	000	1	0	1	00	001
2	-1	010	111	1	0	1	00	001
-1	2	111	010	1	0	1	00	001
3	-2	011	110	1	0	1	00	001
-2	3	110	011	1	0	1	00	001
0	0	000	000	0	0	0	00	000
1	-1	001	111	0	0	0	00	000
-1	1	111	001	0	0	0	00	000
2	-2	010	110	0	0	0	00	000
-2	2	11	010	0	0	0	00	000
-3	3	101	011	0	0	0	00	000

3	-3	011	101	0	0	0	00	000
0	-1	000	111	-1	0	-1	00	111
-1	0	111	000	-1	0	-1	00	111
-2	1	110	001	-1	0	-1	00	111
1	-2	001	110	-1	0	-1	00	111
-3	2	101	010	-1	0	-1	00	111
2	-3	010	101	-1	0	-1	00	111
-1	-1	111	111	-2	0	-2	00	110
0	-2	000	110	-2	0	-2	00	110
-2	0	110	000	-2	0	-2	00	110
-3	1	101	001	-2	0	-2	00	110
1	-3	001	101	-2	0	-2	00	110
-1	-2	111	110	-3	-1	1	11	001
-2	-1	110	111	-3	-1	1	11	001
-3	0	101	000	-3	-1	1	11	001
0	-3	000	101	-3	-1	1	11	001
-3	-1	101	111	-4	-1	0	11	000
-1	-3	111	101	-4	-1	0	11	000
-2	-2	110	110	-4	-1	0	11	000
-3	-2	101	110	-5	-1	-1	11	111
-2	-3	110	101	-5	-1	-1	11	111
-3	-3	101	101	-6	-1	-2	11	110

Table 4

OUTPUTS OF ALL POSSIBLE COMBINATIONS OF A PAIR OF INTERMEDIATE CARRY (A) AND SUM (B)

B A	-2	-1	0	1	2
-1	-3	-2	-1	0	1
0	-2	-1	0	1	2
1	-1	0	1	2	3

We have taken the input range according to our defined rules and hence our output ranges from +3 to -3 and which can be represented by a single digit QSD number hence no further carry is required. Addition operation for higher order digit does not wait for the completion of addition operation of immediate lower order digit resulting in parallel addition of each individual pair of digits.

6.1 MVL: Multiple valued logic (MVL)

Multiple valued logic uses more than two logic levels. Since, multi-valued logic enables more information to be packed in a single digit, researchers have been working on this MVL for many years. MVL allows transmission of more information through a single wire, hence reducing the interconnections. Reducing interconnection directly reduces overall power consumption and circuit area. Development in novel electronic devices and optical devices makes it possible to implement circuits for complicated logic system. Many of such complicated systems are able to deal with more than two logic state, so if we use multiple valued logic for the design of digital circuit their efficiency could be utilized in better way. In binary logic, device size is reduced by reducing transistor size but transistor size cannot be reduced indefinitely. By using MVL number of transistors can be reduced greatly. Therefore we can say that multivalued logic is a best solution for the increasing data storage demand and faster computation. In binary logic, the size of the device is reduced by reducing the size of the transistor. But it has a limit, since the size of transistor cannot be reduced indefinitely. By applying multi-valued logic to the design, word lengths and the number of transistors can be greatly reduced.

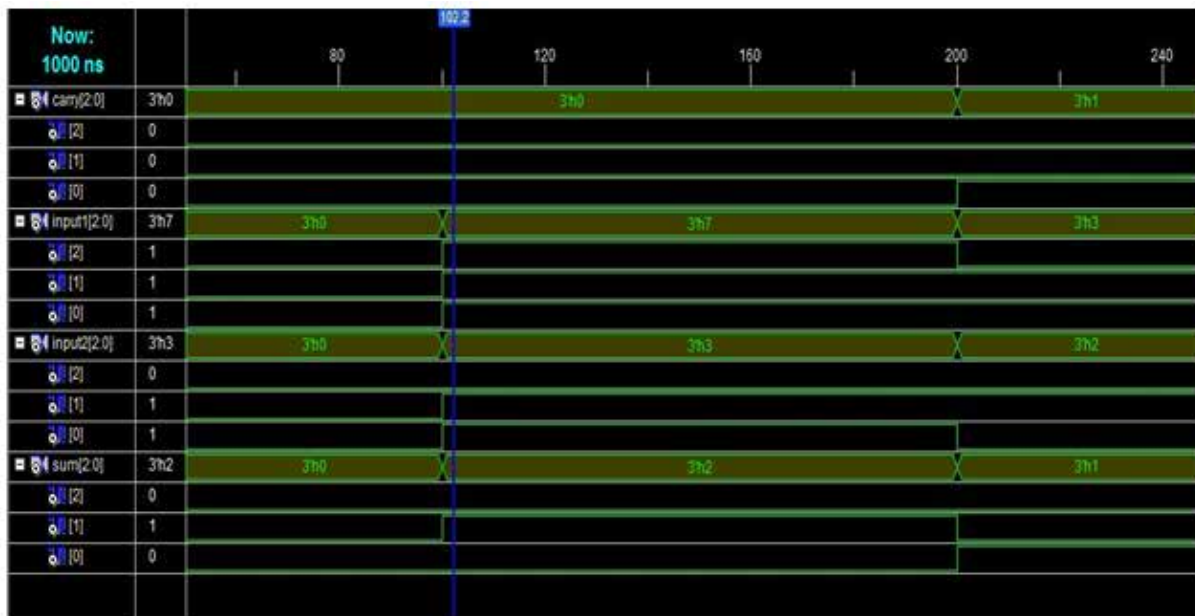


Fig Simulation Results for Quaternary Adder

VII. CONCLUSION

This review paper discussed the idea of both converters; decimal number to QSD number converter and also QSD number to decimal number converter. By using this higher radix number system such as QSD we can perform the operations on large number of bits with constant delay and less complexity. As technologies are becoming more complex, multivalued logic (MVL) will be the future of circuit design. Hence MVL logic scheme can be a solution for the demand of increasing data storage capability and faster processing.

REFERENCES

- [1] Authers Stephen Brown and Zvonko Vranesic "Fundamentals of Digital Logic with VHDL Design" -text book.
- [2] Reena Rani, Neelam Sharma, L.K.Singh, "FPGA Implementation of Fast Adders using Quaternary Signed Digit Number System" IEEEproceedings of International Conference on Emerging Trends inElectronic and Photonic Devices & Systems (ELECTRO-2009), pp 132-135, 2009.
- [3] O. Ishizuka, A. Ohta, K. Tannno, Z. Tang, D. Handoko, "VLSI design of a quaternary multiplier with directgeneration of partial products," Proceedings of the 27th International Symposium on Multiple-ValuedLogic, pp. 169-174, 1997.
- [4] BehroozParhami, "Carry-Free Addition of Recoded Binary Signed- Digit Numbers", IEEE Transactions on Computers, Vol. 37, No. 11, pp. 1470-1476, November 1988.
- [5] Ricardo Cunha, "quaternary lookup tables using voltage mode CMOS logic design", ISMVL 2007, 37th International Symposium on Multiple- Valued Logic, pp.56-56, 2007, 13-16 May, 2007.
- [6] VasundaraPatel K S, K S Gurumurthy, "Design of High Performance Quaternary Adders", International Journal of Computer Theory and Engineering, Vol.2, No.6, pp. 944-952, December, 2010.
- [7] Behroozperhami "generalized signed digit number systems, a unifying frame work for redundant number representation ".IEEE transactions on computers,vol 39,no.1,pp.89-98,January 1990.
- [8] Reena Rani, Neelam Sharma, L.K.Singh, "Fast Computing using Signed Digit Number System" IEEE proceedings of International Conference on Control, Automation, Communication And Energy Conservation - 2009, 4th-6th June 2009.
- [9] HirokatsuShirahama andTakahiro Hanyu et.al, "Design of a Processing Element Based on QuaternaryDifferential Logic for a Multi-Core SIMD Processor", ISMVL, Proceedings of the 37th International Symposium on Multiple-Valued Logic, pp. 43, 2007.

INTRANET BASED E-LEARNING USING REAL TIME TRANSMISSION PROTOCOL

**Hemant Rajput¹, Shekhar Sharma², Amit Mistry³, Sagar Soni⁴,
Mrs. Suvarna Jadhav⁵**

^{1,2,3,4} B.E.INFT Student, Atharva College of Engineering, Malad, Mumbai, (India)

⁵ Project Guide, Department of Information Technology,
Atharva College of Engineering, Malad, Mumbai, (India)

ABSTRACT

Due to increase in use of computers in educational organization there has aroused the need to come up with software which provides communication with machines over Intranet. A LAN based Audio/Video based conferencing system designed for use by individual participants in a conference. In one embodiment one participant in the system is designated as an Instructor. Rest of the participants will be Students. Our proposed idea includes Audio/Video conferencing for a virtual classroom scenario that is E-Learning, Group Chat session between Instructor and all the Participants, Resource Sharing between only Instructor and Participant that is only One to One Sharing for sharing study material and a Questionnaire which is useful for doubt solving or any questions when either Instructor or any Participant is Offline or Unavailable at the moment. Our main focus is to implement Real Time-Transmission Protocol for Broadcasting Audio/Video Conferencing.

Keywords: *Audio/Video Conferencing; E-Learning; Rtp; Real Time Transmission Protocol; Virtual Classrooms*

I. INTRODUCTION

E-learning has a very distinct role to play in the context of scarcity of resources in developing countries. The most significant limitation of educational framework in these countries is the dearth of educational institution and qualified trainers for higher studies. There exist only few institutions facilitating continuing education for the professionals. But, the need for such facilities for professional development of the technologists is well recognized. Its demand is further enhanced by rapid evolution of technology and role of the technologists in economic development of the country. Despite having the potential to contribute in the educational advancement of developing countries, e-learning needs to be designed carefully to overcome the technological and infrastructural limitations. E-Learning provides highlighted improved collaboration and productivity among students as the online environment offers case studies, story-telling, demonstrations, role-playing, and simulations among other tools. Along with this, online training is less intimidating than instructor-led courses. Online learning provides a risk free. Environment that supports trying out new things and making mistakes.

II. POPULAR IMPLEMENTATION MODEL

Success of Instructor Led Online training using web conferencing setup depends on how well it is architecture, designed and deployed in an enterprise[5]. There are various approaches towards implementing a web conferencing solution in an enterprise, [5,6] which depends on the need of having the same. These requirements range from using the web conferencing implementation to conduct formal and informal meeting or important training programs. Primarily enterprise can choose between or on-premise setup

2.1. Hosted Setup with Limited Or Enterprise License

In case of hosted setup, enterprise connects to services that are configured and hosted at vendor's environment. Typically every organization which takes such a service from the vendor, gets a clearly defined storage space, work space and web portal to organize, schedule, plan and record the training programs. Enterprises receives two types of accesses on their respective environments, administrator and user management. User management ensures administrator role can create more administrators and end-users in the environment and add users of the organization to provide them appropriate access to participate in various events, programs, and sessions.[2]

A lot depends on the enterprise-dedicated infrastructure from the Internet Service Provider as hosted implementation uses internet backbone to participate in the events. Since participants are geographically dispersed, the bandwidth requirement drastically reduces and does not become a reason of contention at any specific location. However, if participants are not equally dispersed and are located at specific places in larger numbers for example offshore offices, then the quality of event and training program will depend on how good the internet bandwidth is from localized places. Another important aspect is to ensure there are appropriate proxy configurations to ensure smooth sail for event connections across offshore locations. If participants are joining from outside-office location, then a lot will depend on what connection bandwidth an individual has to join the event. [2]

III. PROPOSED SYSTEM

In Blended model, web conferencing is adopted in enterprise's intranet as well as internet. This means that LAN/WAN is used for candidates to join the event and those candidates who are geographically spread can join using internet bandwidth. Many of the enterprises have their employees located in their local offices along with various geographic locations including customer site. Since in such an enterprise, majority of the workforce is at local offices well connected on corporate LAN/WAN, intranet provides good quality of services and employees, who are geographically spread, can use ISP services to connect to the event. In order to provide a fail safe and reliable architecture, there are multiple servers used within enterprise intranet based on the spread of employees at offshore across locations. Similarly participants connecting through internet also connects to their nearest available server out of many available across geographies. This implementation model ensures every candidate has a list of servers available to connect and in case any of the servers is down, it automatically connects to the next nearest and best responding server. In case a server goes down during the event or training, a typical web conferencing solution will automatically try to connect to the next available server. A unique characteristic about blended model is that users connected through VPN may get hooked to intranet servers or internet servers irrespective of their location. If intranet servers are down then users can make use of servers available across the globe to connect. This brings an extremely reliable and fail safe environment with optimized use of bandwidth. Cost of blended model will be generally lower than the true on premise setup. Enterprises should go for hosted

model and extend the architecture to have web conferencing servers also on premise to consolidate a large pool of available servers both at intranet and at internet. For new candidates, and others who may be intimidated by benefits choices, the E-Learning course will provide an overview to bring all candidates up to a baseline level of Knowledge. Crew members will be guided through the course by an high end GUI and humor will be used, as appropriate, to engage learners. Where appropriate, visuals (e.g., tables, graphs, flow charts) and specific examples will be used to illustrate concepts to Crew members with a variety of learning styles. Throughout the course, links to benefits information on the resource hub will provide another layer of information— more detailed than what is in the course. This will enable learners to get more information on topics that are particularly relevant to them. Once Crew members are ready to make their benefits decisions, we will make it as easy as possible for them to access the specific information they need on the server, thus encouraging them to act as benefits consumers, researching the options and making the decisions that work best for them. All the virtual class would be recorded so as to enable the absentees.

IV. CONFERENCING ARCHITECHTURE

The conferencing architecture gives us the overview of how the system works. Each core in the diagram represents the workstation. Two video and audio conferencing modules will communicate with each other using Real Time Transmission Protocol. Before using these various functionalities shown in the diagram it is essential to set up communication between two PCs i.e. workstations.[1]

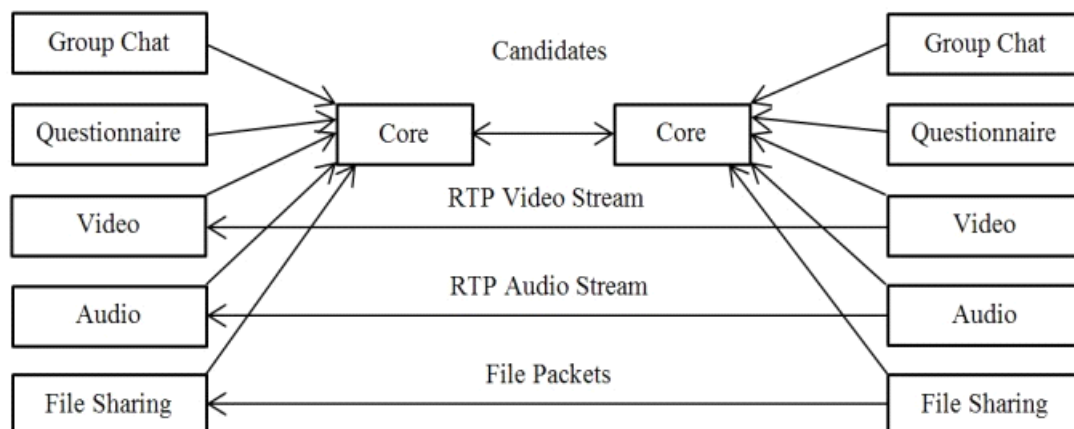


Fig. 1 Architecture

4.1 RTP

The Real-Time Transport Protocol (RTP) is an Internet protocol standard that specifies a way for programs to manage the real-time transmission of multimedia data over either unicast or multicast network services. Originally specified in Internet Engineering Task Force (IETF) Request for Comments (RFC) 1889, RTP was designed by the IETF's Audio-Video Transport Working Group to support video conferences with multiple, geographically dispersed participants. RTP is used extensively in communication and entertainment systems that involve streaming media, such as telephony, video conference applications. RTP itself does not guarantee real-time delivery of data, but it does provide mechanisms for sending and receiving applications to support streaming data. Typically, RTP runs on top of the UDP protocol, although the specification is general enough to support other transport protocols that know how Windows supports Real Time Communication

4.2 RTP Header

The RTP header provides the timing information necessary to synchronize and display audio and video data and to determine whether packets have been lost or arrive out of order. In addition, the header specifies the payload type, thus allowing multiple data and compression types. This is a key advantage over most proprietary solutions, which specify a particular type of compression and thus limit users' choice of compression schemes.

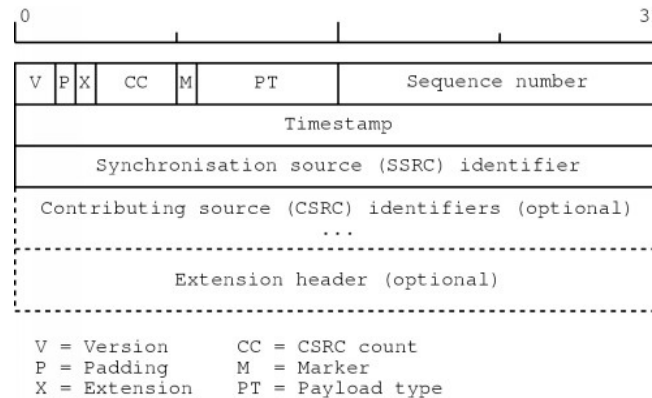


Fig. 2. RTP Header Format

The RTP header has a minimum size of 12 bytes. After the header, optional header extensions may be present. This is followed by the RTP payload, the format of which is determined by the particular class of application. The fields in the header are as follows:

- Version: (2 bits) Indicates the version of the protocol. Current version is 2.
- P(Padding):(1 bit) Used to indicate if there are extra padding bytes at the end of the RTP packet. Padding might be used to fill up a block of certain size, for example as required by an encryption algorithm. The last byte of the padding contains the number of padding bytes that were added (including itself).
- X(Extension):(1bit)Indicates presence of an Extension header between standard header and payload data. This is application or profile specific.
- CC(CSRC Count):(4 bits) Contains the number of CSRC identifiers (defined below) that follow the fixed header.
- M (Marker):(1 bit) Used at the application level and defined by a profile. If it is set, it means that the current data has some special relevance for the application.
- PT(Payload Type):(7 bits) Indicates the format of the payload and determines its interpretation by the application. This is specified by an RTP profile. For example, see RTP Profile for audio and video conferences with minimal control.
- Sequence Number :(16 bits) The sequence number is incremented by one for each RTP data packet sent and is to be used by the receiver to detect packet loss and to restore packet sequence. The RTP does not specify any action on packet loss; it is left to the application to take appropriate action. For example, video applications may play the last known frame in place of the missing frame. The initial value of the sequence number should be random to make known-plaintext attacks on encryption more difficult. RTP provides no guarantee of delivery, but the presence of sequence numbers makes it possible to detect missing packets.
- Timestamp: (32 bits) Used to enable the receiver to play back the received samples at appropriate intervals. When several media streams are present, the timestamps are independent in each stream, and may not be relied upon for media synchronization. The granularity of the timing is application specific. For example, an audio application that samples data once every 125 μ s (8 kHz, a common sample rate in digital telephony) could

use that value as its clock resolution. The clock granularity is one of the details that is specified in the RTP profile for an application.

- SSRC: (32 bits) Synchronization source identifier uniquely identifies the source of a stream. The synchronization sources within the same RTP session will be unique.
- CSRC :(32 bits each) Contributing source IDs enumerate contributing sources to a stream which has been generated from multiple sources.
- Extension header: (optional) The first 32-bit word contains a profile-specific identifier (16 bits) and a length specify

V. SYSTEM BLOCK DIAGRAM

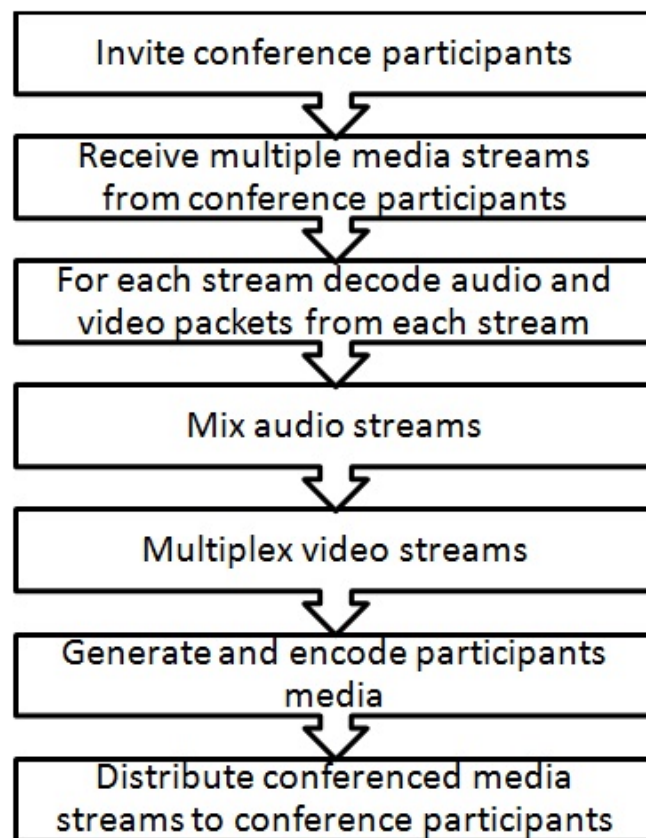


Fig.3 Block Diagram

VI. PROPOSED SYSTEM

Interaction between teacher and students wherein students who are registered in the system can discuss among themselves the topic in consideration and even then if they have any doubts they can consult the teacher available at that time. i.e. there is be ONE TO MANY interaction where one teacher interacts with more than one student discussing the topic at that time and solves their doubts

VII. PROJECT SCREENSHOT

7.1 Parent Form

Which helps user to interact with the application to join or to start the session.

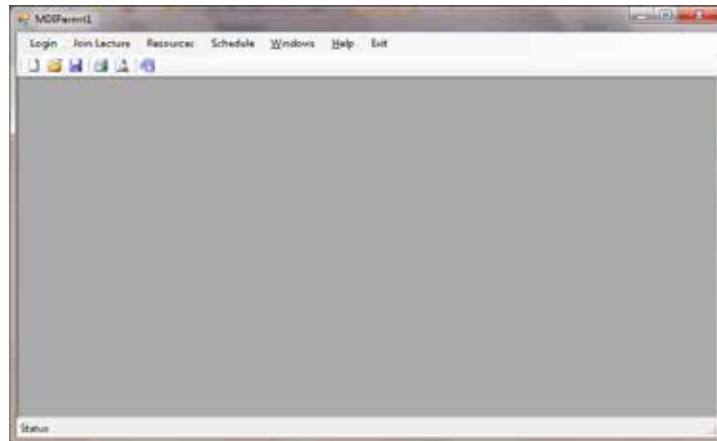


Fig.4 Parent

7.2 Login Form

Teacher and Student both have to enter their username and password to Start or to Join the session, the username and pass will get checked with database



Fig.5 Login window

7.3 Selection and Resource

Student can select various subjects from the list who's lecture s/he wish to join. Also from "Get All Resource" student can download all the necessary notes , assignments or any important information uploaded by teacher/ who started the session.

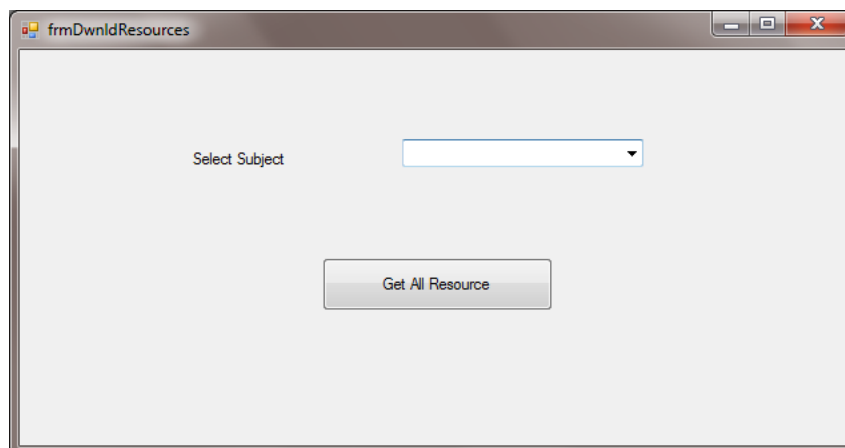


Fig.6 Selection & Resource

7.4 Other features Are

Discussion Forum: It is a forum for all learners and teachers to exchange knowledge with all other users who are registered with e-Learning. This is also meant for learners to interact with teacher to exchange their thoughts on topics taught. One can View other queries replies

- I. Post a query.
- II. Reply a query.
 - Learning is self-directed, allowing students to choose content and tools appropriate to their differing interests, needs, and skill levels
 - Accommodates multiple learning styles using a variety of delivery methods geared to different learners; more effective for certain learners
 - Designed around the learner
 - Geographical barriers are eliminated, opening up broader education options
 - 24/7 accessibility makes scheduling easy and allows a greater number of people to attend classes
 - On-demand access means learning can happen precisely when needed
 - Travel time and associated costs (parking, fuel, vehicle maintenance) are reduced or eliminated
 - Potentially lower costs for companies needing training, and for the providers
 - Fosters greater student interaction and collaboration
 - Fosters greater student/instructor contact
 - Enhances computer and Internet skills
 - Has the attention of every major university in the world, most with their own online degrees, certificates, and individual courses

VIII. FUTURE ENHANCEMENTS & CONCLUSION

The key applications makes course is suitable for new and established computer users, individually or in groups, at home or in the organization. Meeting the highest e-learning instructional design standards, In future projects providing a group discussion among the various students who are registered with the application can be created. Enhanced application may allow the students to share resources among themselves. Flash Animations, Real time videos can be used as teaching aids, in order, to increase the interest of students. Online examinations can be conducted in order to obtain the overall idea of how well students have understood.

REFERENCES

- [1] Kedar Jedhe, Suraj Gosavi, Swapnil Kharche, Rahul Bagul, Prof. S. M. Sangave, "Intranet Conferencing Solution" International Journal of Emerging Technology and Advanced Engineering Website: www.ijetae.com (ISSN 2250-2459, Volume 2, Issue 4, April 2012)
- [2] Alok Tiwari, Amit Tiwary, Yogesh Bhatt, "A Distributed Web Conferencing Architecture to Meet Inorganic Training Needs of an Enterprise" International Conference on Education and Management Technology (ICEMT 2010)
- [3] Alok Tiwari and Amit Tiwary, "Imperative web conferencing tools for effective distance learning in an enterprise," IEEE Xplore, in press.

- [4] Bernard, R. M., Abrami, P.C., Lou, Y., Borokhovski, E., Wade, A., Wozney, L., Wallet, P.A., Fiset, M., and Huang, B.2004. How Does Distance Education Compare With Classroom Instruction? A Meta-Analysis of the Empirical Literature. Review of Educational Research, 74, 3 (Fall 2004),379-439.
- [5] Sue Spielman and Liz Winfeld, The Web Conferencing Book: Understand the technology, choose the right vendors.AMACOM, 2003.
- [6] Snow, C., Pullen, J. and McAndrews, P., An Open-Source Web-Based System for Synchronous Distance Education,IEEE Trans on Education, vol. 4, Nov 2005, pp. 705-712.

CHAIN SYSTEM THE FORMULA WITH INCREASING COMMISSION

Himanshu

Guru Nanak College, Budhlada, Mansa, P.B, (India)

ABSTRACT

In this paper I describe the formula which is useful to determine the profit or loss in chain business having variable commission. I also describe a formula which is helpful to calculate the profit for a participant according to number of members made participants by him in his chain.

Keyword-To Evaluate Total Profit Or Loss, Commission,

I. INTRODUCTION

I had published a article named CHAIN SYSTEM THE FORMULA recently in INTERNATIONAL JOURNAL OF MATHEMATICS TRENDS AND TECHNOLOGY in this paper we can find profit chain business system but in which the commission remains stable at all the stages.

I had also published a article named COMPLEX CHAIN SYSTEM THE FORMULA recently in INTERNATIONAL JOURNAL OF SCIENCE AND RESEARCH in this paper we can find profit of chain business in which not every participant necessarily make other members participant but the commission remains stable.

I had also published a article named CHAIN SYSTEM THE FORMULA WITH CHANGEABLE COMMISSION recently in INTERNATIONAL JOURNAL OF SCIENTIFIC RESEARCH AND EDUCATION in which every participant makes his own members in his chain and they get commission can be changed at different stages.

I had also published a article named COMPLEX CHAIN SYSTEM THE FORMULA WITH CHANGEABLE COMMISSION recently in INTERNATIONAL JOURNAL OF MULTIDISCIPLINARY RESEARCH AND DEVELOPMENT in which not every participant necessarily to make other members in his chain and they get commission can be changed at different stages.

But now in this paper I describe a formula *Chain System The Formula With Increasing Commission* , for this formula we can find profit of chain business in which every participant makes his own members in his chain and they get commission can be changed at different stages. This also helps to find that a company is gaining or losing something with the chain business.

The members which participate in chain they can find their profit easily.

Procedure of commission change used in formula-

I will like to clear it with a example that is- Suppose if a person completes a task and gets A% commission of

starting price and then if second task is also completed by him then he will get $\left\{ \frac{A}{100} * P + A \right\}$

commission(where P is starting price) and $\left\{ \frac{A}{100} * P + 2A \right\}$ commission for next task and so on.

The formulae are-

1. Formula which find the chain's stages through a number of members those participate in the chain system

$$\text{Total member} = \frac{(G^n - 1)}{(G - 1)}$$

- "G" shows the type of group mean number of members which is to be participated by a member this chain, that is a member can make only "G" number of members the participant.

- "n" number of stage.

2. Formula for total profit =

$$\frac{(G^n - 1)P}{G - 1} - \frac{(G^n - G)D}{(G - 1)^2} + \frac{C}{(G - 1)} + (n - 1) \frac{DG}{(G - 1)^2} + \frac{C}{(G - 1)} + \frac{(n - 2)D}{2(G - 1)}$$

- "P" shows the starting price mean the starting investment by each member.

- "C" showing starting commission mean the first profit gained a member after completing his first task.

- "D" Showing number of percent mean if the first profit gained a member after completing his first task like if he get A% commission of starting price THEN $D = A$

3. Formula for evaluating the commission = $(n-1)C + \frac{(n-1)(n-2)D}{2}$

II. METHODOLOGY

- If every member has put "G" member and every "G" member has to put "G" member toward then:-

- Total member = $\frac{(G^n - 1)}{(G - 1)}$

- Total profit =

- $\frac{(G^n - 1)P}{G - 1} - \frac{(G^n - G)D}{(G - 1)^2} + \frac{C}{(G - 1)} + (n - 1) \frac{DG}{(G - 1)^2} + \frac{C}{(G - 1)} + \frac{(n - 2)D}{2(G - 1)}$

Where "P" is starting Price

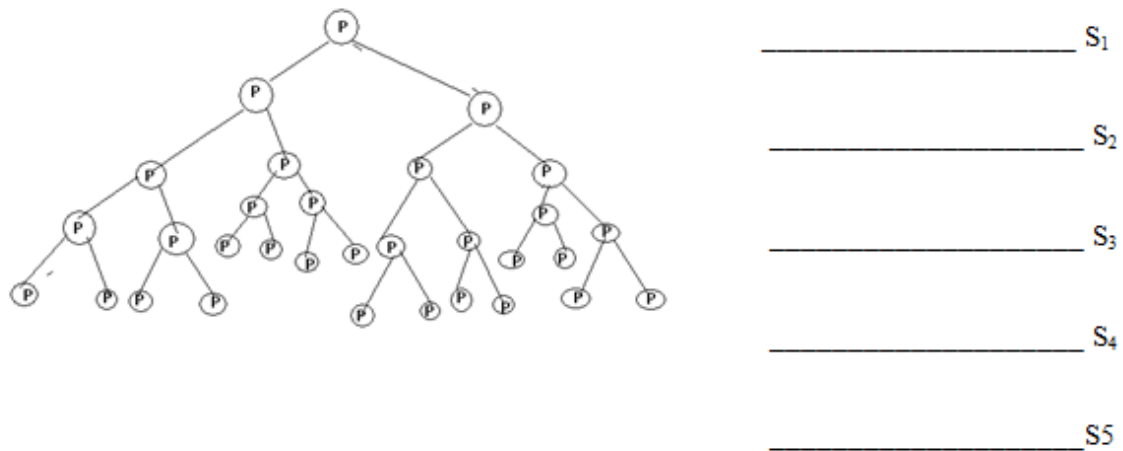
"C" is commission

"n" is no. of Stages

"D" is no. Of %

- For example:- If every member has put 2-2 member for his chain, starting price is 500 Rs., Starting commission is 20% of starting Price, Total member is 31, then find out the profit?

Ans:-



Since Starting Price = 500 RS

Starting Commission = 20% of 500 RS

Then Starting Commission = 100 RS

Profit of S1 = 500 Rs

Profit of S2 = 2(500) - 100 = 900 Rs

Profit of S3 = 4(500) - 2(100) - 120 = 1680 Rs

Profit of S4 = 8(500) - 400 - 240 - 140 = 3220 Rs

Profit of S5 = 16(500) - 800 - 480 - 280 - 160 = 6280 Rs

Total Profit = 12580 Rs.

By his methodology:-

Total member = 31

We know Total member = $\frac{G^n - 1}{G - 1}$

Since G = 2; then $\frac{2^n - 1}{2 - 1} = 31$

$2^n = 32$

$n = 5$

We know total profit =

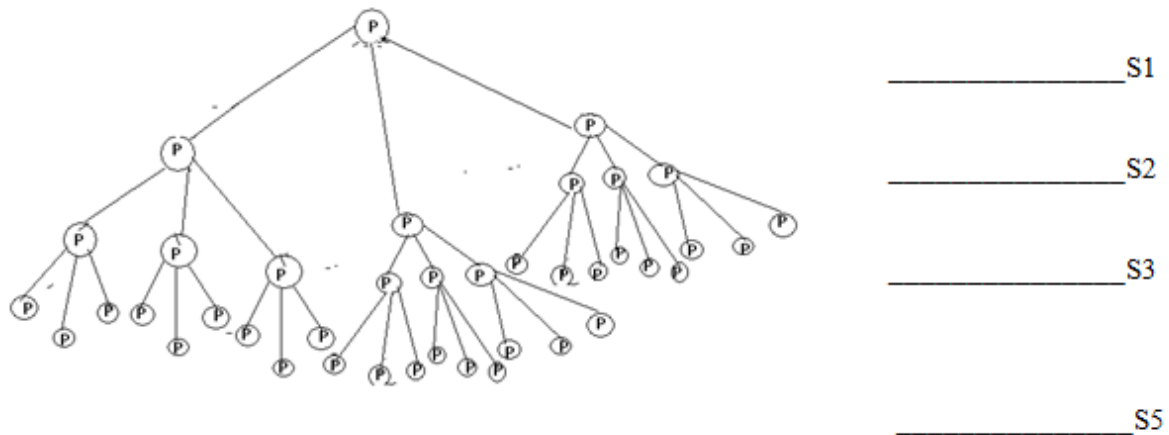
$$\frac{G^n - 1}{G - 1} P - \frac{G^n - G}{G - 1} C + \frac{D}{(G - 1)^2} + \frac{C}{(G - 1)} + (n - 1) \left[\frac{DG}{(G - 1)^2} + \frac{C}{(G - 1)} + \frac{(n - 2)D}{2(G - 1)} \right]$$

Since G = 2; P = 500; n = 5; C = 100; D = 20

$$\begin{aligned} \text{Total profit} &= \frac{2^5 - 1}{2 - 1} \times 500 - \frac{2^5 - 2}{2 - 1} \times \frac{20}{(2 - 1)^2} + \frac{100}{(2 - 1)} + (5 - 1) \times \frac{20(2)}{(2 - 1)^2} + \frac{100}{(2 - 1)} + \frac{(5 - 2)20}{2(2 - 1)} \\ &= 15500 - (30)(20+100) + (4)(40+100+30) \\ &= 15500 - 3600 + 680 \\ &= 12580 \text{ Rs. Ans.....} \end{aligned}$$

For example:- If every member has put 3-3 member for his chain Starting price is 800 RS, Starting commission is 25 of Starting Price ; total member is 40. then find out the total profit?

Ans:-



Since Starting Price = 800 RS
 Starting Commission = 25% of 800 RS
 Then Starting Commission = 200 RS
 Profit of S1 = 800 Rs
 Profit of S2 = 3(800) - 200 = 2200 Rs
 Profit of S3 = 9(800) - 3(200) - 225 = 6375 Rs
 Profit of S4 = 27(800) - 9(200) - 3(225) - 250 = 18875 Rs
 Total Profit = 28250 Rs.

By this Methodology:-

Total member = 40

We know total member = $\frac{G^n - 1}{G - 1}$

Since G = 3, then $\frac{3^n - 1}{3 - 1} = 40$

$3^n = 81$

$n = 4$

We know total profit =

$$\frac{G^n - 1}{G - 1} P - \frac{G^n - G}{G - 1} \frac{C}{G} - \frac{D}{(G - 1)^2} + \frac{C}{(G - 1)} + (n - 1) \frac{DG}{(G - 1)^2} + \frac{C}{(G - 1)} + \frac{(n - 2)D}{2(G - 1)}$$

Since $G = 3; n=4; P = 800; C=200; D=25;$

Now total profit =

$$\frac{3^4 - 1}{3 - 1} (800) - \frac{3^4 - 3}{3 - 1} \frac{200}{3} - \frac{25}{(3 - 1)^2} + \frac{200}{(3 - 1)} + (4 - 1) \frac{(25)3}{(3 - 1)^2} + \frac{200}{(3 - 1)} + \frac{(4 - 2)25}{2(3 - 1)}$$

$$= (40) (800) - (39) \left(\frac{25}{4} + 100 \right) + 3 \left(\frac{75}{4} + 100 + \frac{25}{2} \right)$$

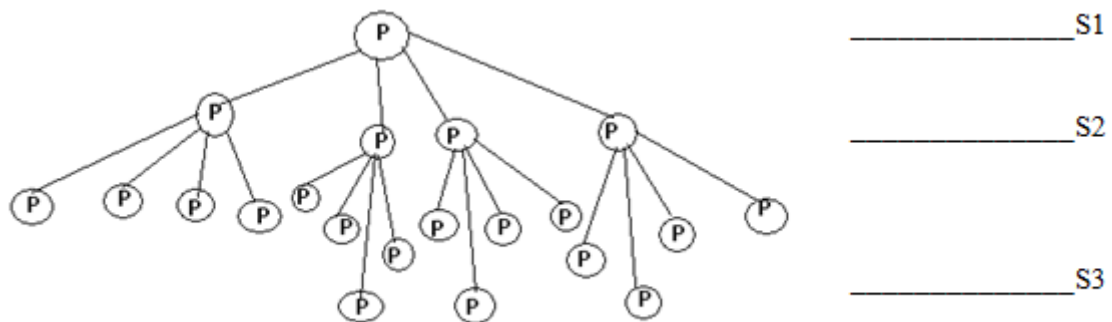
$$= 32000 - \frac{6575}{4} + \frac{575}{4}$$

$$= 32000 - 3750$$

$$= 28250 \text{ RS Ans.....}$$

For example:- If every member has put 4-4 member for his chain Starting price is 400, Starting commission is 20 % of starting price; total member is 21. then find out the total profit?

Ans:-



Since Starting Price = 400 RS

Starting Commission = 20% of 400 RS

Then Starting Commission = 80 RS

Profit of S1 = 400 Rs

Profit of S2 = 4(400) - 80 = 1520 Rs

Profit of S3 = 16(400)-4(80)-100= 5980 Rs

Total Profit = 7900 RS

- By this methodology:-

Total member = 21

We know total member = $\frac{G^n - 1}{G - 1}$

Since G = 4, then $\frac{4^n - 1}{4 - 1} = 21$

$4^n = 64$

$n = 3$

We know that total profit =

$$\frac{G^n - 1}{G - 1}P - \frac{G^n - G}{G - 1}D + \frac{C}{G - 1} + (n - 1)\frac{DG}{(G - 1)^2} + \frac{C}{G - 1} + \frac{(n - 2)D}{2(G - 1)}$$

Since G = 4; n = 3; P = 400; C = 80; D = 20;

Now total profit =

$$\frac{4^3 - 1}{4 - 1}(400) - \frac{4^3 - 4}{4 - 1}20 + \frac{80}{4 - 1} + (3 - 1)\frac{(20)4}{(4 - 1)^2} + \frac{80}{4 - 1} + \frac{(3 - 2)20}{2(4 - 1)}$$

$$= (21)(400) - (20)\left(\frac{20}{9} + \frac{80}{3}\right) + (2)\left(\frac{80}{9} + \frac{80}{3} + \frac{10}{3}\right)$$

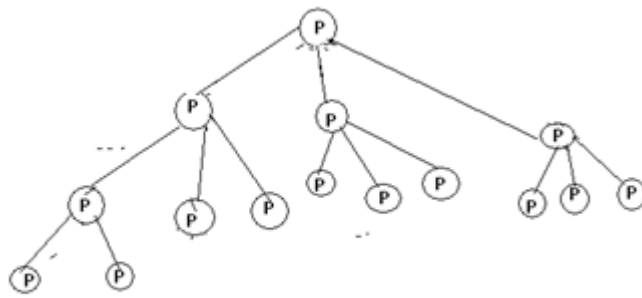
$$= 8400 - \frac{5200}{9} + \frac{700}{9}$$

$$= 8400 - 500$$

$$= 7900 \text{ RS Ans.....}$$

- For example:- If every member has put 3-3 member for his chain Starting price is 1000, Starting commission is 20% of starting price ; total member is 15. then find out the total profit?

Ans:-



_____ S1

_____ S2

_____ S3

Since Starting Price = 1000 RS

Starting Commission = 20% of 1000 RS

Then Starting Commission = 200 RS

Profit of S1 = 1000 Rs

Profit of S2 = 3(1000) - 200 = 2800 Rs

Profit of S3 = 9(1000) - 3(200) - 220 = 8180 Rs

Profit of S4 is = 2(1000) = 2000 Rs

Total Profit = 13980 Rs.

• By this methodology:-

Total member = 15

We know total member = $\frac{G^n - 1}{G - 1}$

Since G = 3, then $\frac{3^n - 1}{3 - 1} = 15$

$3^n = 31$

If this does not express in power of "3" then a smaller number is chosen which can be expressed in power of "3" completely like 27;

$3^n = 27$

$n = 3$

"R" is equal to difference between them

$R = 31 - 27 = 4$

$\Rightarrow R = 4$

We know that total profit =

$$\frac{G^n - 1}{G - 1} P - \frac{G^n - G}{G - 1} \frac{D}{(G - 1)^2} + \frac{C}{G - 1} + (n - 1) \frac{DG}{(G - 1)^2} + \frac{C}{G - 1} + \frac{(n - 2)D}{2(G - 1)}$$

Since G = 3; n = 3; P = 1000; C = 200; D=20;

Now some part of total profit =

$$\begin{aligned} & \frac{3^3 - 1}{3 - 1} (1000) - \frac{3^3 - 3}{3 - 1} \frac{20}{(3 - 1)^2} + \frac{200}{3 - 1} + (3 - 1) \frac{(20)3}{(3 - 1)^2} + \frac{200}{3 - 1} + \frac{(3 - 2)20}{2(3 - 1)} \\ & = 13000 - (12)(5+100)+(2)(15+100+5) \\ & = 13000 -1260+240 \\ & = 11980 \text{ Rs} \end{aligned} \quad \text{_____ (1)}$$

Now find out $I = \frac{R}{G - 1}$

Now we arises three cases:-

Case 1:- If $I < G$ then (IP) add in (1)

Case 2:- If $I = G$ then (IP-C) add in (1)

Case 1:- If $I > G$ then find out $\frac{I}{G} = X$. ____

and arises two cases more

Case 1:- If $X < G$ then add (IP-XC) in (1)

Case 2:- If $X \geq G$ then find out $\frac{X}{G} = Y$. ____

Then add [IP-XC-Y(C+R)] in (1)

Now $I = \frac{R}{G - 1} = \frac{4}{3 - 1} = 2$

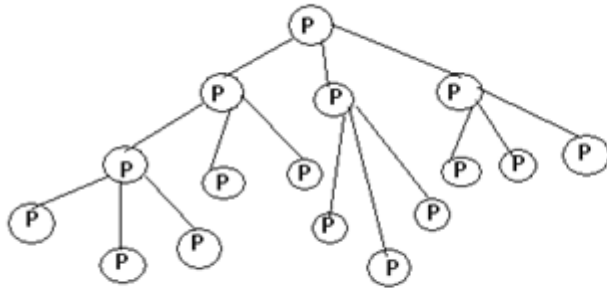
Since $2 < 3$

$I < G$

Then add 2(1000) in (1) _____(By Case:1)

Total profit = 11980 + 2000 = 13980 Rs Ans.....

- For example:- If every member has put 3-3 members for his chain, starting Price is 700 Rs. , Starting commission is 25% of starting price, total member is 16 then find out the total profit?



_____ S2

_____ S3

_____ S4

Since Starting Price = 700 RS

Starting Commission = 25% of 700 RS

Then Starting Commission = 175 RS

Profit of S1 is = 700 Rs

Profit of S2 is = 2100-175 = 1925 Rs

Profit of S3 is = 6300-3(175)-200 = 5575 Rs

Profit of S4 is = 2100-175 = 1925 Rs

Total profit = 10125 Rs

• By this methodology:-

Total member = 16

We know total member = $\frac{G^n - 1}{G - 1}$

Since G = 3, then $\frac{3^n - 1}{3 - 1} = 15$

○ $3^n = 33$

○ R = 6

○ $3^n = 27$

○ n = 3

We know that some part of profit =

$$\frac{G^n - 1}{G - 1} P - \frac{G^n - G}{G - 1} \frac{D}{(G - 1)^2} + \frac{C}{(G - 1)} + (n - 1) \frac{DG}{(G - 1)^2} + \frac{C}{(G - 1)} + \frac{(n - 2)D}{2(G - 1)}$$

Since G = 3; n = 3; P = 700; C = 175; D=25;

Now some part of total profit =

$$\begin{aligned}
 & \frac{3^3 - 1}{3 - 1} (700) - \frac{3^3 - 3}{3 - 1} \frac{25}{(3 - 1)^2} + \frac{175}{3 - 1} + (3 - 1) \frac{25(3)}{(3 - 1)^2} + \frac{175}{3 - 1} + \frac{(3 - 2)25}{2(3 - 1)} \\
 & = (13)(700) - 12 \frac{25}{4} + \frac{175}{2} + (2) \frac{75}{4} + \frac{175}{2} + \frac{25}{4} \\
 & = 9100 - (75 + 1050) + (50 + 175) \\
 & = 8200 \text{ Rs} \quad \text{-----(1)}
 \end{aligned}$$

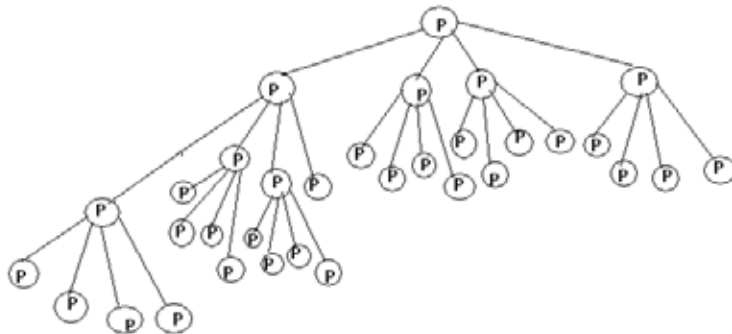
Now $I = \frac{R}{G - 1} = \frac{6}{2} = 3$

I = 3 Since I = G

Then [3(700)-175] add in (1) ----- (By Case:2)

Total profit = 8200 + 1925 = 10125 Rs Ans.....

- For example:- If every member has put 4-4 members for his chain, starting price is 500 Rs. , Starting commission is 40% of starting price, total member is 33 then find out the total profit?



Since Starting Price = 500 RS
 Starting Commission = 40% of 500 RS
 Then Starting Commission = 200 RS
 Profit of S1 is = 500 Rs
 Profit of S2 is = 2000-200 = 1800 Rs
 Profit of S3 is = 8000-800-240 = 6960 Rs
 Profit of S4 is = 6000-600 = 5400 Rs
 Total profit = 14660 Rs

- By this methodology:-

Total member = 33

$$\text{We know total member} = \frac{G^n - 1}{G - 1}$$

$$\text{Since } G = 4, \text{ then } \frac{4^n - 1}{4 - 1} = 33$$

$$\bar{O} \quad 4^n = 100$$

$$\bar{O} \quad R = 36$$

$$\bar{O} \quad 4^n = 64$$

$$\bar{O} \quad n = 3$$

We know that total profit =

$$\frac{G^n - 1}{G - 1} P - \frac{G^n - G}{G - 1} \frac{D}{(G - 1)^2} + \frac{C}{G - 1} + (n - 1) \frac{DG}{(G - 1)^2} + \frac{C}{G - 1} + \frac{(n - 2)D}{2(G - 1)}$$

Since $G = 4$; $n = 3$; $P = 500$; $C = 200$; $D = 40$;

Now some part of total profit =

$$\frac{4^3 - 1}{4 - 1} (500) - \frac{4^3 - 4}{4 - 1} \frac{40}{(4 - 1)^2} + \frac{200}{4 - 1} + (3 - 1) \frac{(40)4}{(4 - 1)^2} + \frac{200}{4 - 1} + \frac{(3 - 2)40}{2(4 - 1)}$$

$$= 10500 - (20) \left(\frac{640}{9} + \frac{200}{3} \right) + (2) \left(\frac{160}{9} + \frac{200}{3} + \frac{20}{3} \right)$$

$$= 10500 - (20) \left(\frac{640}{9} + \frac{820}{9} \right)$$

$$= 10500 - 1240$$

$$= 9260 \text{ Rs} \quad \text{_____ (1)}$$

$$\text{Now } I = \frac{R}{G - 1} = \frac{36}{4 - 1} = 12$$

$$12 > 3 \quad \text{Since } I > G$$

$$\text{Then we find out } \frac{I}{G} = ?$$

$$\frac{I}{G} = \frac{12}{4} = 3$$

Since $3 < 4$

Then add $IP - 3C$ in (1) _____ (By Case:3.1)

$$\text{Mean } (12)(500) - 3(200)$$

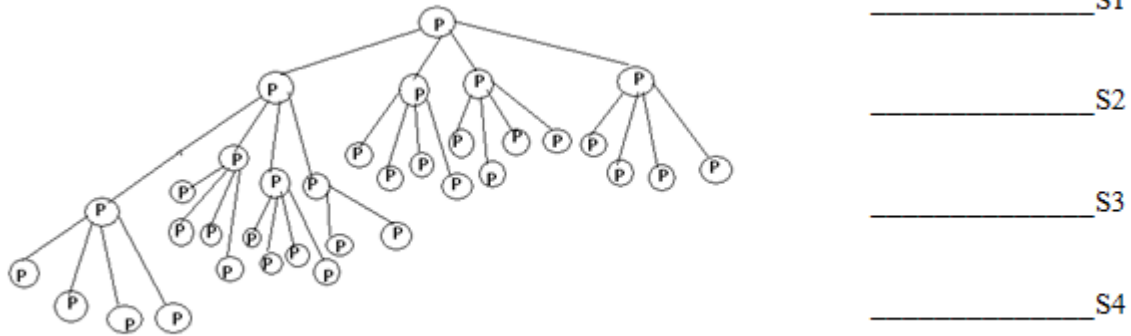
$$= 6000 - 600$$

$$= 5400 \text{ Rs}$$

Add in (1)

Total profit = 9260 + 5400 = 14660 Rs Ans.....

- For example:- If every member has put 4-4 members for his chain, starting price is 1000 Rs. , Starting commission is 50% of starting price, total member is 35 then find out the total profit?



Since Starting Price = 1000 RS
 Starting Commission = 50% of 1000 RS
 Then Starting Commission = 500 RS
 Profit of S1 is = 1000 Rs
 Profit of S2 is = 4(1000)-500 = 3500 Rs
 Profit of S3 is = 16(1000)-4(500)-550 = 13450 Rs
 Profit of S4 is = 14(1000)-3(500) = 12500 Rs
 Total profit = 30450 Rs Ans.....

- By this methodology:-

Total member = 35

We know total member = $\frac{G^n - 1}{G - 1}$

Since G = 4, then $\frac{4^n - 1}{4 - 1} = 35$

- $4^n = 106$
- $R = 42$
- $4^n = 64$
- $n = 3$

We know that total profit =

$$\frac{G^n - 1}{G - 1} P - \frac{G^n - G}{G - 1} \frac{C}{G} - \frac{D}{(G - 1)^2} + \frac{C}{(G - 1)} + (n - 1) \frac{DG}{(G - 1)^2} + \frac{C}{(G - 1)} + \frac{(n - 2)D}{2(G - 1)}$$

Since G = 4; n = 3; P = 1000; C = 500; D=50;

Now some part of total profit =

$$\frac{4^3 - 1}{4 - 1} (1000) - \frac{4^3 - 4}{4 - 1} \frac{500}{4} - \frac{50}{(4 - 1)^2} + \frac{500}{(4 - 1)} + (3 - 1) \frac{50(4)}{(4 - 1)^2} + \frac{500}{(4 - 1)} + \frac{(3 - 2)50}{2(4 - 1)}$$

$$= 21000 - (20) \left(\frac{50}{9} + \frac{500}{3} \right) + (2) \left(\frac{200}{9} + \frac{500}{3} + \frac{25}{3} \right)$$

$$= 21000 - (20) \frac{1550}{9} + (2) \frac{1775}{9}$$

$$= 21000 - 3050$$

$$= 17950 \text{ Rs} \quad \text{-----} (1)$$

$$\text{Now } I = \frac{R}{G - 1} = \frac{42}{4 - 1} = 14$$

$$14 > 4 \quad \text{Since } I > G$$

$$\text{Now } \frac{I}{G} = \frac{14}{4} = 3.5$$

Since 3 < 4

$$X < G$$

Then add in (1) (IP-XC) ----- (By Case:3.1)

Mean 14000-3(500)

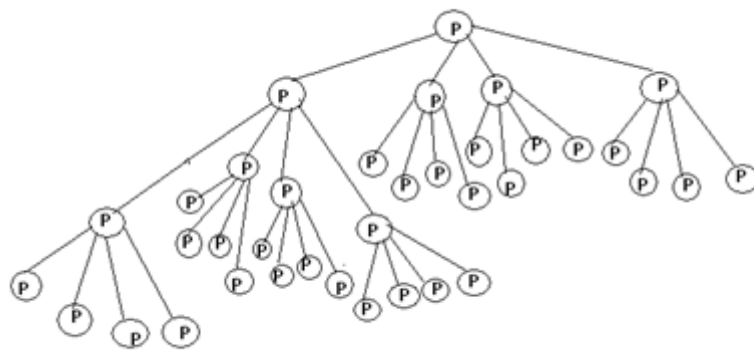
$$= 14000 - 1500$$

$$= 12500 \text{ Rs}$$

Add in (1)

Total profit = 17950 + 12500 = 30450 Rs. Ans.....

- For example:- If every member has put 4-4 members for his chain, starting price is 800 Rs. , Starting commission is 60% of starting price, total member is 37 then find out the total profit?



_____ S1

_____ S2

_____ S3

_____ S4

Since Starting Price = 800 RS

Starting Commission = 60% of 800 RS

Then Starting Commission = 480 RS

Profit of S1 is = 800 Rs

Profit of S2 is = 4(800)-480 = 2720 Rs

Profit of S3 is = 16(800)-4(480)-540 = 10340 Rs

Profit of S4 is = 16(800)-4(480)-540 = 10340 Rs

Total profit = 24200 Rs

· By this methodology:-

Total member = 33

We know total member = $\frac{G^n - 1}{G - 1}$

Since G = 4, then $\frac{4^n - 1}{4 - 1} = 33$

○ $4^n = 112$

○ R = 48

○ $4^n = 64$

○ n = 3

We know that total profit =

$$\frac{G^n - 1}{G - 1} P - \frac{G^n - G}{G - 1} \frac{D}{(G - 1)^2} + \frac{C}{(G - 1)} + (n - 1) \frac{DG}{(G - 1)^2} + \frac{C}{(G - 1)} + \frac{(n - 2)D}{2(G - 1)}$$

Since G = 4; n = 3; P = 800; C = 480; D=60;

Now some part of total profit =

$$\frac{4^3 - 1}{4 - 1} (800) - \frac{4^3 - 4}{4 - 1} \frac{60}{(4 - 1)^2} + \frac{480}{(4 - 1)} + (3 - 1) \frac{(60)4}{(4 - 1)^2} + \frac{480}{(4 - 1)} + \frac{(3 - 2)60}{2(4 - 1)}$$

$$= 16800 - (20) \left(\frac{60}{9} + \frac{480}{3} \right) + (2) \left(\frac{240}{9} + \frac{480}{3} + \frac{10}{1} \right)$$

$$= 16800 - \frac{30000}{9} + \frac{3540}{9}$$

$$= 16800 - 2940$$

$$= 13860 \text{ Rs} \quad \text{-----} (1)$$

$$\text{Now } I = \frac{R}{G - 1} = \frac{48}{4 - 1} = 16$$

$$16 > 4 \quad \text{Since } I > G$$

$$\text{Now } \frac{I}{G} = \frac{16}{4} = 4$$

$$X = 4$$

Since $4 > 3$

So $X > G$

$$\text{Then } \frac{X}{G} = \frac{4}{4} = 1$$

So $Y = 1$

Then add $(IP - XC - 2YC)$ in (1) ----- (By Case:3.2)

$$\text{Mean } (16)(800) - 4(480) - (1)(540)$$

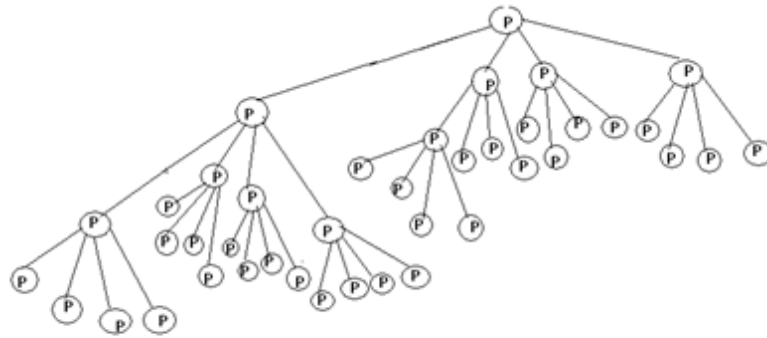
$$= 10340 \text{ Rs}$$

Add in (1)

$$\text{Total profit} = 13860 + 10340$$

$$= 24200 \text{ Rs}$$

- For example:- If every member has put 4-4 members for his chain, starting price is 2000 Rs., Starting commission is 40% of starting price, total member is 41 then find out the total profit?



_____ S1

_____ S2

_____ S3

_____ S4

Since Starting Price = 2000 RS

Starting Commission = 40% of 2000 RS

Then Starting Commission = 800 RS

Profit of S1 is = 2000 Rs

Profit of S2 is = 4(2000)-800 = 7200 Rs

Profit of S3 is = 16(2000)-4(800)-840 = 27960 Rs

Profit of S4 is = 20(2000)-5(800)-840 = 35160 Rs

Total profit = 72320 Rs.

• By this methodology:-

Total member = 41

We know total member = $\frac{G^n - 1}{G - 1}$

Since G = 4, then $\frac{4^n - 1}{4 - 1} = 41$

○ $4^n = 124$

○ R = 60

○ $4^n = 64$

○ n = 3

We know that total profit =

$$\frac{G^n - 1}{G - 1} P - \frac{C}{G - 1} - \frac{D}{(G - 1)^2} + \frac{C}{(G - 1)} + (n - 1) \frac{DG}{(G - 1)^2} + \frac{C}{(G - 1)} + \frac{(n - 2)D}{2(G - 1)}$$

Since G = 4; n = 3; P = 2000; C = 800; D=40;

Now some part of total profit =

$$\begin{aligned} & \frac{24^3 - 1}{4 - 1} (2000) - \frac{24^3 - 4}{4 - 1} \frac{40}{(4 - 1)^2} + \frac{800}{(4 - 1)} + (3 - 1) \frac{40(4)}{(4 - 1)^2} + \frac{800}{(4 - 1)} + \frac{(3 - 2)(40)}{2(4 - 1)} \\ &= 42000 - (20) \left(\frac{40}{9} + \frac{800}{3} \right) + (2) \left(\frac{160}{9} + \frac{800}{3} + \frac{20}{3} \right) \\ &= 42000 - (20) \frac{2440}{9} + (2) \frac{2620}{9} \\ &= 42000 - 4840 \\ &= 37160 \text{ Rs} \end{aligned} \quad \text{_____ (1)}$$

Now $I = \frac{R}{G - 1} = \frac{60}{4 - 1} = 20$
 $20 > 4$ Since $I > G$

Now $\frac{I}{G} = \frac{20}{4} = 5$

\bar{O} $X = 5$

\bar{O} $5 > 4$

\bar{O} $X > G$

Then $\frac{X}{G} = \frac{5}{4} = 1.25$

Then $Y = 1$

Then add in (1) $\{(IP - XC - Y(C+D))\}$ _____ (By Case:3.2)

Mean $(20(2000) - 5(800) - 840)$

$= 35160$ add in (1)

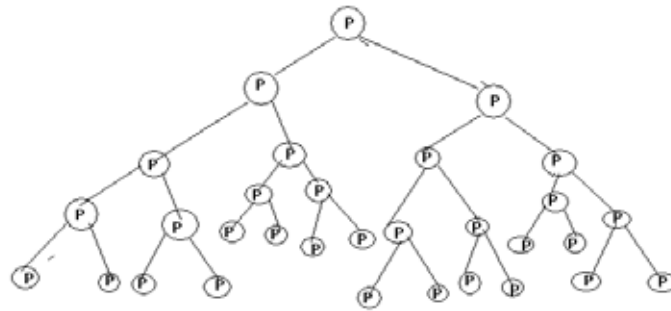
Total profit = $37160 + 35160 = 72320$ Rs Ans.....

For calculating commission = $(n-1)C + \frac{(n-1)(n-2)}{2} D$

For example: If a member has a task of making 2 participants and he have now a total of 31 participants in his chain, if Starting price is 1000 Rs., starting commission is 60% of starting price, then find out the total commission = ?

Sol.

Ts



Since Starting Price = 1000 RS

Starting Commission = 60% of 1000 RS

Then Starting Commission = 600 RS

Since total member is 31

We know total member = $\frac{G^n - 1}{G - 1}$

Since G = 2; then $\frac{2^n - 1}{2 - 1} = 31$

$2^n = 32$

$n = 5$

We know total commission = $(n-1)C + \frac{(n-1)(n-2)}{2}D$

Since n=5, C=600,D=60,

$$= (5-1)600 + \frac{(5-1)(5-2)}{2}60$$

$$= (2400) + (360)$$

$$= 2760 \text{ Rs. Ans.....}$$

II. CONCLUSION

With this formula we can very easily find the profit or loss earned by a company with varying commission. It is very useful to Multiple National Marketing Companies which do this type of business and this type of companies can find easily their profit or loss.

REFERENCE

[1] Himanshu “Chain system the formula” in “International journal of mathematics trends and technology”
 [2] Himanshu “Complex Chain system the formula” in “International journal of science and research”
 [3] Himanshu “Chain system the formula with changeable commission” in “International Journal of Scientific And Education”

[4] Himanshu “Complex Chain system the formula with changeable commission” in “International Journal of Mutidisciplinary Research And Development”

[5] Google

ACKNOWLEDGEMENT

- [1] Dr. Sunil Mehta
HOD Mathematics, Khalsa college Patiala.
- [2] Mr. Anil Jindal
Prof. Bits-Pilani Campus Rajasthan,
- [3] Mr. Rakesh Kumar
Prof. Pbi. Uni. Patiala (PB)
- [4] Mr. Gurmeet Singh
Prof. Mathematics Deptt. Khalsa college Patiala.
- [5] Mrs. Nishu
Prof. Mathematics Deptt. Khalsa college Patiala.
- [6] Mr. Sunil Singla
Principal High Sr. Sec. School Kalipur,
Dist. Mansa
- [7] Mr. Harpreet Singh
Asst. Prof. HOD Mathematics Deptt GNC Budhlada.
- [8] Miss Seema
HOD Mathematics Deptt. Krishna College Rali dist Mansa
- [9] Mr. Happy Kumar
Asst. Prof. Mathematics Deptt GNC Budhlada.
- [10] Mrs. Gurpreet Kaur
Asst. Prof. Mathematics Deptt GNC Budhlada.
- [11] Mr. Sanjiv Singla
Asst. Prof. GNC Budhlada.
- [12] Miss Nitika Singla
Asst. Prof Mathematics Deptt. GNC Budhlada
- [13] Miss Anita Rani
Mathematics Teacher Govt Girl School Boha Dist Mansa
- [14] Miss Manisha Rani
Teacher Manu Vikika , School Budhlada.

FUTURE ASPECTS OF VALVELESS PULSE JET ENGINE

Ashish Kudesia¹, Dr. A. M. Bisen²

¹Department of Mechanical Engineering, MATS University, Raipur (India)

²Professor, Department of Mechanical Engineering, MATS University, Raipur (India)

ABSTRACT

Today there has been a renewed interest among the defense industry in pulsejet technology. With the increasing popularity of the unmanned aerial vehicle, they are trying to find ways to propel these small, lightweight aircrafts with efficient, affordable and durable engines. Pulsejets, because of their simplicity, offer a unique solution to this demand. The main aim of this paper is to study the future aspects of valveless pulsejet engine which can be used as propulsion source.

Keywords: Carburetor; Pulsejet Engine; Thrust; Unmanned Aerial Vehicle; Valveless Pulsejet

I. INTRODUCTION

A pulsejet is a simple form of an air breathing engine. Pulsejet engines can be made with few or no moving parts and are capable of running statically. With valveless pulsejet which have no moving parts it becomes hard for one of these machines to fail in operation. The lack of hardware in pulsejets makes for an engine that is lightweight and dependable. Pulsejets are also known for their exemplary throttle response, as there are no turbines to spool up or flywheels to slow down quickly. Also these machines can take quite a beating and still prove operable. In an environment as demanding as a war zone it is possible for a pulsejet to take a bullet and keep on running. The reason behind choosing valveless pulsejet engine for this paper is the simplicity and robustness of these engines.

There are two main types of pulsejet engines, both of which use resonant combustion. The first is a valved design, in which the combustion process is controlled by valves. This type of engine contains more parts due to which there is a potential for problems. The second type is known as valveless system, in which there are no moving parts. This results in easier construction and are cheaper than the valved ones. In this paper our main focus is on valveless pulsejet system.

II. HISTORY AND BACKGROUND

The pulsejet gained its recognition during world war-II when it was used as the propulsion device for the first cruise missile. This was the German v-1 "buzz-bomb" named for its loud, obnoxious cyclical sound. It operated at 50 Hz, producing a maximum thrust of approximately 360kg. The implementation of the v-1 marked the successful application of a pulsejet as a propulsion device.

Development of pulsating combustion began around 17th century. Christian Huyghens, a renowned mathematician and physicist designed a pulsating engine powered by gun powder.

2.1 Current Approaches

One of the most attractive project on pulsejet engine technology going on is a proprietary developed by Boeing known as the Pulse Ejector Thrust Augmenter (PETA), which proposes to use pulse jet engines for vertical lift in military and commercial vertical take-off and landing aircraft (VTOL). The Boeing design embeds the pulse jet inside a thrust augmenting duct which entrains surrounding air into the exhaust stream. This entrained air improves thrust and cools the pulse jet.



Fig. 1: An Aircraft with Pulse Ejector Thrust Augmenter (PETA) Modules

III. WORKING OF PULSEJET

The primary effect behind the function of a pulsejet is the fact that gases are compressible and tend to act like a spring. This springiness is crucial to the way a pulsejet draws in a fresh mixture of air and fuel then expels the hot burning gasses that are generated when that fuel is ignited. The two most popular theories to describe the pulsejet engine cycle are the kadenacy effect and acoustical resonance.

- The kadenacy effect describes the movement of the gases through pressure waves and the inertia of the gases. It is named after Michel kadenacy who obtained a patent for an engine in 1933. To understand this effect let us take an example, now something very similar happens when we take a sealed container and fill it with compressed air. If we suddenly release that pressure by removing the cork, the compressed air will rush out but even once the pressure inside falls to match the pressure outside, the air will continue to flow out.
- This will cause the pressure inside the container to fall below the pressure outside and then the gas will flow back inwards. This cycle of increasing and decreasing pressure will repeat a number of times, decreasing in magnitude each time.
- That’s the kadenacy effect in action driven by the springiness of air.

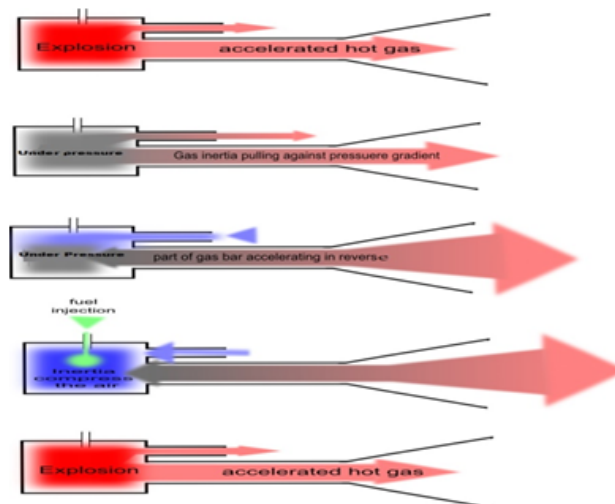


Fig. 2: WORKING OF PULSEJET ENGINE

3.1 Pulsejet Cycle

A pulsejets operates by combination of two cycles: the Lenoir cycle and the Humphrey cycle

The Lenoir cycle consists of the intake of air and fuel at a point a, isochoric combustion from a to b, and an adiabatic expansion to c.

Process a-b: Heat addition at constant volume

Process b-c: Isentropic expansion

Process c-a: Heat rejection at constant pressure

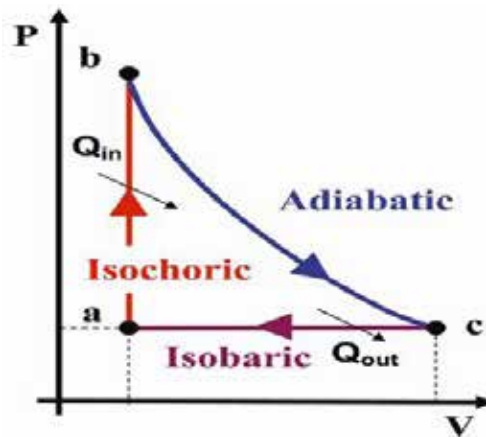


Fig. 3: LENOIR CYCLE

The Humphrey cycle is shown below, in this process it adds a small amount of compression before combustion, step a to b.

Process a-b: Isentropic compression

Process b-c: Constant volume heat addition.

Process c-d: Isentropic Expansion of the gas

Process d-a: Constant pressure heat rejection

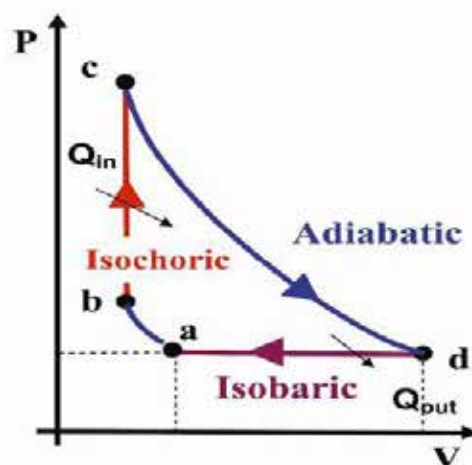


Fig. 4: HUMPHREY CYCLE

IV. DESIGN

The valveless pulsejet that has been designed is known as the thermo- jet engine. It contains no rotating or vibrating parts. The engine is being operated on petrol, methanol and variety of different liquid fuels. The length and diameter of the engine determine the frequency of the pressure pulses. Fuel, flows through the fuel nozzles

at high velocity inside the carbureted inlet tubes forcing the surrounding air to also enter the inlets and mix with the fuel in a ratio of approximately 15 to 1. Fuel and air then flow into the combustion chamber where they are ignited initially by a spark plug only during starting of the engine and then from left out heat of the previous combustion.

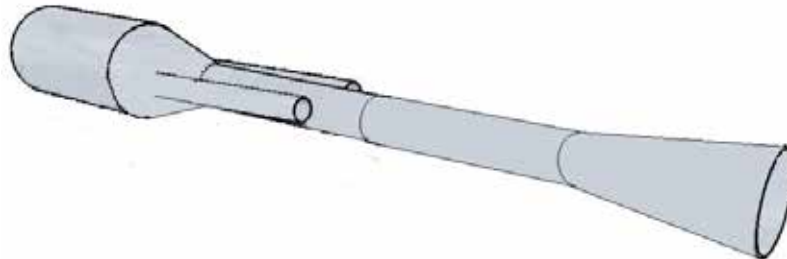


Fig. 5: PULSEJET DESIGN

4.1 Combustion Chamber

Designing the combustion chamber is the most important part of the designing. Whole engine's dimension depends on the length, diameter and volume of the combustion chamber. From statistical analysis there comes a relation through which thrust can be calculated using volume of combustion chamber.

$$\text{Thrust} = 4453.98V_{cc} + 1.448$$

Where V_{cc} is the volume of combustion chamber.

4.2 Carburetor

A carburetor is used at an intake which will maintain air to fuel ratio of 15:1. Fuel will be automatically draws due to the vacuum created inside the carburetor. Thus the amount of air entering the carburetor will draw the required amount of fuel.



Fig. 6: CARBURATED INTAKE

4.3 Efficiency

Reviewing Lenoir and Humphrey cycle it can be understood that combustion of varying pressure and volume occurs along the line a-b in Lenoir cycle and along b-c in Humphrey cycle. Isentropic expansion along b-c in Lenoir cycle and along c-d in Humphrey cycle. The heat added is $C_{PV} (T_C - T_B)$. C_{PV} is the effective average specific heat intermediate between C_V & C_P . Heat rejected is $C_p (T_D - T_A)$.

The cycle efficiency is then

$$\eta = \frac{C_{PV} (T_C - T_B) - C_p (T_D - T_A)}{C_{PV} (T_C - T_B)} = 1 - \frac{C_p (T_D - T_A)}{C_{PV} (T_C - T_B)}$$

C_p is average specific heat for a constant pressure reaction. T_B is equal to T_A for a stationary thermojet. The pressure ratio P_C/P_D is relatively small, therefore the temperature T_D cannot differ much from the temperature T_C .

Thus the fraction $(T_D - T_A) / (T_C - T_B)$ cannot be much less than 1, whereas

$$C_p / C_v$$

Is greater than 1 and the efficiency will have a low positive value. To increase the efficiency, it is necessary to increase the value of T_C , at higher aircraft velocities the compression and expansion ratios will increase, thereby improving the engine efficiency.

4.4 Exhaust Tube

This is the long tube which is connected to the combustion chamber. The exhaust tube serves two important roles. Firstly, it is this tube that accounts for around 60% of the thrust produced by an valveless engine. Hot gases from the combustion chamber exiting through this tube produce a reaction that creates the thrust.

Secondly, this is the pump that drives the engine. For this reason, its dimensions are critical. In order to provide the necessary pumping action to draw in the next charge of fresh air, the gases in the tailpipe must contain sufficient energy to create a partial vacuum in the combustion chamber. The energy or momentum of those gases is determined by their mass and their velocity using the formula.

$$P = mV$$

Based on observations the exhaust tube's internal diameter should be half the maximum combustion chamber's internal diameter

4.5 Intake Tubes

The intake tube's internal diameter should be around three fourth of the exhaust's internal diameter. Its shorter than the exhaust tube because it needs to be able to pass enough air to pretty much fill the combustion chamber during the engine's intake phase. If the intake tube were too long, the engine would simply end up sucking back the exhaust gasses that filled it during the last combustion phase.

However, the intake tube also needs to be long enough that it can hold a large enough slug of cold, dense air to help air to contain the combustion gasses during the early phase of the combustion cycle.

Table 1 Design Dimensions

PARAMETER	MAGNITUDE	UNITS
INTERNAL DIA OF COMBUSTION CHAMBER	7.62	CM
LENGTH OF CC	10.16	CM
VOLUME OF CC	463.33	CM ³
INTERNAL DIA OF EXHAUST TUBE	3.17	CM
LENGTH OF EXHAUST TUBE	36.83	CM
VOLUME OF EXHAUST TUBE	290.68	CM ³
INTERNAL DIA OF INTAKES	1.27	CM
LENGTH OF INTAKES	7.62	CM
VOLUME OF INTAKES	19.3	CM ³
No Of Intakes	2	

V. DISCUSSIONS

During the operation of pulsejet it was noticed that pulsejets are highly dependent on the way the fuel is introduced to the combustion chamber, also they are sensitive to the location of the fuel injector. It is desired to achieve a high pressure drop at the injector interface so that the fuel can be sprayed into the combustion chamber at the higher velocity. This promotes turbulent flows and mixing. Flares at the exhaust and inlet aid in the operation of pulsejets.

Pulsejets are simple propulsion devices, and it is the characteristic that makes them attractive for propulsion applications. The next step in the development of valveless pulsejet engine technology is almost certainly going to be in the pulse detonation engine which will provide a useful way of propelling manned and un manned crafts to speeds well in excess of Mach 3 and with vastly greater efficiencies than existing engine technologies. Methods have been developed to make the design more predictable. This is pushing the pulsejet closer to practical applications. Those applications will come if the problem of vibration is addressed. The simplest way to cut at least some vibration is having two identical pulsejets work out of phase will cancel some of the vibrations out. Experiments made so far indicate that some useful reduction in vibration is indeed available by this method. Pairing of engines will achieve not only the reduction of vibration but also a boost of operating efficiency. Like the opposed twin piston engine, two pulsejets working together can be made to cancel the vibrations out. Next, the use of surge chambers, sound-deadening materials etc. should be considered.

VI. CONCLUSIONS

The valveless pulsejet engine can be an alternate solution for propulsion of target drones and unmanned Ariel vehicle after some more improvements in the pulsejet research. In order to further improve the pulsejet research, several things can be done during the testing phase that would enhance the results. Effects of optimum fuel to air ratios and maximizing flow into the inlets could potentially show improvements in thrust and efficiency within the engine, also tests could be done to see the effects of different fuels on the pulsejet. Finally, tests could be done to increase the engines compression ratio and decrease the level of vibrations that engine produces.

Nomenclature

T-Temperature

P -Pressure

V – Volume

V_{CC} -Volume of combustion chamber

C_V . Specific Heat at Constant Volume

C_P –Specific Heat at constant Pressure

C_{PV} –Average Specific Heat

REFERENCES

- [1] Kentfield, J „The Potential of Valveless Pulsejets for Small UAV Propulsion Applications“ *AIAA Journal* 1998, No. 3879
- [2] “Design and Build a Pulse Jet Engine And Thrust Measurement Stand,” Univ. Of Adelaide, School. Of Mechanical Engineering. Level IV Design Project 2007, May 2007
- [3] Tharatt, C „The Propulsive Duct“ *Aircraft Engineering*, November 1965, pp 327- 337, December 1965, p 359-371
- [4] Ogorelec, B 2005 Valveless pulsejet 1.5 – a historical review of valveless pulsejet designs.
- [5] Simpson, B 2007 , the valveless pulse jet, Accessed 15 april 2007.
- [6] www.pulsejetbook .com
- [7] Reynst, F H 1961, pulsating combustion, Pergamon press, London,UK.
- [8] Sunnhordvik, A 2007, Valveless Pulse Jet, Accessed 10 May 2007
- [9] Cotrill, L., “First Principles: The Kadenacy Effect,”http://jetzilla.com/topic_003_01.html
- [10] <http://aardvark.co.nz/pjet/valveless.html>